

# MAXIMUM MONTHLY RAINFALL BEHAVIOR ALONG THE FRONT RANGE OF COLORADO

by

JEREMY M. MULCAHEY

(Under the direction of Lynne Seymour)

## ABSTRACT

This work investigates long term trends in observed monthly maximum 24-h precipitation for Boulder, Colorado, which experienced a historic 24-h rainfall in September, 2013. The long term precipitation trends for four cities (Fort Collins, Evergreen, Lakewood, and Greeley) in the area around Boulder are also analyzed, yet the historic event observed in Boulder was not observed in those cities. The maximum precipitation trends for Fort Collins, Lakewood, and Boulder, which have presumably similar geographic features, showed increases in the mean, variance, and probability of experiencing certain rainfall thresholds over time. Each of the aforementioned values were decreasing over time in the city of Evergreen, which appears to be geographically dissimilar from the other cities investigated. Lastly, the trend lines for Greeley were highly variable, yet have an increasing trend since the mid 1900s. The trend lines for individual months showed that these increasing trends are not spread among the 12 months. Certain months are experiencing greater maximum rainfall on average, while others are experiencing less.

INDEX WORDS: 24-h maximum rainfall; flooding; Fort Collins; Boulder; Colorado;  
Climate trends

MAXIMUM MONTHLY RAINFALL BEHAVIOR ALONG THE FRONT  
RANGE OF COLORADO

by

JEREMY M. MULCAHEY

B.S. Statistics, California Polytechnic University, 2015

A Thesis Submitted to the Graduate Faculty  
of The University of Georgia in Partial Fulfillment  
of the  
Requirements for the Degree

MASTER OF SCIENCE

ATHENS, GEORGIA

2016

© 2016

Jeremy M. Mulcahey

All Rights Reserved

MAXIMUM MONTHLY RAINFALL BEHAVIOR ALONG THE FRONT  
RANGE OF COLORADO

by

JEREMY M. MULCAHEY

Approved:

Major Professor: Lynne Seymour

Committee: Nicole Lazar  
Jaxk Reeves

Electronic Version Approved:

Suzanne Barbour  
Dean of the Graduate School  
The University of Georgia  
December 2016

## ACKNOWLEDGMENTS

Countless people have contributed, in various and immeasurable ways, to my transition from high school dropout to college graduate. First and foremost I would like to thank my best friend, Will Rinehart, for years of guidance and mental, emotional, and financial support. Will took the first step to leading me down this path and I followed. I would like to thank State Farm, particularly Jonathan Sauls, Andy Pulkstenis, and Bob Trefzger, for accepting me to the MAGNet program that lured me to UGA, and for believing in me once I got there. I would like to thank Dr. Lynne Seymour for providing me with the opportunity to complete this EDA as my thesis and for being a good listener. I would like to thank my committee, Dr. Jaxk Reeves and Dr. Nicole Lazar, for volunteering their time and energy to help me complete this process. I would like to thank the educators at Cuesta Community College in San Luis Obispo for a competitive education that prepared me for, and served me well at, Cal Poly SLO. I would like to thank the Cal Poly SLO Statistics department for a rigorous education that prepared me for “real world” statistics and built the foundation required to be relatively successful in a Master’s program with a theoretical emphasis. I would also like to thank Dr. Beth Chance, of Cal Poly SLO, for her continued support, friendship, and pushing for me to do bigger and better things. I would like to thank Caleb Miller for being a comrade in arms during our time at Cal Poly, and for reminding/showing me everyday that successful applications of intellect are 5 parts hard-work and 5 parts extremely hard-work. Lastly, I would like to thank my family, teammates, and friends that know they contributed to this portion of my life in one way or another.

# TABLE OF CONTENTS

	Page
ACKNOWLEDGMENTS . . . . .	iv
LIST OF FIGURES . . . . .	vii
LIST OF TABLES . . . . .	xiii
CHAPTER	
1 INTRODUCTION . . . . .	1
1.1 FOREWORD . . . . .	1
1.2 MOTIVATION . . . . .	1
2 CLIMATE SIGNAL EXPLORATORY DATA ANALYSIS (EDA) . . . . .	5
2.1 BOULDER . . . . .	9
2.2 FORT COLLINS . . . . .	24
2.3 EVERGREEN . . . . .	32
2.4 LAKEWOOD . . . . .	39
2.5 GREELEY . . . . .	45
3 GEOSPATIAL EXPLORATORY DATA ANALYSIS . . . . .	52
4 CONCLUSIONS . . . . .	57
4.1 CLIMATE SIGNAL EDA . . . . .	57
4.2 GEOSPATIAL EXPLORATORY DATA ANALYSIS . . . . .	58
4.3 SHORTCOMINGS . . . . .	58
4.4 FUTURE WORK . . . . .	59
REFERENCES . . . . .	62

APPENDIX . . . . .	64
A.1 DISTRIBUTION TESTING WITH FITDISTRPLUS IN R . . . . .	64
B.1 CHANGE POINT ANALYSIS IN R . . . . .	69
C.1 SEASONAL EFFECTS FOR CLIMATE SIGNAL EDA . . . . .	78
D.1 STANDARD DEVIATION PLOTS FOR CLIMATE SIGNAL EDA . . . . .	81
E.1 GEOSPATIAL SUPPORT PLOTS . . . . .	84

## LIST OF FIGURES

1.1	Relative locations of cities/weather stations investigated . . . . .	3
2.1	Estimated Gamma (left) and Exponential (right) Distributions from Lake- wood Colorado in 1993 (left) and 1994(right) . . . . .	6
2.2	Observed monthly maximum 24-h rainfall for Boulder Colorado 1898-2012 (left) and 1898-2014 (right) . . . . .	9
2.3	Observed monthly maximum 24-h rainfall for Boulder, Colorado 1898-2012 (left) and 1898-2014 (right) with smoothing trend and highest observed value indicated . . . . .	10
2.4	Centered moving average trend line for monthly observed 24-h maximum pre- cipitation for 1898 to 2012 and group means (15.60 mm, 18.24 mm) from change point analysis (left); Box Plot for pre-change point and post-change- point group (right) . . . . .	11
2.5	Left: Centered moving average trend line for monthly observed 24-h maximum precipitation prior to the 9/13 Event (black), and the full data (blue); Right: Information from left plot for only the last decade of the data with third time series in which the 9/13 Event has been omitted (red) . . . . .	13
2.6	Smoothed time series for long term trend . . . . .	14
2.7	Observed variances and smoothed trend lines . . . . .	16
2.8	Seasonal time series (by month) . . . . .	17
2.9	Left: Box plot of each month over the full range of the data (1898 to 2014), Right: Split into groups (before and post-change-point), Bottom: Each month by group . . . . .	18



2.10	Left: Box plot for the smoothed values for each month over the full range of the data (1898 to 2014), Right: Split into groups (before and post-change-point), Bottom: Each month by group . . . . .	19
2.11	Top Left: All probabilities (meeting and/or exceeding 1 in, 2 in, or 3 in of rainfall), Top Right: Probability of meeting and/or exceeding 1 in of rainfall with smoothing lines, Bottom Left: Same with 2 in, Bottom Right: Same with 3 in . . . . .	23
2.12	Observed monthly maximum 24-h rainfall for Fort Collins, Colorado 1896-2014	24
2.13	Centered moving average of 24-h observed maximum rainfall (black line) smoothed with 25 year window (green), 50 year window (red), 75 year window (blue) . . . . .	25
2.14	Centered moving average trend line for monthly observed 24-h maximum precipitation for 1896 to 2014 and group means (13.31 mm, 15.03 mm) from change point analysis (left); Box Plot for pre-change-point and post-change-point groups (right) . . . . .	26
2.15	Observed variances smooth with window sizes of 15 year, 30 year, and 50 year	27
2.16	Seasonal time series (by month) . . . . .	28
2.17	Left: Box plot of each month for full dataset (1896 to 2014), Right: Split into groups (before and post-change-point), Bottom: Each month by group . . . .	29
2.18	Left: Box plot of each month for smoothed data (1896 to 2014), Right: Split into groups (before and post-change-point), Bottom: Each month by group .	30
2.19	Top Left: All probabilities (meeting and/or exceeding 1 in, 2 in, or 3 in of rainfall), Top Right: Probability of meeting and/or exceeding 1 in of rainfall with smoothing lines, Bottom Left: Same with 2 in, Bottom Right: Same with 3 in . . . . .	31
2.20	Observed monthly maximum 24-h rainfall for Evergreen, Colorado 1962-2014	32

2.21	Centered moving average of 24-h observed maximum rainfall (black line) smoothed with 10 year window (green), 20 year window (red), 50 year window (blue) . . . . .	33
2.22	Centered moving average trend line for monthly observed 24-h maximum precipitation for 1962 to 2014 and group means (15.41 mm, 14.22 mm) from change point analysis (left); Box Plot for pre-change-point and post-change-point group (right) . . . . .	34
2.23	Observed variances with smoothed trend lines . . . . .	35
2.24	Seasonal time series (by month) . . . . .	36
2.25	Left: Box plot of each month for smoothed data (1962 to 2014), Right: Split into groups (before and post-change-point), Bottom: Each month by group .	37
2.26	Top Left: All probabilities (meeting and/or exceeding 1 in, 2 in, or 3 in of rainfall), Top Right: Probability of meeting and/or exceeding 1 in of rainfall with smoothing lines, Bottom Left: Same with 2 in, Bottom Right: Same with 3 in . . . . .	38
2.27	Observed monthly maximum 24-h rainfall for Lakewood, Colorado 1963-2014	39
2.28	Centered moving average of 24-h observed maximum rainfall (black line) smoothed with 10 year window (green), 20 year window (red), 50 year window (blue) . . . . .	40
2.29	Centered moving average trend line for monthly observed 24-h maximum precipitation for 1963 to 2014 and group means (13.58 mm, 15.87 mm) from change point analysis (left); Box Plot for pre and post-change-point groups (right) . . . . .	40
2.30	Observed variances smooth with window sizes of 10 year, 20 year, and 50 year	41
2.31	Seasonal time series (by month) . . . . .	42
2.32	Left: Box plot of each month for smoothed data (1963 to 2014), Right: Split into groups (before and post-change-point), Bottom: Each month by group .	43

2.33	Top Left: All probabilities (meeting and/or exceeding 1 in, 2 in, or 3 in of rainfall), Top Right: Probability of meeting and/or exceeding 1 in of rainfall with smoothing lines, Bottom Left: Same with 2 in, Bottom Right: Same with 3 in . . . . .	44
2.34	Observed monthly maximum 24-h rainfall for Greeley, Colorado 1893-2014 . . . . .	45
2.35	Centered moving average of 24-h observed maximum rainfall (black line) smoothed with 25 year window (green), 50 year window (red), 75 year window (blue) . . . . .	46
2.36	Centered moving average trend line for monthly observed 24-h maximum precipitation for 1963 to 2014 and group means (11.67 mm, 13.66 mm) from change point analysis (left); Box Plot for pre-change-point and post-change-point group (right) . . . . .	47
2.37	Observed variances smooth with window sizes of 10 year, 20 year, and 50 year . . . . .	48
2.38	Seasonal time series (by month) . . . . .	49
2.39	Left: Box plot of each month for smoothed data (1893 to 2014), Right: Split into groups (before and post-change-point), Bottom: Each month by group . . . . .	50
2.40	Top Left: All probabilities (meeting and/or exceeding 1 in, 2 in, or 3 in of rainfall), Top Right: Probability of meeting and/or exceeding 1 in of rainfall with smoothing lines, Bottom Left: Same with 2 in, Bottom Right: Same with 3 in . . . . .	51
3.1	Density and frequency for 1 in of rainfall observed in the data set from 1963 to 2014 . . . . .	52
3.2	Density and frequency for 2 in of rainfall observed in the data set from 1963 to 2014 . . . . .	54
3.3	Density and frequency for 3 in of rainfall observed in the data set from 1963 to 2014 . . . . .	56

A.1	Distributions of Observed 24-Hour Maximum Rainfall for Intervals that failed K-S GoF tests with parameter estimates from MLE (Boulder) . . . . .	65
A.2	Boulder time interval 45, suboptimal fit . . . . .	66
A.3	Boulder time interval 3, optimal fit . . . . .	67
B.1	QQ plot (left); Distribution of smoothed precipitation values (right) . . . . .	69
B.2	Box plot for pre and post-change-point groups for full dataset (event omitted)	70
B.3	QQ plot (left); Distribution of smoothed precipitation values (right) . . . . .	71
B.4	Box plot for pre and post-change-point groups for full dataset . . . . .	72
B.5	QQ plot (left); Distribution of smoothed precipitation values (right) . . . . .	72
B.6	Box plot for pre and post-change-point groups for full dataset . . . . .	73
B.7	QQ plot (left); Distribution of smoothed precipitation values (right) . . . . .	74
B.8	Box plot for pre and post-change-point groups for full dataset . . . . .	75
B.9	QQ plot (left); Distribution of smoothed precipitation values (right) . . . . .	76
B.10	Box plot for pre and post-change-point groups for full dataset . . . . .	76
C.1	Left: Box plot of each month for full dataset (1962 to 2014), Right: Split into groups (before and post-change-point), Bottom: Each month by group (Evergreen) . . . . .	78
C.2	Left: Box plot of each month for full dataset (1963 to 2014), Right: Split into groups (before and post-change-point), Bottom: Each month by group (Lakewood) . . . . .	79
C.3	Left: Box plot of each month for full dataset (1893 to 2014), Right: Split into groups (before and post-change-point), Bottom: Each month by group (Greeley)	80
D.1	Observed Standard deviations over time (Boulder) . . . . .	81
D.2	Observed Standard deviations over time (Fort Collins) . . . . .	81
D.3	Observed Standard deviations over time (Evergreen) . . . . .	82
D.4	Observed Standard deviations over time (Lakewood) . . . . .	82
D.5	Observed Standard deviations over time (Greeley) . . . . .	83

E.1	Number of times the weather stations recorded 1 in of rain or more for qualifying each month in the data set . . . . .	84
E.2	Number of times the weather stations recorded 2 in of rain or more for each qualifying month in the data set . . . . .	85
E.3	Number of times the weather stations recorded 3 in of rain or more for each qualifying month in the data set . . . . .	86

## LIST OF TABLES

2.1	Table III-2 Urban Flash Flood Guidance from Urban Drainage and Flood Control District in Colorado . . . . .	21
3.1	Number of times at least 1 in of rain was recorded for qualifying months . .	53
3.2	Number of times at least 2 in of rain were recorded for qualifying months . .	55
3.3	Number of times at least 3 in of rain were recorded for qualifying months . .	56
A.1	Goodness-of-Fit test results using K-S GoF Test . . . . .	64
A.2	Goodness-of-Fit test results using K-S GoF Test . . . . .	68
A.3	Goodness-of-Fit test results using K-S GoF Test . . . . .	68
A.4	Goodness-of-Fit test results using K-S GoF Test . . . . .	68
A.5	Goodness-of-Fit test results using K-S GoF Test . . . . .	68

## CHAPTER 1

### INTRODUCTION

#### 1.1 FOREWORD

I believe one of the most important components of a statistician's work is the story they tell. If no one can understand the results and conclusions, an insightful analysis can fall on deaf ears. One afternoon Dr. Lynne Seymour and I discovered we could expedite my graduation if I were to complete a thesis, as opposed to taking the qualification exams and two extra classes. From there, I was given five datasets containing maximum precipitation values for five cities in Colorado and told to find the climate signals for each. This thesis tells the story of the insights I gained into the motivation behind the analysis of these datasets (and similar analyses), what I uncovered about the rainfall component of the climate signal in the cities, and ways to make use of this exploratory data analysis moving forward.

#### 1.2 MOTIVATION

Climate change is a well-documented component of the Earth's history. The Earth and its many systems function on natural cycles. The natural global warming cycle is unavoidable and has a direct impact on the global hydrological cycle. Since the hydrological cycle is a closed system, meaning that water cannot be created or destroyed on a large scale, water shifts from one area to another as the climate changes (Doodge 1968). This can lead to less rainfall in previously arid locations and an increase in rainfall for more lush climates. The greater concern is that areas receiving additional precipitation tend to experience more severe storms (Marvel and Bonfils 2013).

In the absence of human inhabitants the shifts in the hydrological cycle associated with the global warming cycle might go unnoticed. As of 2008, it is estimated that 95% of the world's population lives on 10% of the land (JRC 2008). The inhabited areas range from arid to tropical, which can leave respective locals without access to fresh water or an over abundance of water and potentially hazardous rainfall conditions. The latter situation has wrought havoc on American states such as Colorado, Texas, and South Carolina in recent years. Three separate flood periods in these three states since 2013 have resulted in an estimated \$6 billion in damages and the loss of 65 lives (NOAA 2016).

Colorado was the first of the aforementioned states to experience a historic level of rainfall (in excess of 15 in) in September 2013 (HDSC 2013). The unprecedented surge in rainfall caused an estimated \$1.5 billion in damage and claimed 9 lives (NOAA 2016). In the immediate wake of the flooding in Colorado, the National Weather Service (NWS)/National Oceanic and Atmospheric Administration (NOAA) Hydrometeorological Design Studies Center produced a paper sharing the geospatial probabilities that precipitation of this magnitude occurred in the affected area (HDSC 2013). The probability plots illustrate that the event was extremely improbable, but the paper does not offer results or conclusions for the analysis.

The intent of this report is to identify, analyze, and explore elements of the climate signal for select cities (Fort Collins, Boulder, Evergreen, Lakewood, and Greeley) in Colorado through exploratory data analysis (EDA) of monthly maximum precipitation. The amount of data available differs by city. For instance, Fort Collins and Boulder have observations as far back as the 1890's, while Evergreen and Lakewood date back to only the 1960s. The information from each city's weather station is subset and referred to as observed monthly maximum 24-h rainfall data, where 24-h refers to a calendar day. The subset data is created by selecting the highest value of observed rainfall in a 24-h period (recorded  $\frac{1}{10}$  mm) from a qualifying month. In order for a month to qualify, at least 80% of the days need to have a record for rainfall. The observed maximum 24-h rainfall for months that do not have at least



80% of the days recorded are treated as missing and coded as NA. Ideally, this is necessary for producing the most informative and representative subset for maximum value analysis since false maxima could underestimate trends, distribution parameters, and probabilities that are calculated in this report.

The climate signals for the select cities aid in understanding if the storms in the analyzed region of Colorado are increasing in intensity (i.e. experiencing greater precipitation in a 24-h period), or if the precipitation has remained relatively constant over time. Specifically, the maximum precipitation trends are analyzed to provide a more in depth understanding of the probability of the September 2013 event. Finally, an analysis is done to understand the probability of exceeding 1 in, 2 in, and 3 in of rainfall in a day for the select cities.

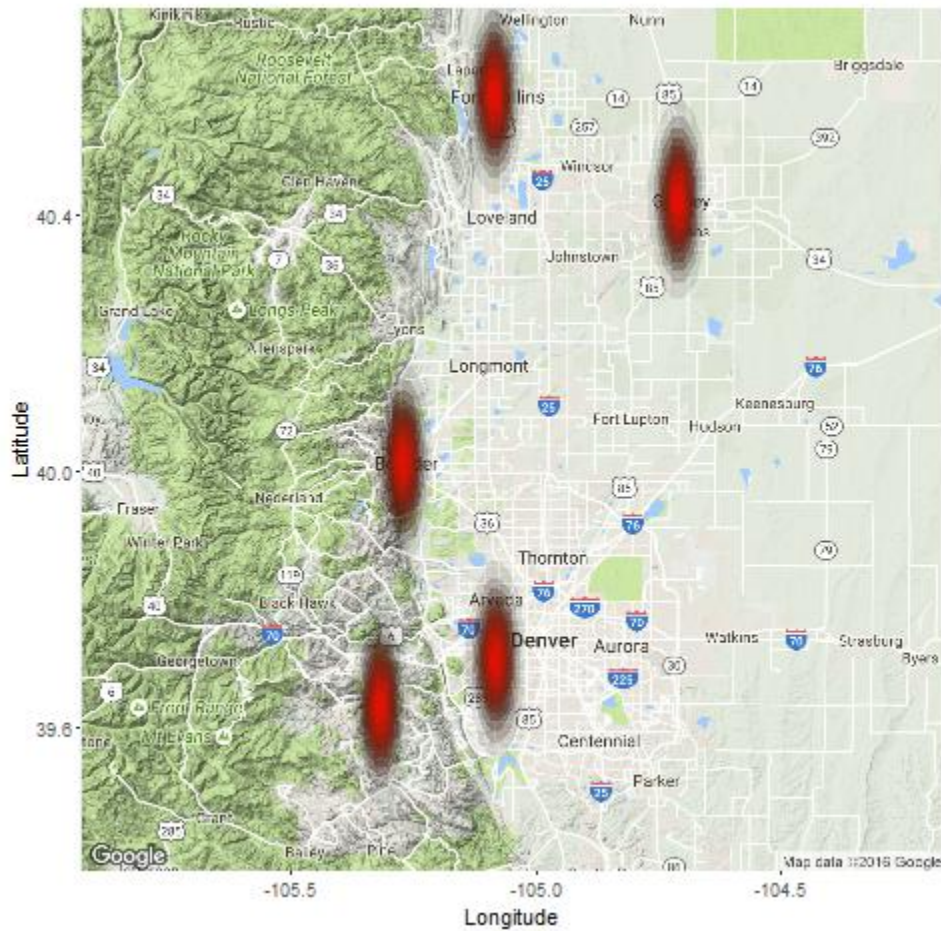


Figure 1.1: Relative locations of cities/weather stations investigated

The less complex approaches in the analysis involve investigating changes to the distribution of monthly maximum observed 24-h rainfall over time, changes to the means and variances of estimated distributions for maximum 24-h rainfall over time, changes in the maximum observed 24-h rainfall by month, and geospatial comparisons of observed rainfall thresholds. The more complex approach utilizes estimated distributions to obtain the probabilities that observed precipitation exceed the defined rainfall thresholds, and examines the change in those probabilities over time.

The structure of this investigation is to introduce methodology in detail as it arises in the context of the analysis, then provide only the results for subsequent applications of previously introduced methodology. The bulk of the methodology is explained in the Climate Signal EDA introduction and the analysis of the first city/weather station (Boulder, Colorado). The report itself primarily relies on EDA methods and does not make firm inferences based on statistically significant results at this time.

## CHAPTER 2

### CLIMATE SIGNAL EXPLORATORY DATA ANALYSIS (EDA)

A pre-project EDA on observed monthly maximum 24-h rainfall performed by Dr. Lynne Seymour revealed that many decade long intervals appeared to follow a gamma distribution (with many intervals following the exponential distribution, which is a special case of the gamma distribution - see Figure 2.1, page 6) (Mattingly et al., 2016). The time intervals were created by starting at the first year in a dataset, selecting all valid monthly 24-h maximum rainfall data points (as defined in the Introduction) for a decade, then incrementing by one year and repeating. For example, the first time interval for Fort Collins was 1896 to 1905, followed by 1897 to 1906. The conjecture was, given recently observed impacts of climate change on the hydrological cycle discussed in Chapter 1, these gamma distributions would shift to the right and flatten as time passed (indicating that the mean and variance were slowly increasing over time). This could indicate that the area of Colorado, which experienced the historic rainfall, is affected by a shift in the hydrological cycle - if the hydrological cycle is in fact shifting at this time.

The first step to assess the conjecture was to estimate the distributions for the time intervals. The gamma distribution is defined as

$$f(x|\alpha, \beta) = \frac{\beta^\alpha}{\Gamma(\alpha)} x^{\alpha-1} e^{-\beta x} \text{ for } x \geq 0, \text{ and } \alpha, \beta > 0.$$

Estimating the distributions means estimating the  $\alpha$  and  $\beta$  parameters that control the distribution from the available data. The  $\alpha$  parameter is responsible for the shape of the distribution while  $\beta$  controls the scale of the distribution. The conjecture implies that the  $\alpha$  and  $\beta$  parameters are both subtly increasing over time. The increase in the  $\alpha$  parameter yields

the shift from the exponential distribution shape to the unimodal gamma distribution, and the increase in the  $\beta$  parameter pulls the height of the unimodal hump lower while flattening and widening the distribution (increasing the variance which leads to more probable extreme rainfall values).

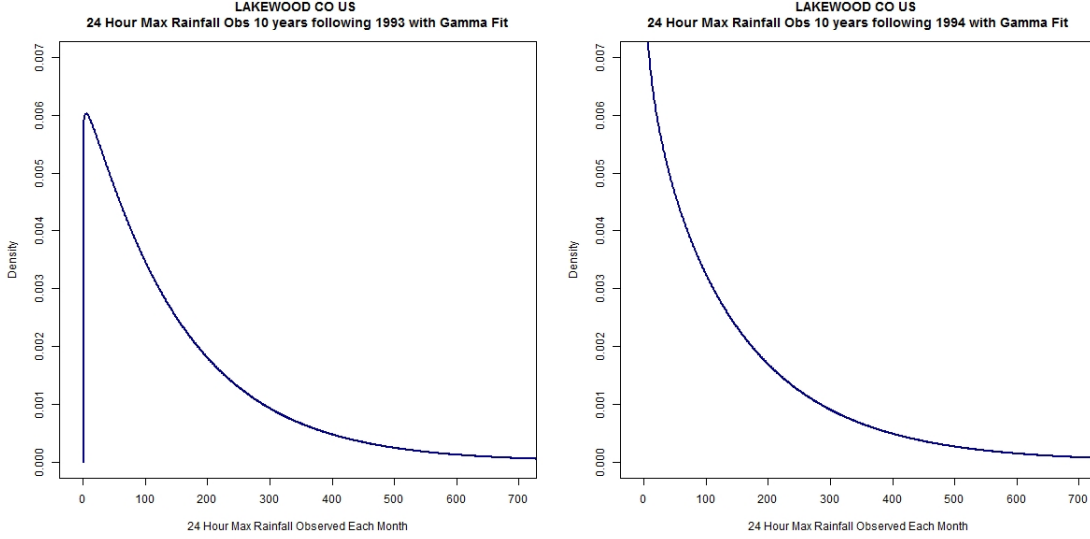


Figure 2.1: Estimated Gamma (left) and Exponential (right) Distributions from Lakewood Colorado in 1993 (left) and 1994(right)

The parameters for all intervals from all cities were estimated using maximum likelihood estimation with the `fitdistrplus` package in R (Delignette-Muller and Dutang 2015). The  $x_i$  values referenced below are the observed maximum 24-h rainfall for the  $i^{th}$  month. The maximum possible number of  $x$  values for any parameter estimation is 120. This occurs when the decade long interval, for which the distributions is being fit, has at least 80% of the daily rainfall totals recorded for all 120 months.

The maximum likelihood estimates for the gamma distribution are found by determining the values of the parameters that maximize the likelihood function

$$L(\alpha, \beta | x) = \left( \frac{\beta^\alpha}{\Gamma(\alpha)} \right)^n \cdot (x_1 x_2 \dots x_n)^{\alpha-1} e^{-\beta(x_1 + x_2 + \dots + x_n)}.$$

This is achieved by determining the log likelihood function and taking the partial derivatives for  $\alpha$  and  $\beta$ . The partial derivative functions are then set to 0 and solved to find the value

that corresponds to the unimodal maximum where the slope is 0:

$$\ln L(\alpha, \beta | x) = n(\alpha \ln \beta - \ln \Gamma(\alpha)) + (\alpha - 1) \sum_{i=1}^n \ln x_i - \beta \sum_{i=1}^n x_i,$$

$$\frac{\partial}{\partial \alpha} \ln L(\hat{\alpha}, \hat{\beta} | x) = n(\ln \hat{\beta} - \frac{d}{d\alpha} \ln \Gamma(\hat{\alpha})) + \sum_{i=1}^n x_i = 0,$$

$$\frac{\partial}{\partial \beta} \ln L(\hat{\alpha}, \hat{\beta} | x) = n \frac{\hat{\alpha}}{\hat{\beta}} - \sum_{i=1}^n x_i = 0.$$

Solving the partial derivative of  $\beta$  yields the relationship

$$\bar{x} = \frac{\hat{\alpha}}{\hat{\beta}}.$$

Plug into the partial derivative for  $\alpha$  to yield

$$n(\ln \hat{\alpha} - \ln \bar{x} - \frac{d}{d\alpha} \ln \Gamma(\hat{\alpha})) + \sum_{i=1}^n x_i = 0.$$

Similarly, and more simply, the exponential distribution parameter  $\beta$  is estimated by maximizing the likelihood function where the  $\alpha$  parameter is equal to 1. Maximum likelihood estimation of the exponential distribution parameter is done with the derivative of the log-likelihood function with respect to  $\beta$  instead of partial derivatives with respect to  $\alpha$  and  $\beta$  separately (Watkins, 2011).

The test for the fit of the distribution for each decade interval was also performed using the `fitdistrplus` package in R. The Kolmogorov-Smirnov (K-S) Goodness of Fit (GoF) Test uses the empirical distribution function (ECDF),

$$E_N = \frac{n(i)}{N},$$

where  $n(i)$  is the number of points less than  $x_i$ . This is a step function that increases by  $\frac{1}{N}$  at the value of each data point. The K-S test statistic is:

$$D = \max_{1 \leq i \leq N} |F(x_i) - \frac{i}{N}|,$$

with the hypotheses:

$$H_o : \text{Data follows specified distribution,}$$

$H_a$  : Data does not follow specified distribution.

The K-S Goodness of Fit test was chosen because it works with continuous distributions, it does not depend on an underlying cumulative distribution (which is important since that distribution is what was estimated in the previous step), it does not require large sample sizes, and because the lack of power was not a concern since there was little-to-no negative implications of rejecting the fit of a distribution (Chakravarti et al. 1967). A caveat that is not addressed is the K-S GoF test requires a custom critical value for testing when the tested distribution's parameters were estimated from the data. Empirically, this was not a concern for evaluating the conjecture since the observed distributions for the data were similar to estimated density curves.

The initial behavior, assessed by plotting the estimated distributions and animating the changes over time, did not adhere to the conjectured pattern. As the time windows progressed, few subsequent intervals demonstrated a visual shift in the distribution that would be associated with an increase in the mean and/or variance. Instead, the patterns in Figure 2.1, page 6, in which the preceding interval follows a gamma distribution and the subsequent interval follows an exponential distribution (the opposite pattern of the conjecture) were present.

The next stage was to investigate the individual weather stations in terms of means and variances over time. Since the prior stage had shown the distributions were not changing as conjectured, there were no expectations for how the mean and variances would change. Additional subsections of analysis include time series for observed monthly maximum 24-h rainfall, which involves smoothing to expose trends that the noise in the full time series mask, looking at any time points of interest (such as September 2013), and examining further subsets of the data such as time series for observed maximum 24-h rainfall in January throughout the time range vs. in July throughout the time range. The analysis for each city is iterative and guided by what is found in the previous stage(s). Therefore, the structure of the analysis across the cities is not identical.

## 2.1 BOULDER

The city of Boulder experienced 9.08 in (23.1 mm) of rain on September 9, 2013. It was one of the greatest amounts of rainfall ever recorded in Colorado in a single day, making Boulder the ideal starting point of these analyses. This historic rainfall will henceforth be referred to as the 9/13 Event. Subsequent investigations of the surrounding cities will aid in understanding the climate signal of the area involved in the 9/13 Event.

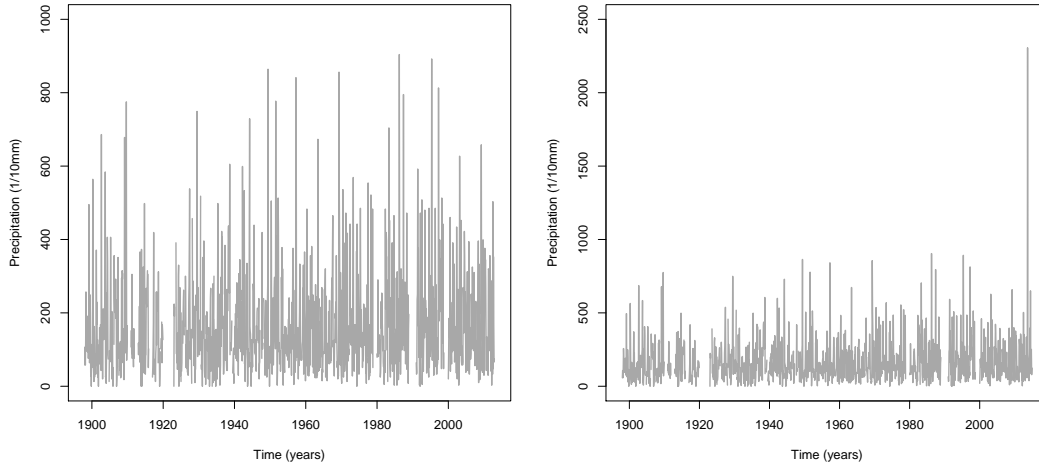


Figure 2.2: Observed monthly maximum 24-h rainfall for Boulder Colorado 1898-2012 (left) and 1898-2014 (right)

The maximum rainfall trend for a station is initially investigated by creating univariate time series plots. Univariate time series, which are used throughout this report, are ordered pairs of the observed data points and the time that corresponds to the observation (e.g.  $\{x_t = (x_i, t_i) | i = 1, 2, \dots, n\}$ ).

Boulder requires two time series plots to assess the initial behavior of the maximum values being studied. The left plot (see Figure 2.2) shows the time series for Boulder prior to the 9/13 Event experienced in September 2013. Looking at the highest points from 1898 to 2012, it appears that the maxima are increasing over time. Recall, the plotted values for precipitation are the maximum observed 24-h rainfall values recorded in qualifying months. An increase in these peak values could indicate an increase in the variance of precipitation,

but does not guarantee an increase in mean rainfall. The right plot shows the time series for the entire time range of the data for Boulder (1898-2014). The pattern of increasing peaks also appears evident in this plot. Looking at both plots, it appears the 9/13 Event is an outlier and could not have been predicted - this is investigated further.

Building from Figure 2.2 the smooth trend lines and highest observed values have been indicated in Figure 2.3, page 10. The trend lines are generated using a centered moving average (`runmean()` in R),

$$\hat{x}_i = \frac{1}{n+1} \sum_{k=i-\frac{n}{2}}^{i+\frac{n}{2}} x_k = \frac{x_{i-\frac{n}{2}} + x_{i-\frac{n}{2}+1} + \dots + x_i + \dots + x_{i+\frac{n}{2}}}{n+1},$$

which reduces the noise to better represent the underlying trend. The smoothing window used is the same size as the intervals considered for the distributions in the prior section (i.e. 120 months or 10 years). The red dotted line at the top marks the highest observed

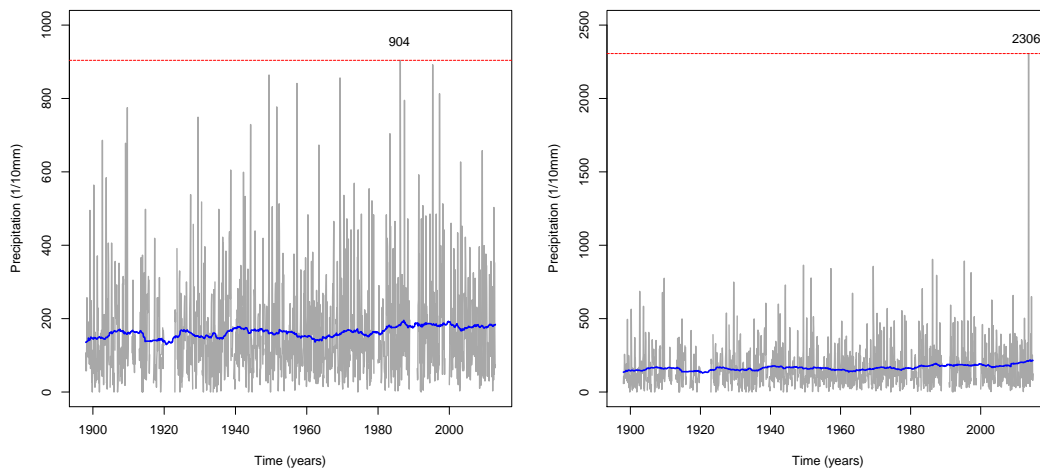


Figure 2.3: Observed monthly maximum 24-h rainfall for Boulder, Colorado 1898-2012 (left) and 1898-2014 (right) with smoothing trend and highest observed value indicated

values. The blue trend lines at the bottom are the centered moving average time series. These plots show that precipitation observed during the 9/13 Event was 2.55 times higher than any qualified monthly maximum 24-h rainfall record dating back to 1898. Additionally, these plots do show a subtle increase in the trend line over time. For certain analyses moving



forward, the 9/13 Event will be omitted as an outlier. The omission of that event will be explicitly noted in context.

### 2.1.1 TREND ANALYSIS FOR BEHAVIOR OF MEAN

The trend lines calculated using the centered moving average in the previous section are the basis for the trend analysis. In Figure 2.4, page 11, only the trend line from Figure 2.3, page 10 (left) is shown. Rescaling the trend line plot adds information that was not easily observed before. For example, the left plot indicates that there are stable long term changes in the trend line (i.e. the mean appears to be changing over time).

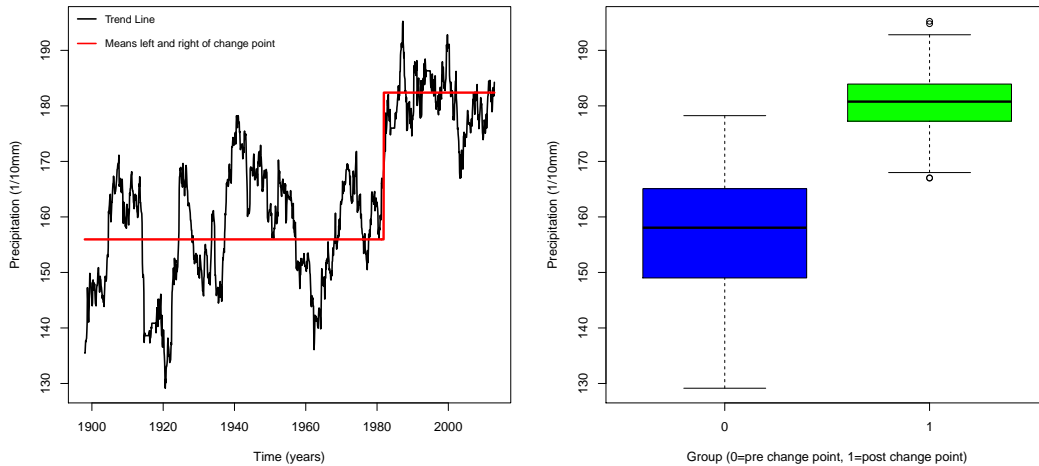


Figure 2.4: Centered moving average trend line for monthly observed 24-h maximum precipitation for 1898 to 2012 and group means (15.60 mm, 18.24 mm) from change point analysis (left); Box Plot for pre-change point and post-change-point group (right)

Focusing on the point just beyond 1981 in the left plot (Figure 2.4), it appears there is a significant increase in the smoothed time series precipitation values. Based on the information gained from the time series plot a change point analysis was performed using the **changepoint** package in R (Killick and Eckley 2014). The **changepoint** package performs a likelihood ratio test to determine if there is a point in which the mean prior to the test point is significantly

different from the mean after the test point. The hypotheses are:

$$H_o : \text{No change point was detected,}$$

$$H_a : \text{A single change point was detected.}$$

The change point is formally defined as the existence of a time,  $t \in \{1, \dots, n - 1\}$  such that the statistical properties of  $\{x_1, \dots, x_t\}$  and  $\{x_{t+1}, \dots, x_n\}$  are different (e.g. the mean is significantly different between the group before and after some point in time,  $t$ ). The smoothed values are assumed to be normally distributed to satisfy the distribution needs of the likelihood ratio test approach. Per the likelihood ratio test, the log-likelihood is maximized under the null and alternative hypotheses. The maximum under the null hypothesis is  $\log p(x_1 : n | \hat{\theta})$ , which is the probability under the normality assumption that the data is observed given the parameters estimates  $\hat{\theta}$ . The alternative hypothesis has to consider a time  $t$  where the change point is believed to exist. Therefore, the alternative hypothesis is maximized by

$$ML(t_i) = \log p(x_{1:t_i} | \hat{\theta}_1) + \log p(x_{(t_i+1):n} | \hat{\theta}_2),$$

where  $\hat{\theta}_1$  refers to the parameter estimates for the data left of the change point and  $\hat{\theta}_2$  refers to the parameter estimates for the data right of the change point. The test statistic incorporates information for all possible change points by maximizing  $ML(t_i)$  for all time points. The statistic is provided as

$$\lambda = 2[\max_{t_i} ML(t_i) - \log p(x_{1:n} | \hat{\theta})].$$

It is not stated in Killick and Eckley's referenced Journal of Statistical Software article, but this appears to be the Wilk's lambda form  $(-2\ln(\lambda))$ , which is presumably tested against the Chi-square distribution (per Wilk's Theorem) (2014).

In addition to the normality assumption, change point detection requires an assumption of independence. Due to the nature of rolling means, these values are dependent since each data point is calculated with overlap from points preceding and following it. Figure 2.4 shows

the situational robustness of change point detection (note the underlying trimodal symmetric distribution in Appendix Figure B.1) with both the time series on the left and the box plot on the right. Both assumptions, normality and independence, are violated, however, it is clear that a change point exists and that it was accurately detected (Appendix B.1).

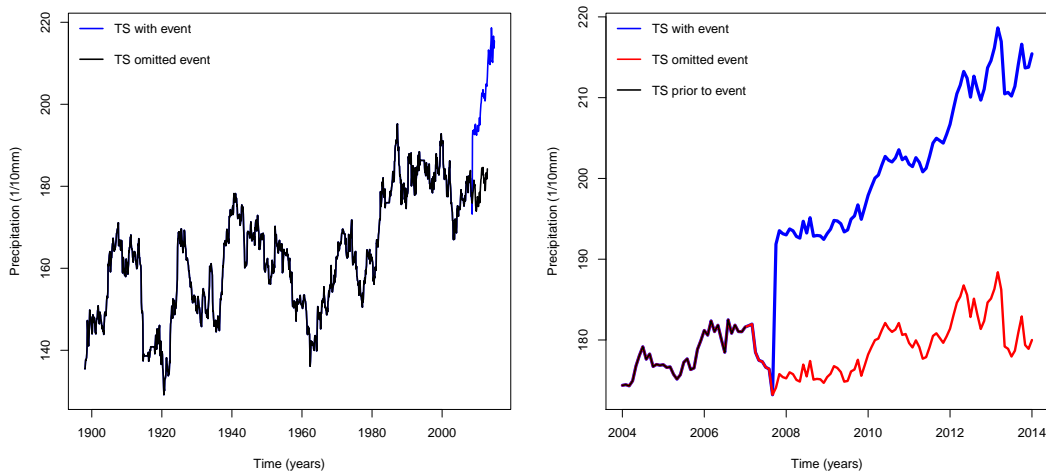


Figure 2.5: Left: Centered moving average trend line for monthly observed 24-h maximum precipitation prior to the 9/13 Event (black), and the full data (blue); Right: Information from left plot for only the last decade of the data with third time series in which the 9/13 Event has been omitted (red)

Once the change point (November 1981) was determined, the trend line was divided into two groups. The first group contains all observations prior to and including the change point (January 1898 to November 1981). The second group contains all observations after the change point (December 1981 to December 2014). The red line added to the plot on the right is the mean of the first group (15.60 mm) and the mean of the second group (18.24 mm). The vertical portion of the line is the transition from the prior mean to the current mean (at the change point). The change point analysis is helpful in understanding the climate signal for Boulder, and potentially adds insight about the 9/13 Event as well (which could be a new change point 33 years after the previous change point). The right plot in Figure 2.4 shows the box plots of the two groups. It aids in understanding the impact of the change point as well as contrast what it means to detect a statistically significant change point in a

univariate time series instead of determining statistically significant differences between two groups. Due to the variance in the actual data (see Appendix Figure B.2), a valid statistical test is highly unlikely to detect a difference between the groups.

Investigating the data prior to the 9/13 Event provides insight, but a key feature of trend analysis is that trends can change over time. This was observed and noted in the change point analysis where a shift in the mean of monthly maximum 24-h rainfall in excess 2.6 mm occurred. In many applications the most recent changes in a trend are the most valuable to understand. To this end, Figure 2.5, incorporates the full range of the data in attempt to learn about the most recent changes to the trend line.

The left plot in Figure 2.5 contains two smoothed time series: the time series prior to the 9/13 Event year (black), and the time series for the full data range (January 1898 to December 2014) (blue). Looking at that last decade, the blue trend line appears to significantly increase. This could be the result of another shift in the climate signal, as previously observed around November 1981, or the 9/13 Event could be an outlier pulling the trend higher than the true climate signal.

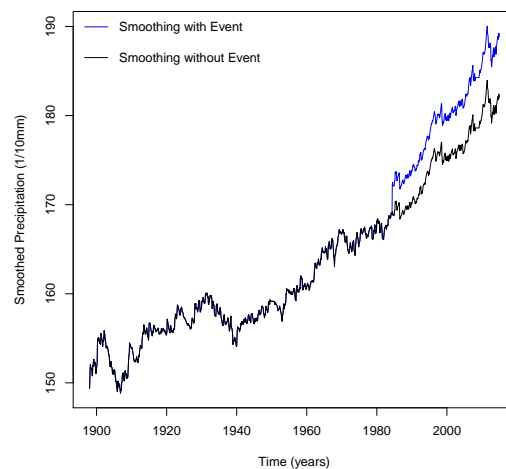


Figure 2.6: Smoothed time series for long term trend

The right plot focuses only on the last decade of the data (2004 to 2014). In order to help determine the effect of the 9/13 Event on the true climate signal a third time series

has been added (red). The new time series is a smoothed trend line (also 120 month window size) for the entire range of the data, however, the 9/13 Event itself has been omitted as an outlier. Examining the time series simultaneously, the conclusion is similar to what was shown in Figure 2.3: the 9/13 Event appears to be a clear outlier. The red time series in the right plot does show a slight increasing trend toward the end of data range (2010 to 2014), but nothing of the same magnitude as the data with the 9/13 Event included or the shift in the means around change point from 1981. Therefore, a change point detection will not be performed for 2007 and the 9/13 Event will continue to be removed as needed.

The final point to examine for the mean climate signal can be seen in Figure 2.6. The figure shows two time series; each smoothed with a window size of half the number of data points (702). Increasing the window size of the smoothing function reduces the noise in an attempt to expose the true trend line and change to maximum rainfall. The two lines in the plot show that regardless of the 9/13 Event, there is a long term increase in mean observed monthly 24-h maximum rainfall. The only notable impact the 9/13 Event has on the long term behavior of the trend line is a vertical shift; the behavior/pattern in the tail of the time series are essentially identical otherwise.

Based on the trend analysis for the behavior of mean maximum precipitation in Boulder, Colorado, from January 1898 to December 2014, there is evidence to support that mean maximum precipitation has primarily been increasing since the early 1900's. The rate of increase appears to be around 3 mm (or 0.12 in) over the last one hundred and fifteen years. Given that the data points are smoothed observed monthly 24-h maximum precipitation, an increase in the mean of these values indicates that larger amounts of rain are being observed in 24-h periods.

### 2.1.2 TREND ANALYSIS FOR BEHAVIOR OF VARIANCE

The context of the data makes the mean signal, which was examined in the previous section, more intuitive and interpretable, than the variance signal, when drawing conclusions.

In learning that the mean of the maximum values has increased, it is evident that the amount of rain seen in a 24-h period is also increasing. The variance tells a different, less intuitive, story unless further investigation is done. The variances can be inflated due to missingness during a time interval since less qualifying months would create a higher weight for larger observed values. The variances can also increase due to a higher amount of large 24-h monthly maximum rainfalls observed in a time interval, which is the desired explanation for an increase in variance. The most informative investigation for the behavior of variance over time would come from the original dataset and not from the monthly observed 24-h maximum rainfall investigated in this report.

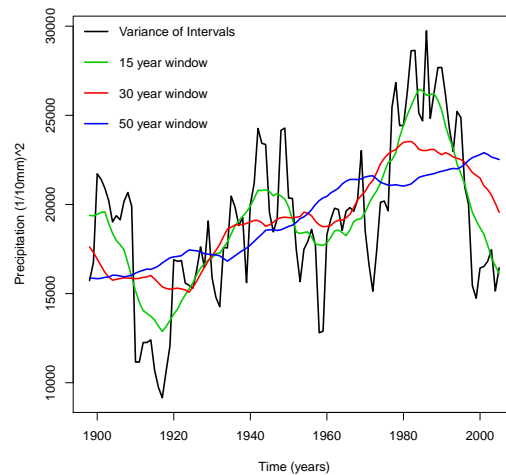


Figure 2.7: Observed variances and smoothed trend lines

With that in mind, Figure 2.7 depicts the aspects of the variance that will be focused on. First, the observed variances for each 10 year interval were plotted as the black line in the background. Without smoothing, it is difficult to determine if the observed variances have a constant mean over time or if the signal slightly increases over time. Focusing on the medium smoothing window used, 25 years (red line), it is a little clearer to see that the variance is increasing over time, yet has seemingly cyclical behavior that causes it to decrease after steady periods of increase. The largest smoothing window (blue line - half a century) exposes the true trend of the variance over time. The observed variances, if converted to

standard deviations (see Appendix Figure D.1), increase over time at an overall rate that is roughly the same as the observed increase in the mean signal - approximately 3 mm or 0.12 in.

### 2.1.3 SEASONAL EFFECT AND CLIMATE SIGNAL

The focus of the seasonal exploration is not on the traditional quarterly seasons (Fall, Winter, Spring, Summer), but on the months over time. The intent is to discover if any

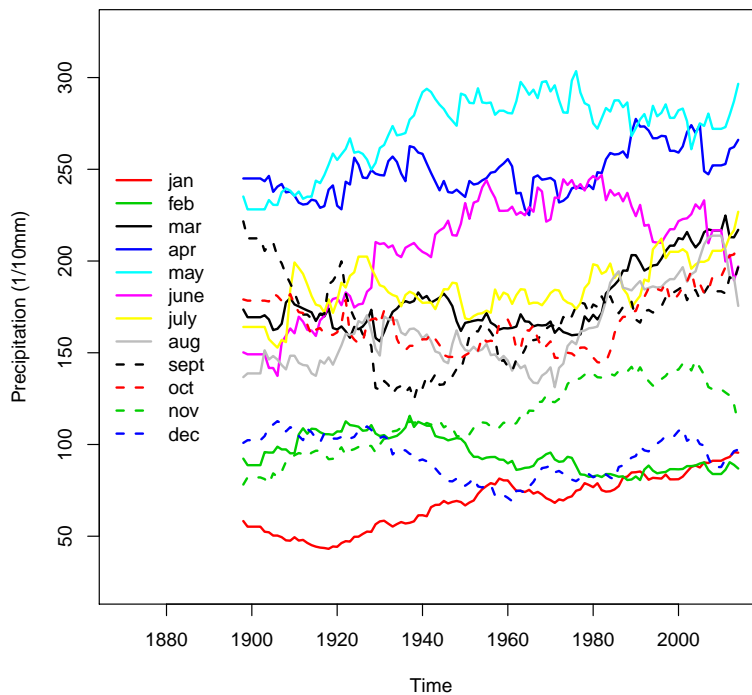


Figure 2.8: Seasonal time series (by month)

particular months have contributed to the observed change point, or if the observed shift in the smooth trend line can be attributed to increased rainfalls in some months (implying a decrease in rainfall for other months). Similar to the previous sections, where trend lines were utilized to understand the underlying behavior, the trend lines can be used to investigate trends for the individual months over time (see Figure 2.8). The plot shows that in general the behavior of the individual time series are within reason. There is some interesting

behavior among the months March (solid black line), June (solid purple line), and September (dotted black line). Note that March and September appear to behave opposite of June; in particular March and September appear to have sharp increases in their previously stable mean maximum rainfall around the change point.

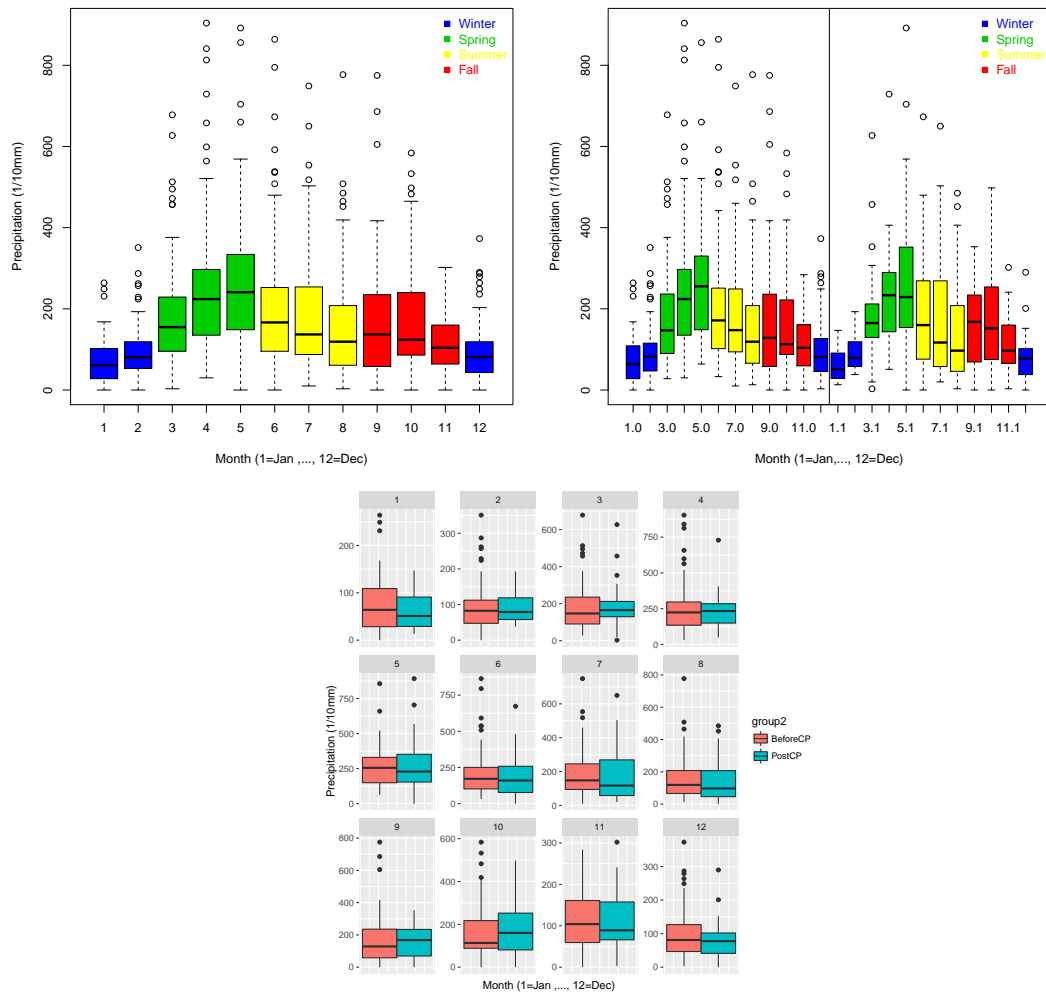


Figure 2.9: Left: Box plot of each month over the full range of the data (1898 to 2014), Right: Split into groups (before and post-change-point), Bottom: Each month by group

The box plot in Figure 2.9, page 18, provides a box for each month for the full time range of the data (i.e. panel one is a box plot for the data points January 1898, January 1899, ..., January 2013, January 2014). Practically speaking, there are observable differences in the behavior of the each month and of the quarterly seasons. For instance, the mean rainfall for



April and May appears higher than the other months, the highest observed rainfalls appear to occur only between April and September, and the Winter months appear to be, relatively, the driest time of the year. The highest observed rainfall in the winter months would not be considered outliers in the other months. Looking at the right plot, the variability observed during the mean Climate Signal EDA is visible in the before-change-point group. Focusing on the inner quartile ranges (not the outliers and whiskers) there does appear to be some shifts in the maximum rainfall behaviors. Post-change-point, rainfall in June appears fairly

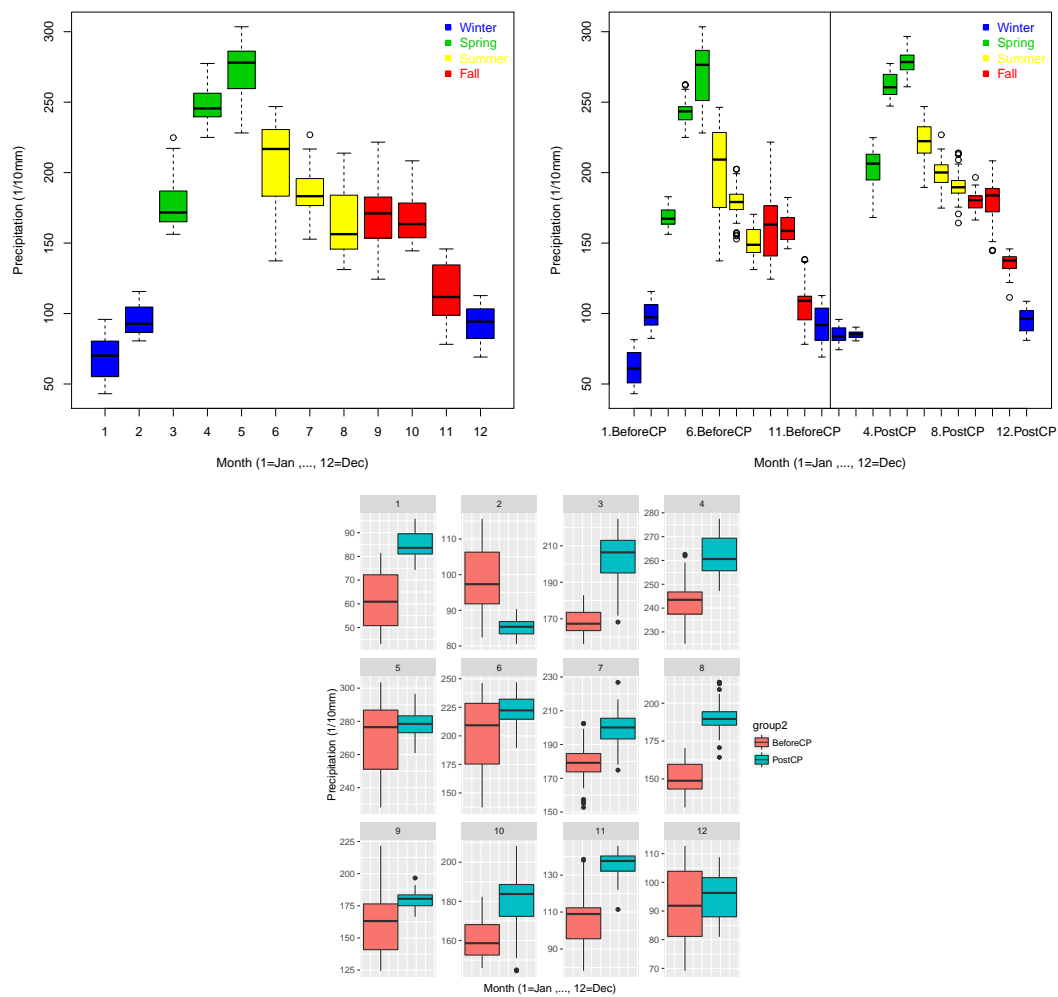


Figure 2.10: Left: Box plot for the smoothed values for each month over the full range of the data (1898 to 2014), Right: Split into groups (before and post-change-point), Bottom: Each month by group

consistent around the mean while rainfall in September appears more variable. Directly comparing the months in the bottom plot confirms the observed behavior in the right plot in which the inner quartile range of June has notably decreased and the inner quartile range has ballooned in September (after the change point).

The smoothed trend line values can also be used to generate box plots to further investigate the seasonal behavior pre and post-change-point. In Figure 2.10 the plots are provided in the same layout as Figure 2.9, but these plots were generated using the smoothed trend line data to gain insight about the underlying trends. The left plot in Figure 2.10 shows similar behavior to the left plot in Figure 2.9, but the underlying differences in the behavior of the months is more apparent. Splitting the smoothed data into pre-change-point and post-change-point leads to the right and bottom plots in 2.10. Focusing on the bottom plot, it appears the underlying signal for each month could differ pre and post-change-point. For instance, the average maximum 24-h rainfall for January, March, April, July, August, September, October, and November appears to have increased. Meanwhile, February shows a potential decrease, and the other months appear relatively stable. The information gained by looking at the individual months is that the observed 24-h maximum rainfall shows a steady increase over time - that increase is potentially explained by 8 of the 12 months. The implication is if 24-h maximum rainfall is increasing on average and that increase is not evenly spread across the months, then the peak rainfall observed in a 24-h period is arguably becoming more extreme.

#### 2.1.4 PROBABILITIES OF EXCEEDING SELECT RAINFALL THRESHOLDS OVER TIME FROM ESTIMATED DISTRIBUTIONS

This section focuses on understanding how the probabilities of exceeding certain rainfall thresholds have changed with the climate signal. It is important to note that while flooding and rainfall are often related, flooding can occur in the absence of rain. In the presence of rain, there are still several considerations as to whether or not floods will occur such as

the distribution of rain coverage (how evenly spread over an area the rainfall is)(Stewart 2010), and covariates that can be time dependent such as soil characteristics, vegetation cover (including forest density), slope, land use and urbanization, and seasonal effects like wildfire (Clark et al. 2014). Since the data in this investigation pertains to precipitation, the Urban Drainage and Flood Control District in Colorado was able to provide a table that relates the two for the area of interest (see Table 2.1). The table provides the rainfall values that will be examined here (1 in, 2 in, and 3 in), however, these values are guidelines intended for urban areas and change under conditions as described above (Stewart 2010)(Clark et al. 2014). The last row of the table states that the flood potential guidelines are for rainfalls observed within one hour. Since the data used are observed 24-h calendar day values, we cannot make direct statements about flood potential; however, we can look at the trend lines for the probability of exceeding the values for forecast rainfall within the 24-h calendar day. The significance here is days that do not exceed 1 in of rainfall in total did not exceed 1 in of rainfall within one hour.

Table 2.1: Table III-2 Urban Flash Flood Guidance from Urban Drainage and Flood Control District in Colorado

FORECAST RAINFALL	FLOOD POTENTIAL	RECOMMENDED ACTIONS
Total Amt less than 1.0 in	Streets, low-lying areas intersections	Prepare for routine nuisance
Total Amt = 1.0 to 2.0 in	All of the above plus small streams, bankfull	Prepare for flooding of frequent problem areas
Total Amt = 2.0 to 3.0 in	All of the above plus floodplain inundation	Prepare for street closures
Total Amt more than 3.0 in	Major overbank flooding expected	Prepare for floodplain evacuations
Note: Rainfall amounts and guidance information apply to short duration storms ( $\leq 1 - hour$ )	Note: refer to basin flood warning plans for site specific data	Note: use judgment on when to warn public, maintain contact with meteorologist

The Kolmogorov-Smirnov GoF test rejected a proportion of the distribution fits estimated using the maximum likelihood method as described in the introduction to Chapter 2 Climate

Signal EDA (see Appendix Table A.1). Due to the observed distributions of the data, it seemed best to utilize an alternative estimation method to see if the distributions that failed the testing could be retained (since the failed distributions looked similar to many distributions that did not fail - see Appendix Figure A.1 and note the gamma shape in the histograms). Each distribution estimated with the alternative method (also provided by the **fitdistrplus** package in R), Maximum Goodness-of-Fit with Anderson-Darling right-tailed distances (MGoF with ADR), passed the K-S GoF test (see Appendix Table A.1).

The MGoF estimation is performed using a random sample from a distribution function  $F(x; \theta)$ , where  $\theta$  is an unknown parameter. Let  $F_n(x)$  represent the empirical distribution function based on the data. If there exists a  $\hat{\theta} = \hat{\theta}(X_1, \dots, X_n)$  in  $R^k (k \geq 1)$ , such that

$$d[F(x; \hat{\theta}), F_n(x)] = \inf d[F(x, \theta), F_n(x)],$$

it is called a minimum distance estimate of  $\theta$ , where  $d[F(x; \hat{\theta}), F_n(x)]$  is any non-negative “distance” function that measures “how far apart” are the CDFs (Drossos and Philippou, 1980). The distance function used for the remainder of the probability related analyses is the Right-tail AD (ADR), which is defined as

$$\int_{-\infty}^{\infty} \frac{(F_n(x) - F(x))^2}{1 - F(x)} dx.$$

The distances are calculated using the form

$$\frac{n}{2} - 2 \sum_{i=1}^n F_i - \frac{1}{n} \sum_{i=1}^n (2i - 1) \ln(\bar{F}_{n+1-i}).$$

These distances put more weight on the right tail of the data when fitting the distribution, which makes the distribution fit robust against gaps in the histograms seen in Appendix Figure A.1. Examples of optimal and suboptimal fits that passed the K-S test can be found in Appendix Section A.1 (Figures A.2 and A.3). The fit plots show that even when the original test of the MLE parameter estimate failed, the estimate is still a decent fit of the data. The worst fits produced using MGoF-ADR were quite good (as determined by Figure A.2), which lends confidence to the accuracy of the trends detected for probabilities related to the rainfall thresholds.

The change in the parameter estimation method, and all estimates passing a statistical test of significance, enables the generation of full trend lines for the probabilities of interest (since the trend line is the primary focus of the analysis, not the individual probabilities themselves). The top left plot in Figure 2.11 shows the probabilities of meeting and/or exceeding

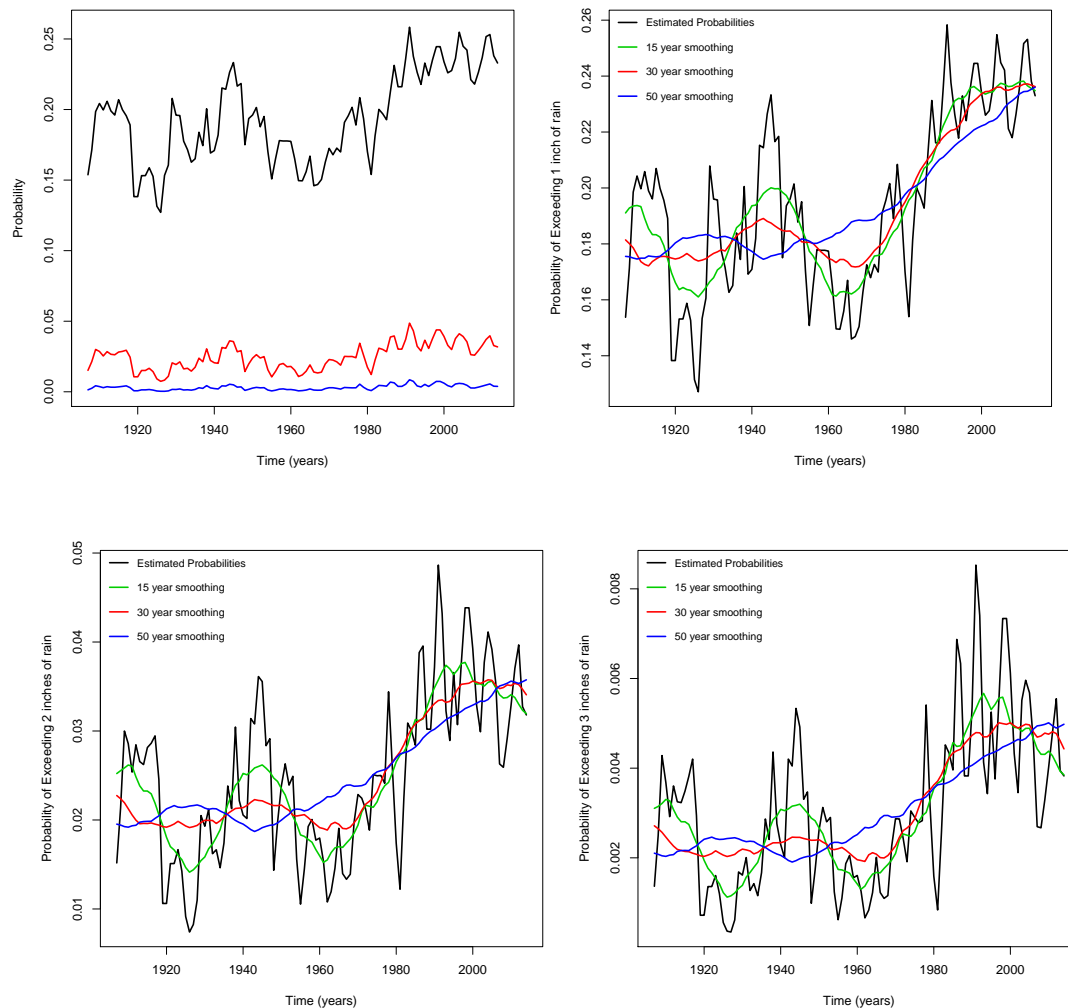


Figure 2.11: Top Left: All probabilities (meeting and/or exceeding 1 in, 2 in, or 3 in of rainfall), Top Right: Probability of meeting and/or exceeding 1 in of rainfall with smoothing lines, Bottom Left: Same with 2 in, Bottom Right: Same with 3 in

the rainfall levels of interest (1 in, 2 in, and 3 in). Looking at the probability of exceeding 1 in and 2 in (black and red lines, respectively) there appears to be a slight increase in the probability of these rainfall amounts since the change point (1981). The accompanying plots

in Figure 2.11 show the individual trend lines with smoothing to determine the underlying behavior of the probabilities over time. Starting with the top right plot, it is apparent that the probability of meeting and/or exceeding 1 in of rainfall has been increasing since the change point (all lines), and the 50 year smoothing line (blue) shows that the probabilities has been steadily increasing since the 1940s. The bottom plots show similar behavior with one exception: the most recent years show a slight decline in the probability of exceeding 2 and 3 in of rainfall in a 24-h calendar day (with the probability of exceeding 3 in of rainfall decreasing more dramatically than the probability of exceeding 2 in).

## 2.2 FORT COLLINS

The data for the city of Fort Collins ranges from January 1896 to December 2014. Fort Collins is 65 miles from Boulder, yet it does not have an outlier from the September 9, 2013 event. The greatest amount of rainfall observed in the data is 117.6 mm (approximately 4.63

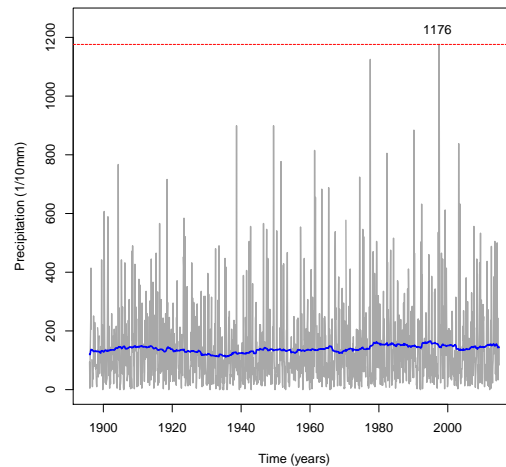


Figure 2.12: Observed monthly maximum 24-h rainfall for Fort Collins, Colorado 1896-2014 in), which was recorded in July 1997 (see Figure 2.12). If this point were to be treated as an outlier, the next highest peak, just prior to 1980, is reported as 112.5 mm (approximately 4.43 in). If both points were removed, the third and fourth highest peaks are 89.9 mm (approximately 3.54 in) recorded in September 1938 and June 1949. Unlike Boulder, where

it was of interest to investigate the possibility of a trend that could have indicated the 9/13 Event was approaching, we do not have an interest in the trends leading to the peaks observed in 1980 and 1997.

### 2.2.1 TREND ANALYSIS FOR BEHAVIOR OF MEAN

The overall behavior of the trend line for observed 24-h maximum rainfall for Fort Collins appears to be increasing over time (see black in Figure 2.13), however, it is not as obvious as the increase noted during the investigation of Boulder's rainfall trend. Looking at the 50

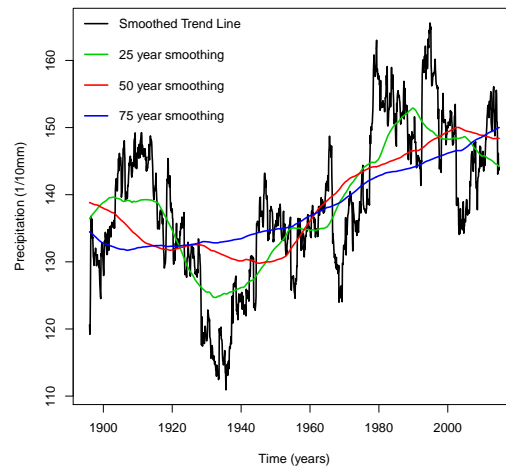


Figure 2.13: Centered moving average of 24-h observed maximum rainfall (black line) smoothed with 25 year window (green), 50 year window (red), 75 year window (blue)

year smoothed trend line, the increase in mean maximum rainfall seems to have a relatively constant rate of change from around 1940 to 2000. In the most recent years, there appears to be a decrease in mean maximum rainfall (as noted by the 25 year (green) and 50 year smoothing lines (red)). The data required a 75 year smoothing window to see that the mean maximum 24-h rainfall has steadily increased over time.

Similar to the trend line for maximum rainfall in Boulder, there is a statistically significant change point in the smooth trend line for Fort Collins (see Appendix B.1). The change point occurs in April of 1977 and, like Boulder, is an increase in the mean. The similarity of

the change points between Boulder and Fort Collins, juxtaposed with the difference in the rainfall received during the September 2013 event, is interesting. If there is a shift in the area's climate signal, we can attempt to identify the rainfall component as we move through the investigations of the remaining cities (Evergreen, Lakewood, and Greeley). Like Boulder, this change point in Fort Collins is an intuitive separator for the two groups (as noted by the vertical shift in the time series pre and post-change-point). It is difficult to fully understand the significance of the change point in the smoothed data; however, it is a visible positive shift in the mean of the maximum values. This means that more rain is recorded in 24-h calendar days, on average, than prior to 1977. Appendix Figure B.4 is provided as a reminder that these shifts and trends do not carry the same weight as a statistically significant difference between two groups when considering the full dataset.

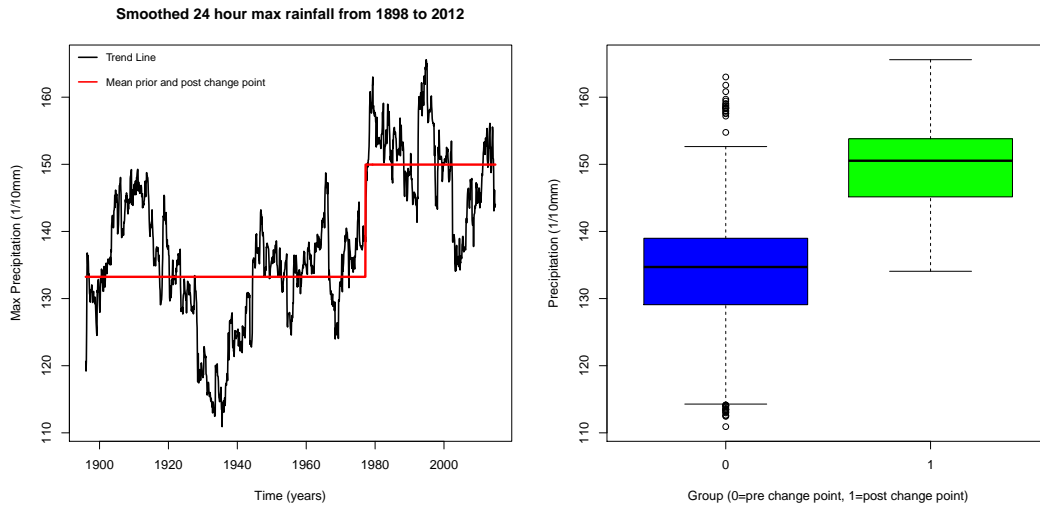


Figure 2.14: Centered moving average trend line for monthly observed 24-h maximum precipitation for 1896 to 2014 and group means (13.31 mm, 15.03 mm) from change point analysis (left); Box Plot for pre-change-point and post-change-point groups (right)

### 2.2.2 TREND ANALYSIS FOR BEHAVIOR OF VARIANCE

The variance for the intervals in Fort Collins have some interesting behaviors. Looking at Figure 2.15 it appears there are somewhat evenly spaced peaks throughout the entire time range. The width of the base of the peaks appears to be around 15 years, where the



base is considered to start at a low value, climb to the peak, then return to a low value. There are no statements that can be made about the peaks at this point, yet this pseudo

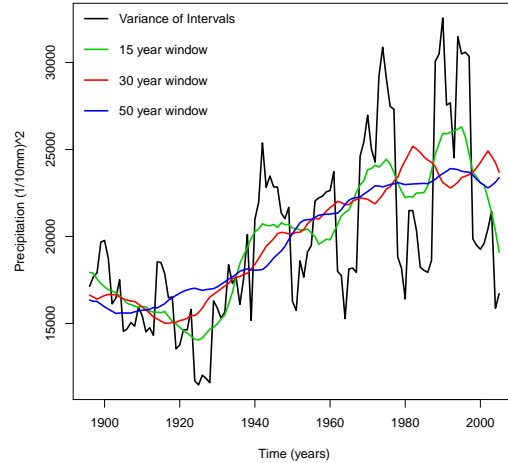


Figure 2.15: Observed variances smooth with window sizes of 15 year, 30 year, and 50 year

periodicity is present in several time series plots throughout the investigation. Overall, the variance appears to periodically increase since the 1920's. This results in an overall increase in the variance of observed 24-h maximum rainfall for Fort Collins (as noted by the 50 year smoothing window (blue line)). The smaller smoothing windows are more sensitive to the pseudo periodicity and show a decline in the variance of these maximum values over recent years. Based on the time series, we expect that the decrease will be followed by a sharp increase in the variance until it hits a peak point and starts to decrease (following the observed pattern throughout the time range).

### 2.2.3 SEASONAL EFFECT AND CLIMATE SIGNAL

The time series for the individual months (Figure 2.16) exhibit quite different behaviors. Months such as May and June show a decreasing trend since the 1960s while May, July, and August show an increasing trend since the 1940s. In recent years (since the 1980s), smoothed time series such as November, December, and January are relatively constant.

The observed 24-h maximum rainfall values are used to generate the plots in Figure 2.17. The left plot shows, similar to Boulder, the Winter months have much less extreme observed

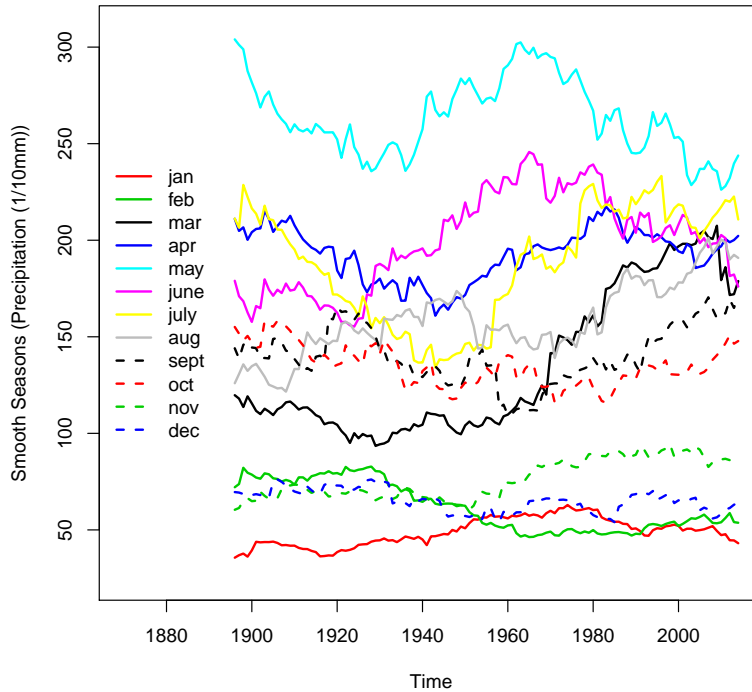


Figure 2.16: Seasonal time series (by month)

rainfall since the values are close to the means and the highest recorded rainfalls are in within the box and whiskers of most other seasons. The right plot shows the box plots for all of the values split into the pre and post-change-point groups. This plot shows that many of the previous peak rainfalls were pre-change-point; however, the highest observed rainfalls were both in July post the change point. It is not evident from the right plot that an increasing trend in mean observed 24-h maximum rainfall was identified during the investigation of the mean trend line. The bottom plot shows little difference between the pre and post-change-point groups by month. The full data box plots show much less information than the box plots based on the smooth data. Having addressed the full data box plots for Boulder and Fort Collins, the box plots will be referenced from the Appendix for subsequent analyses.

The smoothed trend line values from Figure 2.16 are used to generate the plots in Figure 2.18. The left plot shows that average 24-h maximum precipitation increases from January

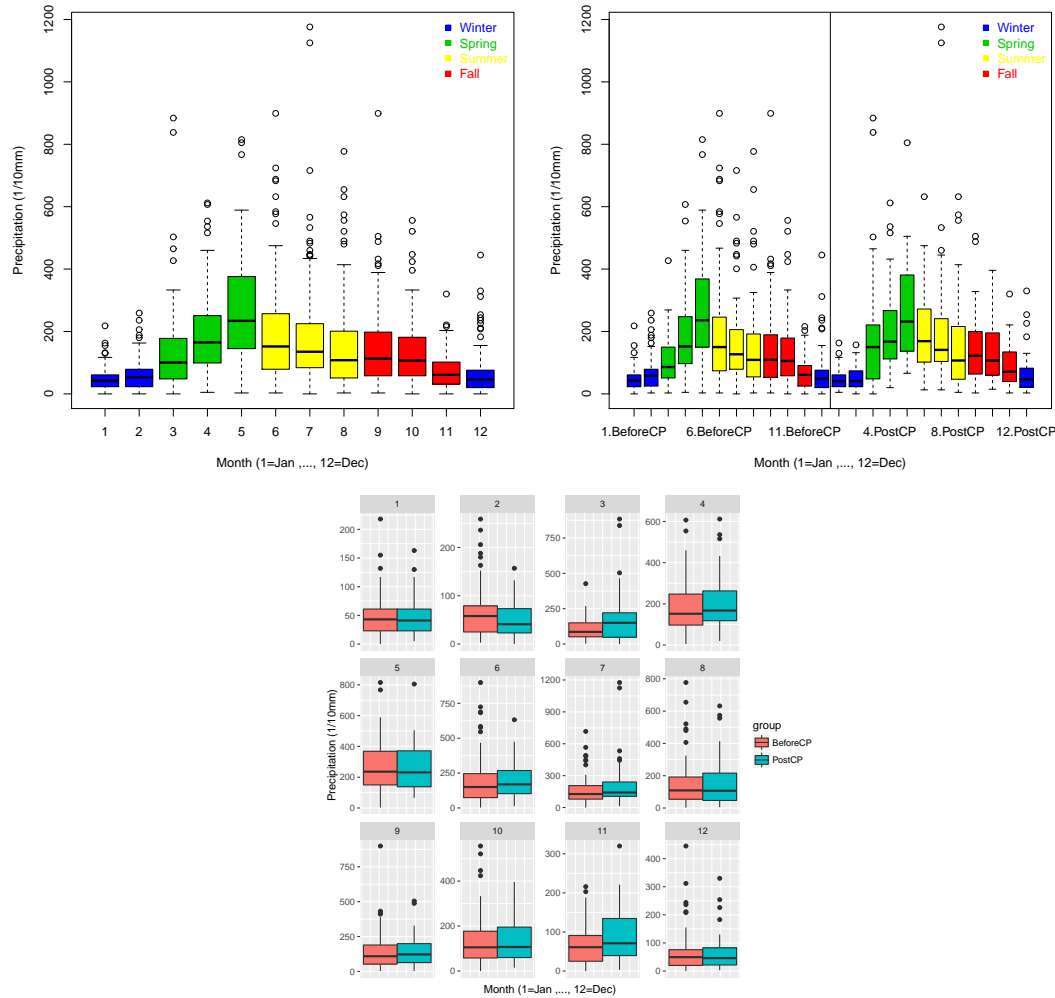


Figure 2.17: Left: Box plot of each month for full dataset (1896 to 2014), Right: Split into groups (before and post-change-point), Bottom: Each month by group

to May, then decreases from May to December. Looking at the right plot it appears that many months in the Spring and Summer have higher average maximum rainfall after the change point than before the change point, and that the smoothed values after the change point deviate much less from the means of their group (where the groups referred to this time are the months). The bottom plot helps tie the story together: here, it can be seen that the general increase in the mean trend line is most related to the increases in mean maximum

rainfall in March, April, July, August, and November, while months such as February and May show relatively large decreases in average maximum rainfall. Similar to Boulder, it appears that certain months are experiencing an increase in average maximum values, which could imply that rainfall is becoming more extreme in some months while rainfall in other months is becoming less extreme.

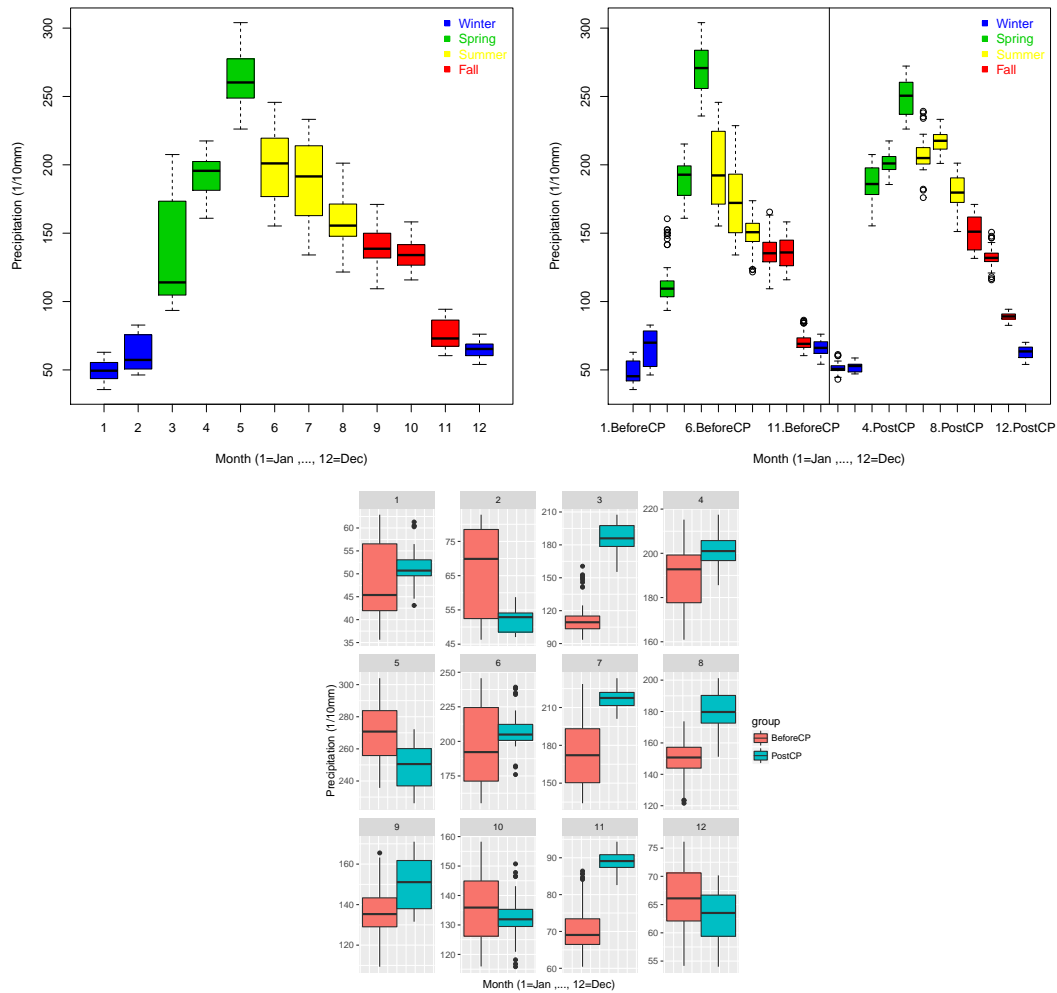


Figure 2.18: Left: Box plot of each month for smoothed data (1896 to 2014), Right: Split into groups (before and post-change-point), Bottom: Each month by group

## 2.2.4 PROBABILITIES OF EXCEEDING RAINFALL THRESHOLDS OVER TIME FROM ESTIMATED DISTRIBUTIONS

The top left plot in Figure 2.19 shows less obvious increases to the probability trend lines than the investigation of the rainfall thresholds for Boulder. Overall, each of the three time series (for meeting and/or exceeding 1 in (black), 2 in (red), and 3 in (blue) of rainfall) show a subtle increase in the probability of meeting and/or exceeding the rainfall thresholds. The 75 year smoothing window used in the top right plot (blue) confirms the long term

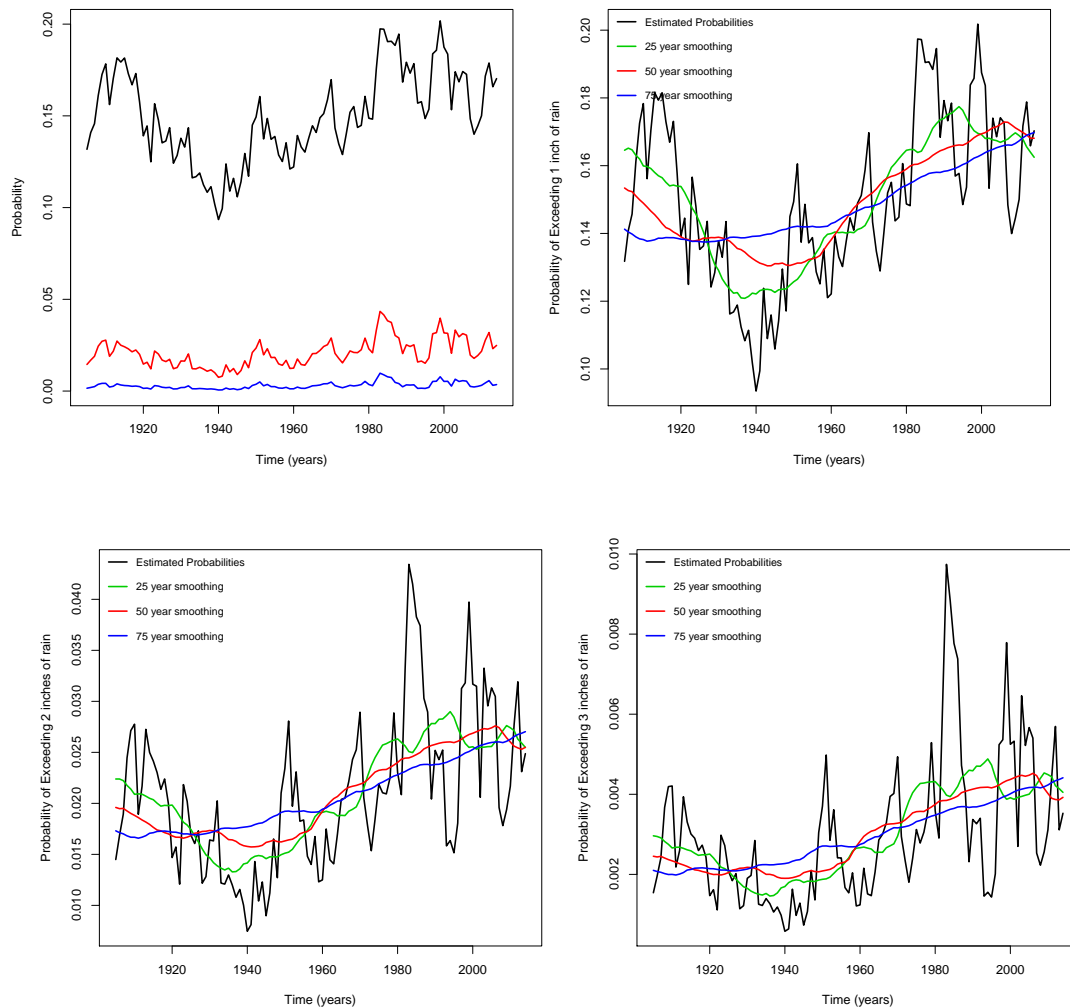


Figure 2.19: Top Left: All probabilities (meeting and/or exceeding 1 in, 2 in, or 3 in of rainfall), Top Right: Probability of meeting and/or exceeding 1 in of rainfall with smoothing lines, Bottom Left: Same with 2 in, Bottom Right: Same with 3 in

increase, however the 25 year smoothing window (green) shows a steady increase from the 1940s to 1990s followed by a recent decrease in the probability of meeting and/or exceeding 1 in of rainfall in a 24-h calendar day. The bottom left plot shows similar behavior, but required a larger smoothing window to expose the same underlying trends. The 50 year smoothing window (red) shows the relatively steady increase in the probability of meeting and/or exceeding 2 in of rainfall from the 1950s to the 2000s where a slight downward trend is currently occurring. Finally, the probability of exceeding 3 in of rainfall (bottom right plot) has been steadily increasing over time, yet in the most recent years (1980 to present) the probabilities appear to be much more variable. This behavior is also visible in the lower left plot. It appears the 24-h maximum rainfalls are becoming more extreme in recent years leading to an increase in the probability of subsequent maximums.

### 2.3 EVERGREEN

The data for the city of Evergreen ranges from January 1962 to December 2014. Evergreen is 40 miles south (in the semi-opposite direction from Fort Collins) from Boulder, yet it does

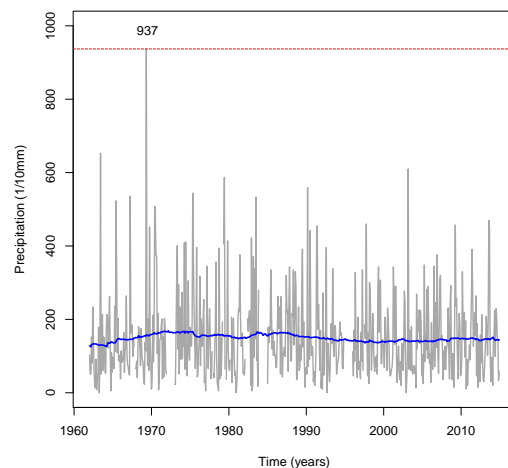


Figure 2.20: Observed monthly maximum 24-h rainfall for Evergreen, Colorado 1962-2014 not have an outlier from the September 9, 2013 event. The greatest amount of rainfall observed in the data is 93.7 mm (approximately 3.69 in), which was recorded in May 1969

(see Figure 2.20). If this point were to be treated as an outlier, the next highest peak, June 1960, is reported as 65.3 mm (approximately 2.57 in). From the initial time series Evergreen appears to have much lower maximum rainfalls and, as the data is defined, the city has not experienced any rainfalls on the magnitude of the potential outliers seen in the Boulder and Fort Collins investigations. Looking at the relative terrain in Figure 1.1, Evergreen is in the lower left of the plot behind the line delineating the national forest/mountain range. The Evergreen area is gray while the rest of the range/forest appears green/lush. The delineating line in the plot could indicate a barrier in which the flood plain regions to the east of the line experience more extreme rainfalls than the forest regions to the west.

### 2.3.1 TREND ANALYSIS FOR BEHAVIOR OF MEAN

The underlying signal for Evergreen shows a decrease in the smoothed trend line over time unlike the trend lines for Boulder and Fort Collins, which increased over time and

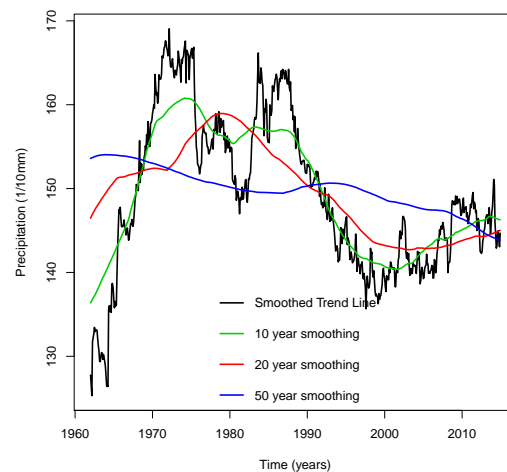


Figure 2.21: Centered moving average of 24-h observed maximum rainfall (black line) smoothed with s10 year window (green), 20 year window (red), 50 year window (blue)

showed prominent change points that were detectable by visual inspection or change point detection. Looking at Figure 2.21 the largest smoothing window (50 years - blue) shows a slow decreasing trend in the mean over time. The medium smoothing window (20 years -

red) shows a decline in the mean over time starting around 1980, but more interestingly the signal is relatively stable since 2000. The smallest smoothing window (10 years - green) confirms some behavior of the red line, which is helpful since the green line best parallels the mean trend line's behavior while still denoising the data to help expose certain trends. It also shows a slight increasing trend since 2000. Both of the smaller smoothing windows indicate that the long term decline in the mean trend does not appear to represent the most recent mean maximum rainfall trend in Evergreen.

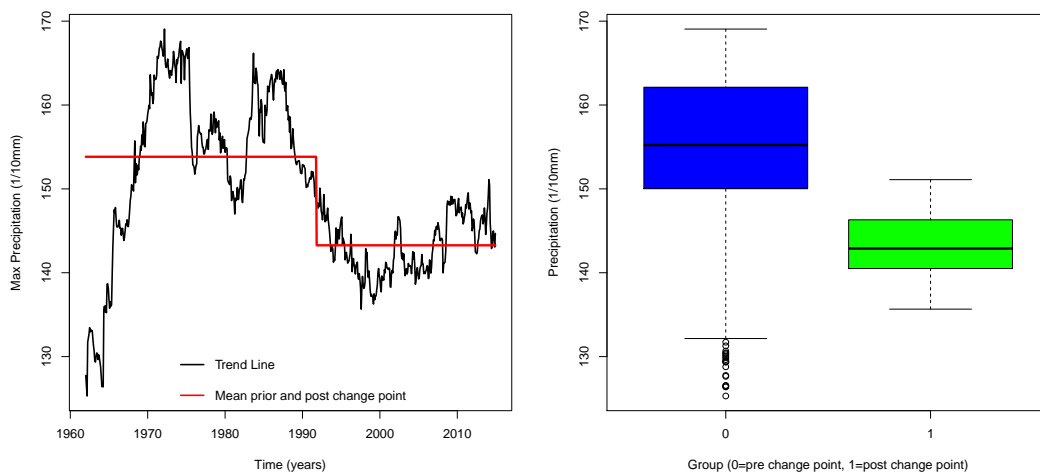


Figure 2.22: Centered moving average trend line for monthly observed 24-h maximum precipitation for 1962 to 2014 and group means (15.41 mm, 14.22 mm) from change point analysis (left); Box Plot for pre-change-point and post-change-point group (right)

A change point detection was performed even though the maximum rainfall trend line does not indicate the existence of an obvious change point (unlike Boulder and Fort Collins). The results for the change point test can be viewed in Appendix B.1. The left plot in Figure 2.22 shows the group means on either side of the change point plotted over the mean trend line. This change point is much less obvious than the two prior change points in which clear vertical shifts were present in the time series plots for the mean signal. The plot on the right shows the difference in means for the smoothed data groups and helps confirm the change point detected by the change point analysis. The box plot for the full data can be found in the Appendix as Figure B.6. The appendix figure clearly shows that a difference in the



original data would not be statistically significant, however, the trend line data does indicate a difference.

### 2.3.2 TREND ANALYSIS FOR BEHAVIOR OF VARIANCE

The variance of the observed distributions has been steadily declining for the full range of the data. Figure 2.23 confirms that regardless of the smoothing window size used, the observed variance decreases over time. The smallest smoothing window (15 years - green line) does show a slight stabilization of the variances since the 1990s.

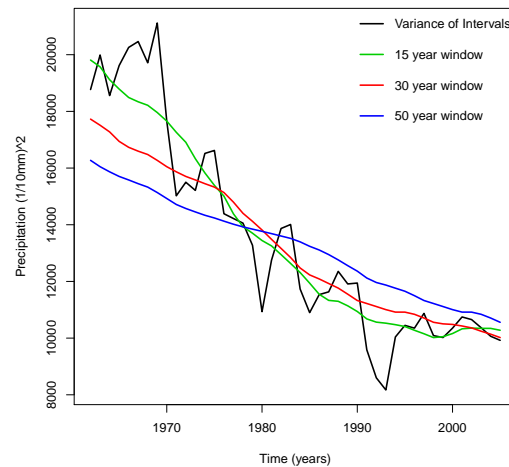


Figure 2.23: Observed variances with smoothed trend lines

### 2.3.3 SEASONAL EFFECT AND CLIMATE SIGNAL

The decreasing trends in the previous sections could indicate the time series for the individual months are all decreasing as well. Figure 2.24 shows that this is not the case. Many of the months have had stable mean rainfall or experienced slight increases over time. The decrease in the mean signal appears to be associated with sharp decreases in mean maximum rainfall for the months of May, June, and November.

The box plot on the left in Figure 2.25 shows a greater contrast among the months than the previous box plots for Boulder and Fort Collins (where the variability is much lower in

this plot than the others). The smaller boxes and lower perceived variability is due to the smoothing used for the mean trend line in the seasonal effect section. The smoothing uses a

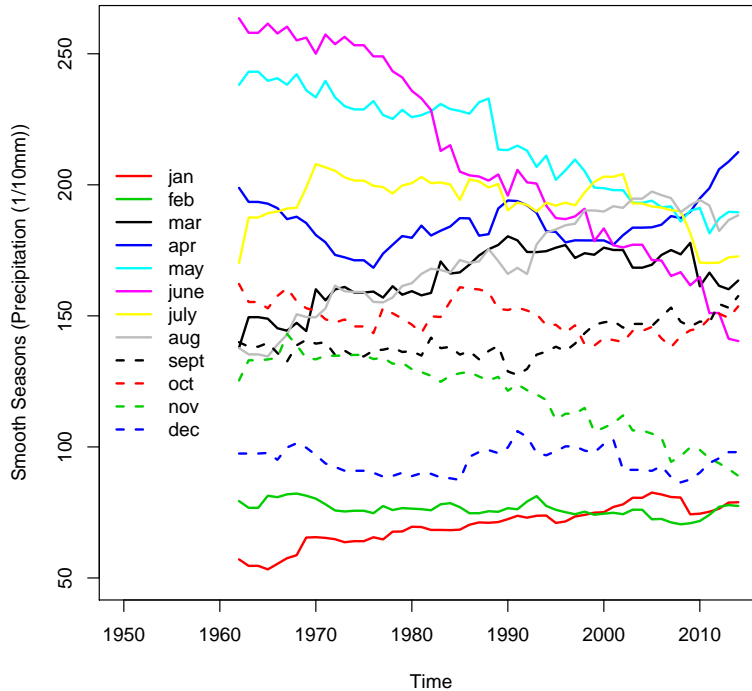


Figure 2.24: Seasonal time series (by month)

40 year window for all the weather stations regardless of the amount of data available from the weather station. This leads to smaller boxes with values clustered around the means for Lakewood and Evergreen - as compared to the weather stations with data as far back as the 1890's (Boulder, Fort Collins, and Greeley).

The right plot in Figure 2.25 shows some interesting behaviors between the pre and post-change-point groups. It appears months like June and November have far greater variability in the smoothed data, and that the peak Spring and Summer month's values, which were higher than the rest in the left plot, have decreased to a point where all the Spring and Summer months post-change-point are relatively similar. Looking at the comparisons of the individual months in the bottom plot confirms some of the sharp decreases in mean values for May, June, and November in Figure 2.24, but adds the information that the decline happens

post-change-point. It also shows increases in mean maximum rainfall for January, March, and August beyond the change point.

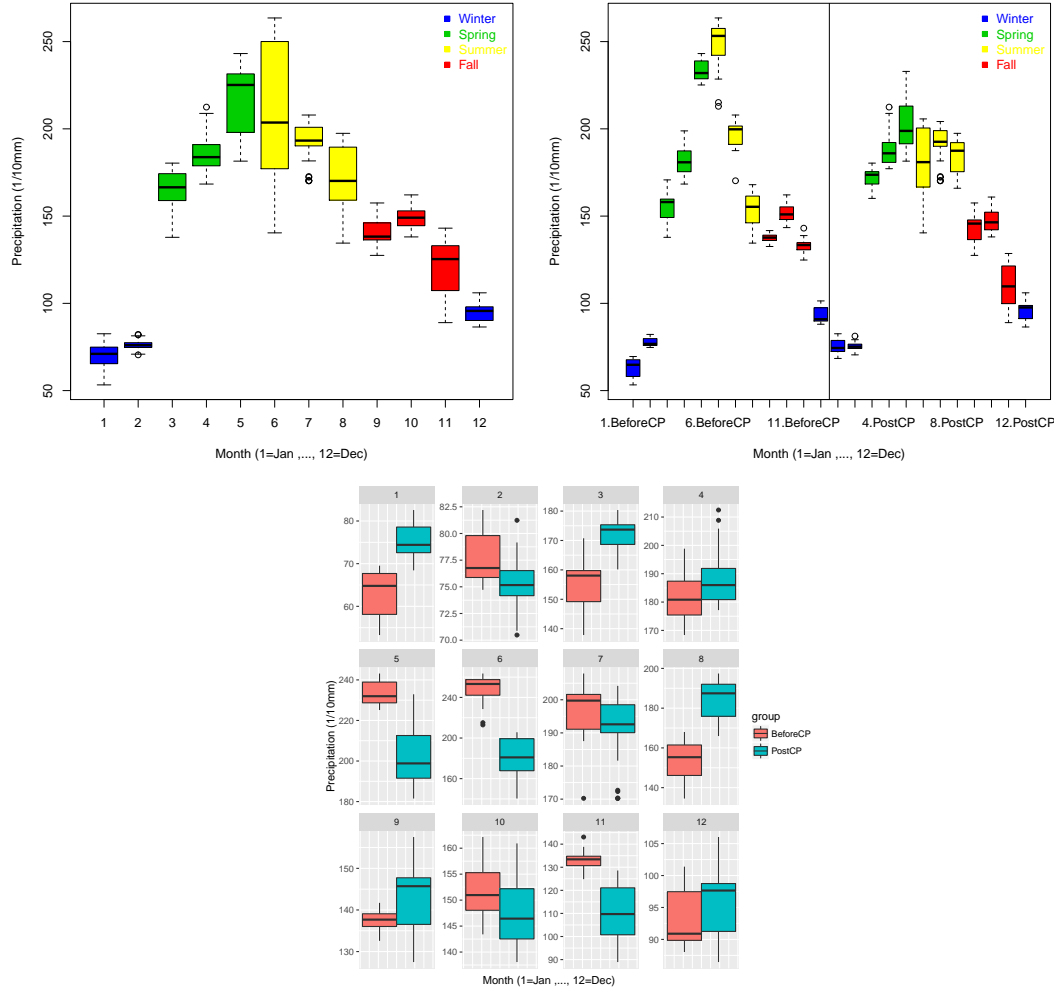


Figure 2.25: Left: Box plot of each month for smoothed data (1962 to 2014), Right: Split into groups (before and post-change-point), Bottom: Each month by group

### 2.3.4 PROBABILITIES OF EXCEEDING RAINFALL THRESHOLDS OVER TIME FROM ESTIMATED DISTRIBUTIONS

The top left plot in Figure 2.26 shows the shape of the probability plots are similar to that of the mean and variance plots (as expected due to the declines in both values over time). The individual rainfall threshold plots show the same long term behavior (each blue line) in

which the probability of meeting and/or exceeding the rainfall threshold has been decreasing over time. Focusing on the top right plot (which is the probability of recording at least 1 in

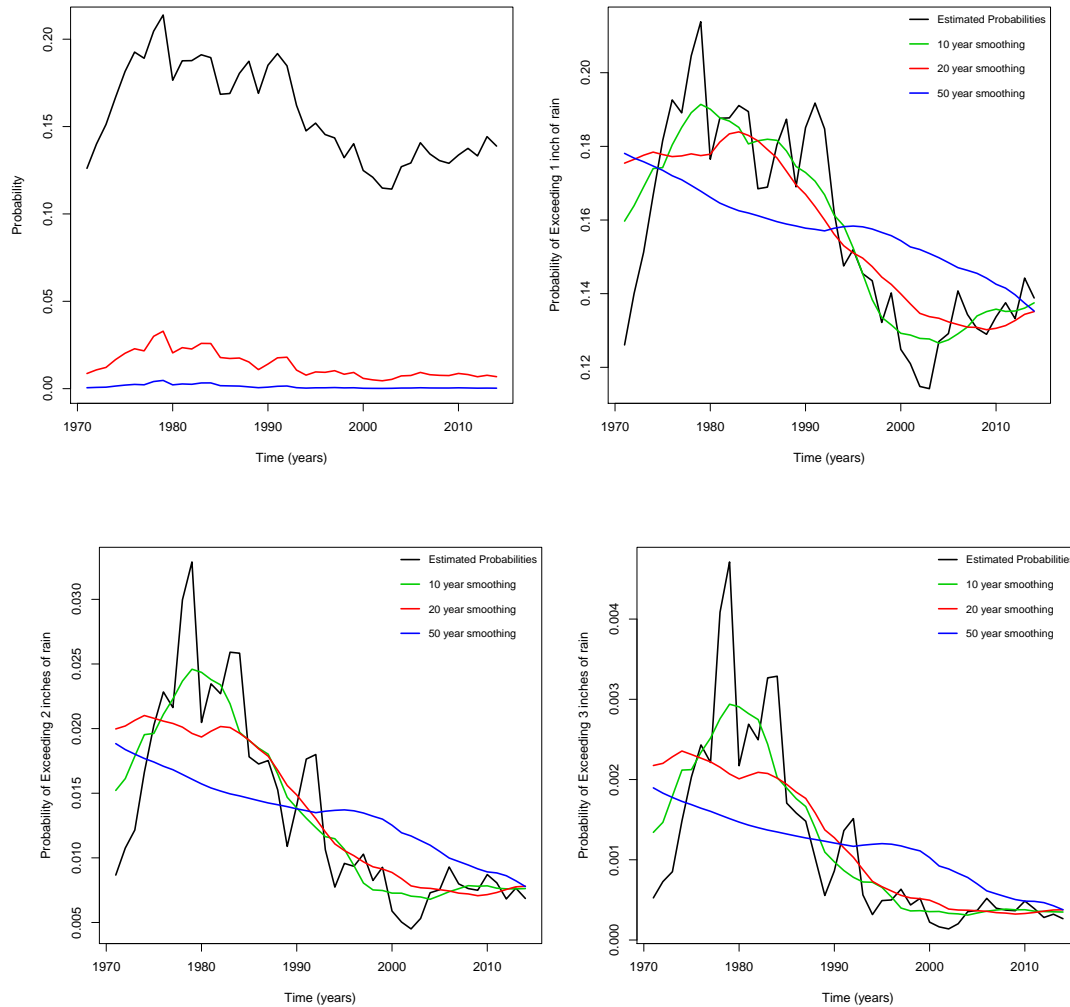


Figure 2.26: Top Left: All probabilities (meeting and/or exceeding 1 in, 2 in, or 3 in of rainfall), Top Right: Probability of meeting and/or exceeding 1 in of rainfall with smoothing lines, Bottom Left: Same with 2 in, Bottom Right: Same with 3 in

of rainfall in a 24-h calendar day at least once in a month) the smaller smoothing windows (red and green) show that in the most recent years, mid 2000's to 2014, the probabilities have stabilized, or increased, counteracting the steady decrease in the estimated probabilities since approximately 15 years prior. The bottom left plot shows the same behavior, but the recent years show more of stable/relatively constant trend than a possible increasing trend

(as seen by a flattening of the red and green lines). Lastly, the bottom right plot shows a stable probability for at least 3 in of rainfall being recorded in a 24-h calendar day for the last 20 years.

## 2.4 LAKEWOOD

The data for the city of Lakewood ranges from January 1963 to December 2014. Lakewood is 34 miles from Boulder, yet it does not have an outlier from the September 9, 2013 event. The greatest amount of rainfall observed in the data is 88.9 mm (approximately 3.5 in), which was recorded in March 2003 (see Figure 2.27). If this point were to be treated as an outlier, the next highest peak, October 1984, is reported as 74.4 mm (approximately 2.93 in). From the initial time series Lakewood appears to have an increasing mean maximum rainfall over time (blue line), similar to Boulder and Fort Collins - even though it is the closest city (in miles) to Evergreen.

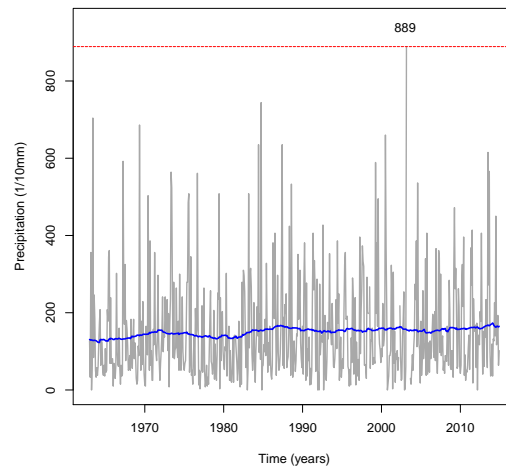


Figure 2.27: Observed monthly maximum 24-h rainfall for Lakewood, Colorado 1963-2014

### 2.4.1 TREND ANALYSIS FOR BEHAVIOR OF MEAN

The trend lines in Figure 2.28 confirm that the mean signal appears to increase over time. Now, the rainfall trends among the three cities investigated so far (Boulder, Fort Collins,

and Lakewood), not in the national park area, have shown similar increasing trends. It is clear in the plot that there is a change point in the climate signal, around the time of the previous two change points (not including Evergreen). The behavior of the mean signal for

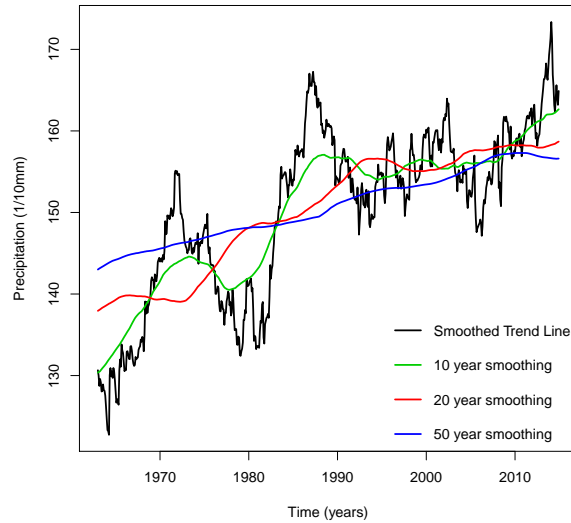


Figure 2.28: Centered moving average of 24-h observed maximum rainfall (black line) smoothed with 10 year window (green), 20 year window (red), 50 year window (blue)

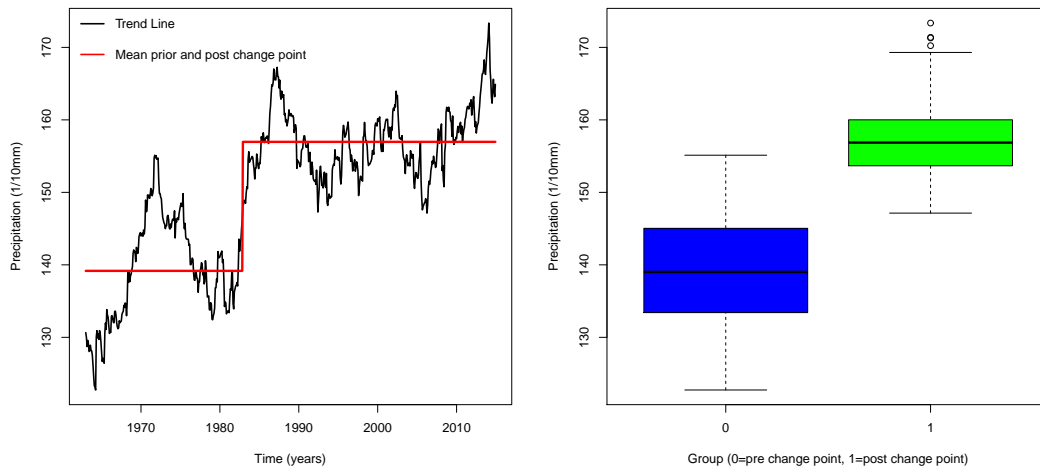


Figure 2.29: Centered moving average trend line for monthly observed 24-h maximum precipitation for 1963 to 2014 and group means (13.58 mm, 15.87 mm) from change point analysis (left); Box Plot for pre and post-change-point groups (right)

Lakewood is similar to the mean signal for Boulder such that after a certain point the mean appears relatively stable for a period of time. Another similarity between the two signals is the peak in the last couple years of the data.

The change point analysis determined the location of the change point is November 1982 (see Appendix B.1). The plots in Figure 2.29 show the difference in the means of the pre and post-change-point groups. Looking at the left plot, the vertical shift in the early 1980s is very similar to Boulder in both the point in time they occur and magnitude ( $\sim 2.7$  mm for Boulder vs.  $\sim 2.3$  mm for Lakewood). Fort Collins did exhibit relatively similar behavior as well; however, the greater similarity between Lakewood and Boulder could be due to closer proximity of the two cities (which possibly means greater geographically similar features as well).

#### 2.4.2 TREND ANALYSIS FOR BEHAVIOR OF VARIANCE

The behavior of the observed variances for Lakewood also mirror the behavior of the variances observed for the time intervals in Boulder (see Figure 2.30) such that there appear

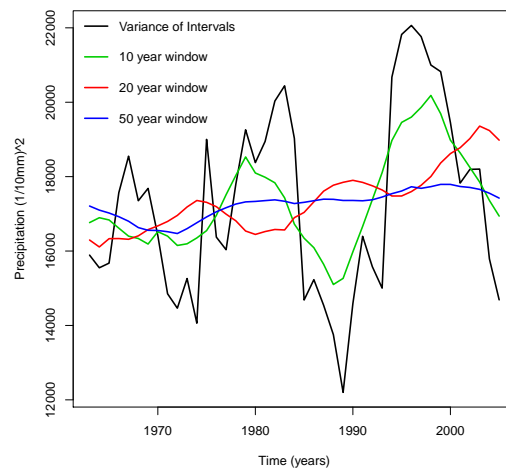


Figure 2.30: Observed variances smooth with window sizes of 10 year, 20 year, and 50 year

to be distinct peaks in which the variances consistently climb to a point then decrease as sharply as they rose. Unfortunately, the range of the data for Lakewood is much shorter

than Boulder (starting in 1963 vs. 1898), so only three peaks of this pseudo periodicity are observed. The long term smoothing window (50 years - blue line) shows a subtle increase in the variance over time, but the green smoothing window is of the most consequence here since the behavior of the observed variances appears to be so extreme. Based on the pseudo periodicity present in the observed data we would expect a continued decrease in the observed variances until a low point is reached, then a sharp increase for approximately 10 years - assuming the recent trends will hold over the next 12-20 years.

### 2.4.3 SEASONAL EFFECT AND CLIMATE SIGNAL

The full time series plot, Figure 2.31, shows a sharp decline in the mean trend with the greatest precipitation (June - purple) while several signals are increasing (March, April, July, and August), and the remaining are relatively constant.

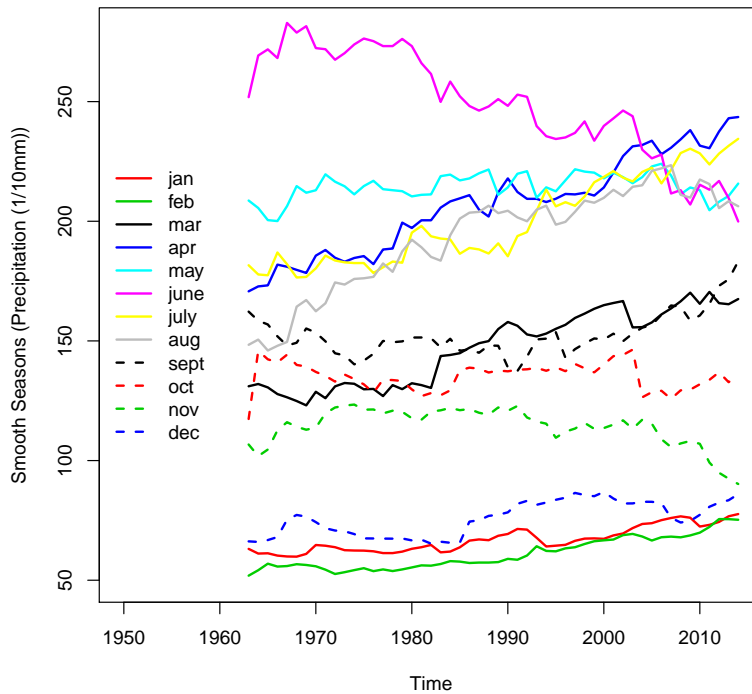


Figure 2.31: Seasonal time series (by month)



The box plots for the smooth trend lines shows the similar behavior to what has been seen throughout the report (see Figure 2.32). The separation due to the change point in the right plot shows similar behavior to the same plot in the Evergreen investigation in which the Spring and Summer months have comparable mean rainfall after the change point (even

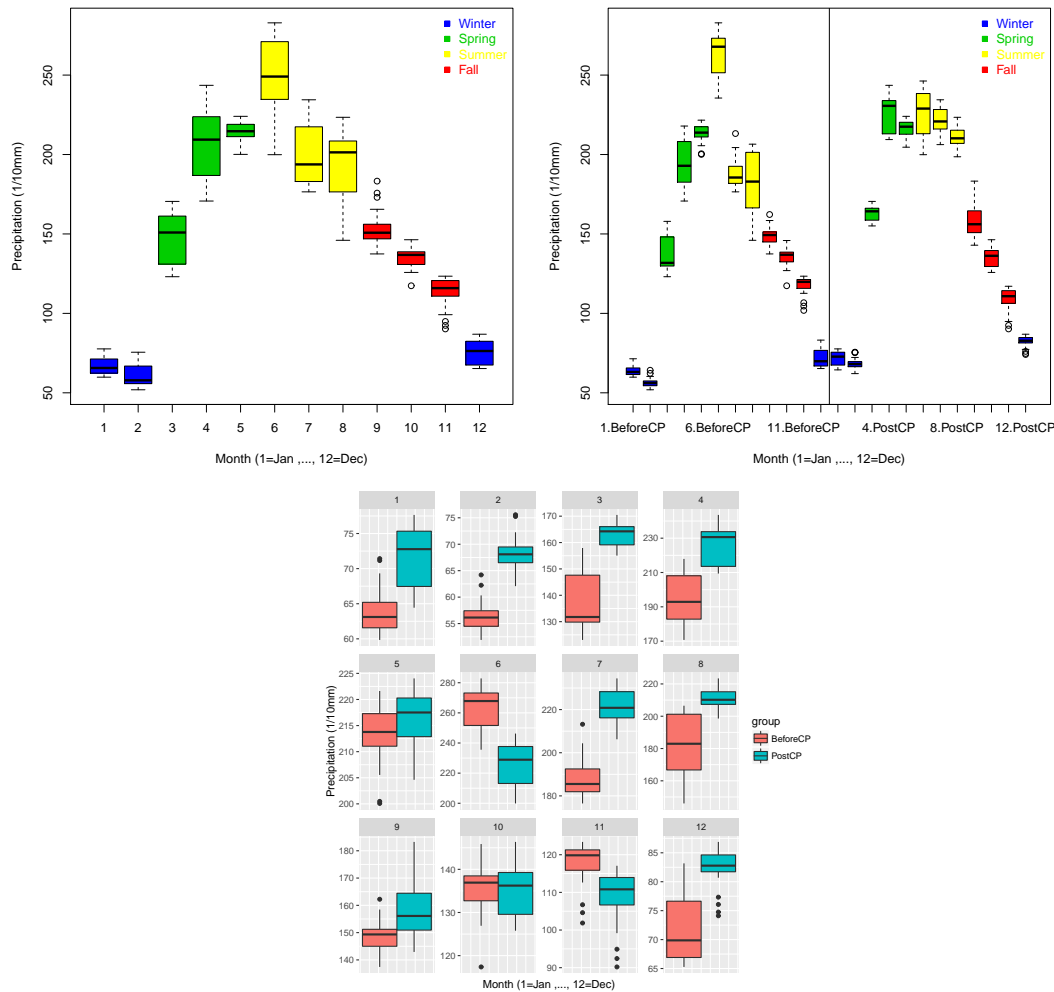


Figure 2.32: Left: Box plot of each month for smoothed data (1963 to 2014), Right: Split into groups (before and post-change-point), Bottom: Each month by group

though Lakewood's climate signal is much closer to Boulder's). Looking at the bottom plot, the box plots add the change point information to the trends noted in Figure 2.31, which shows that June does have an unexpectedly lower mean for the post-change-point group

while several other months have increased means for the post-change-point group (such as January, February, March, July, and December).

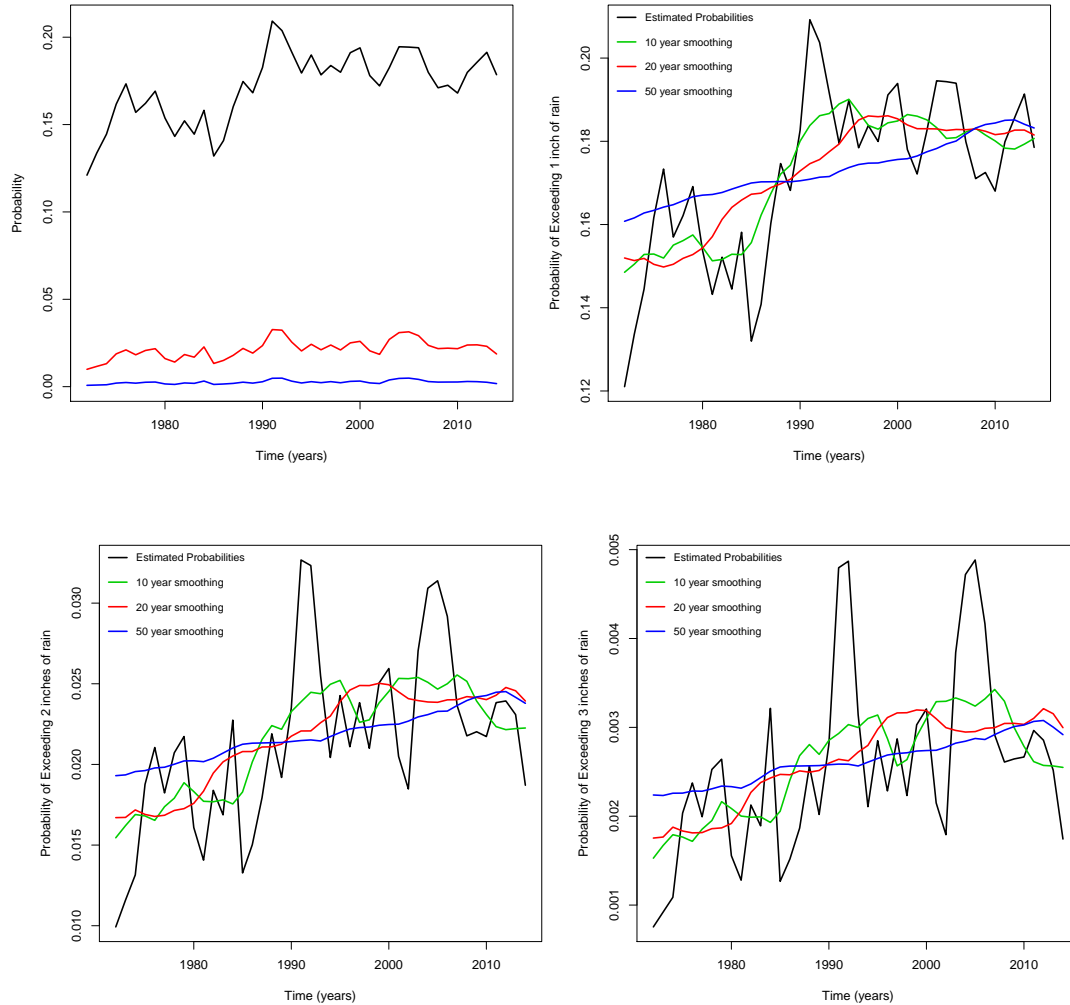


Figure 2.33: Top Left: All probabilities (meeting and/or exceeding 1 in, 2 in, or 3 in of rainfall), Top Right: Probability of meeting and/or exceeding 1 in of rainfall with smoothing lines, Bottom Left: Same with 2 in, Bottom Right: Same with 3 in

#### 2.4.4 PROBABILITIES OF EXCEEDING RAINFALL THRESHOLDS OVER TIME FROM ESTIMATED DISTRIBUTIONS

The top left plot of Figure 2.33 (which is the probability of recording at least 1 in of rain in a 24-h calendar day during a qualifying month) is similar to the mean maximum rainfall

trend line. The probability signal, while increasing over the full range of the data (blue line), appears to be relatively stable over the last 20 years (red) (or subtly decreasing - green). The bottom plots show extremely similar behavior. Both the probability of at least 2 in and 3 in of precipitation are increasing over time. The medium size smoothing window (red) shows a relatively stable probability of meeting and/exceeding these rainfall thresholds since around 2000, yet the observed data and the smallest smoothing window show a decrease in those probabilities over the last five years of the data. Due to the observed variance in the bottom plots, the green smoothing line provides better information since the peaks and valleys are so extreme. If the previous trends hold, there should be an increase in the probabilities of seeing at least 2 and 3 in of rain shortly after 2014.

## 2.5 GREELEY

The data for the city of Greeley ranges from January 1893 to December 2014, making it the weather station with the greatest time range of data available. Greeley is 64 miles from Boulder, and it does not have an outlier from the September 9, 2013 event. The greatest

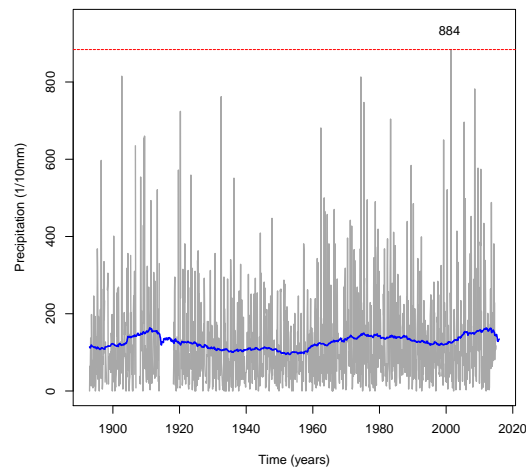


Figure 2.34: Observed monthly maximum 24-h rainfall for Greeley, Colorado 1893-2014

amount of rainfall observed in the data is 88.4 mm (approximately 3.48 in), which was recorded in July 2001 (see Figure 2.34). If this point were to be treated as an outlier, the

next highest peak, September 1902, is reported as 74.4 mm (approximately 3.21 in). The figure shows a large chunk of data missing before 1920, which will have a marginal affect on the overall trend, and is outside the range of the largest smoothing window considering when looking at recent trends (which is a 75 year window). The most recent points affected by the missing data will be in the mid 1950s.

### 2.5.1 TREND ANALYSIS FOR BEHAVIOR OF MEAN

The mean signal for Greeley is the most variable throughout the range of the data (see Figure 2.35). The overall trend of the data (blue line) appears to show an increase over time, but given the missingness in the data, and the length of time available it is best to focus on a practical time range. The plot shows that if we consider from the 1950s on, then all 3 levels of smoothing show that the mean signal has been increasing over the last 60 or so years. The smoothed trend line for the observed data does show a severe drop at the end of data (2014), however, this is such a short time period that the most sensitive smoothing window (25 years - green) was seemingly unaffected by the down turn.

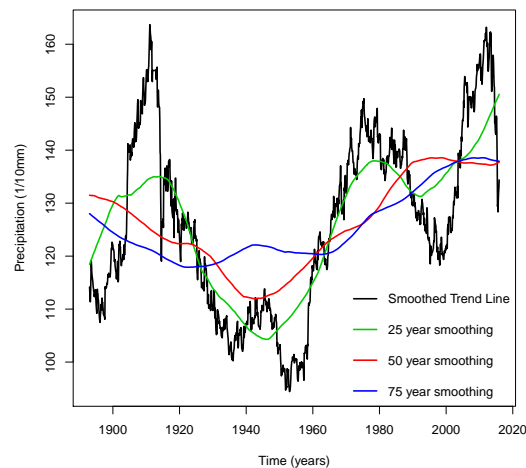


Figure 2.35: Centered moving average of 24-h observed maximum rainfall (black line) smoothed with 25 year window (green), 50 year window (red), 75 year window (blue)

An obvious change point does not appear in Figure 2.35 because it is challenging to visually assess the impact of the variability on the mean signal before 1960 and after. A change point analysis was performed (see Appendix for Change Point Detection) that determined December 1965 is a statistically significant change point. This change point happens before all of the previously presented change points, and at the beginning of the data range for Lakewood and Evergreen. The change point and the box plot for the groups it creates are in Figure 2.36. The left plot shows that the data before 1960 does confound the change point since the peak that occurs between 1900 and 1920 shifts the change point to the right of where it would be in the absence of the peak. The box plot on the right shows that the magnitude of the difference in the smoothed means is higher than suspected ( $\sim 2$  mm).

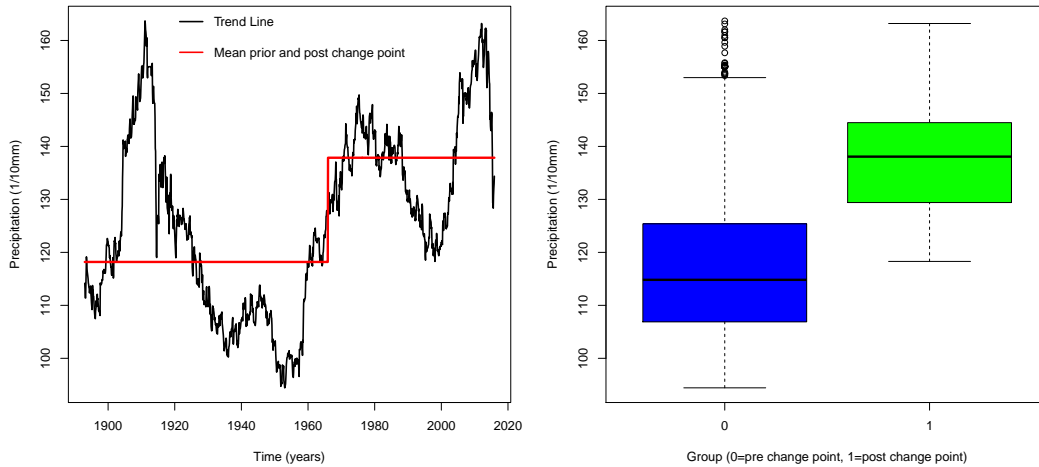


Figure 2.36: Centered moving average trend line for monthly observed 24-h maximum precipitation for 1963 to 2014 and group means (11.67 mm, 13.66 mm) from change point analysis (left); Box Plot for pre-change-point and post-change-point group (right)

### 2.5.2 TREND ANALYSIS FOR BEHAVIOR OF VARIANCE

The observed variances are equally challenging when it comes to assessing the long term change in the variance of the observed distributions. Overall, it appears the variance has roughly the same average value from the beginning of the time range to the end. The overall information also does not help understand this signal since a lack of change in the variance

over the time range does not accurately express how the data varies throughout the time range. The relevant information is there appears to be an increasing trend in the observed

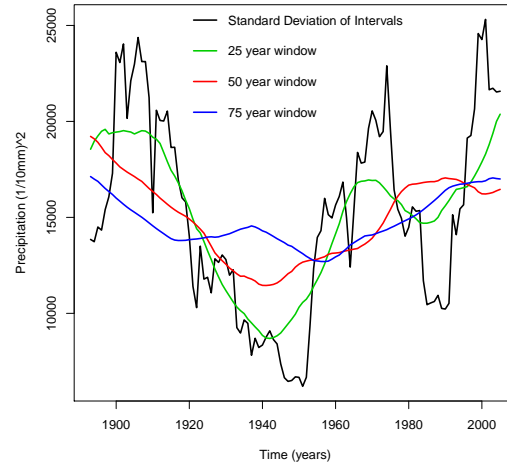


Figure 2.37: Observed variances smooth with window sizes of 10 year, 20 year, and 50 year

variance since the 1950s, and the variance reached its highest peak just before the end of the data set (after 2010), which could indicate the long term increasing trend will hold.

### 2.5.3 SEASONAL EFFECT AND CLIMATE SIGNAL

The individual time series for the months in Figure 2.38 show that the months with higher values of precipitation have similar behavior to the mean maximum trend line. Given the similarities between the mean trend lines for the individual months and the mean maximum trend line, the only month that stands out is August, which over doubles in mean value from the starting point (1893) to the ending point (2014).

The right plot in Figure 2.39 shows some relatively similar behavior between the pre and post-change-point data (which is atypical behavior for this report). The similarities are related to the quadratic (bowl) shape present in the mean maximum trend line. As observed in Figure 2.38, August appears to be quite different pre and post-change-point. The bottom plot shows a slightly more balanced comparison of the months than the previous weather stations, such as the increases in June and November and the decreases in February and

December. The lack of change in the variance for the entire time range is best reflected in the right plot and Figure 2.37.

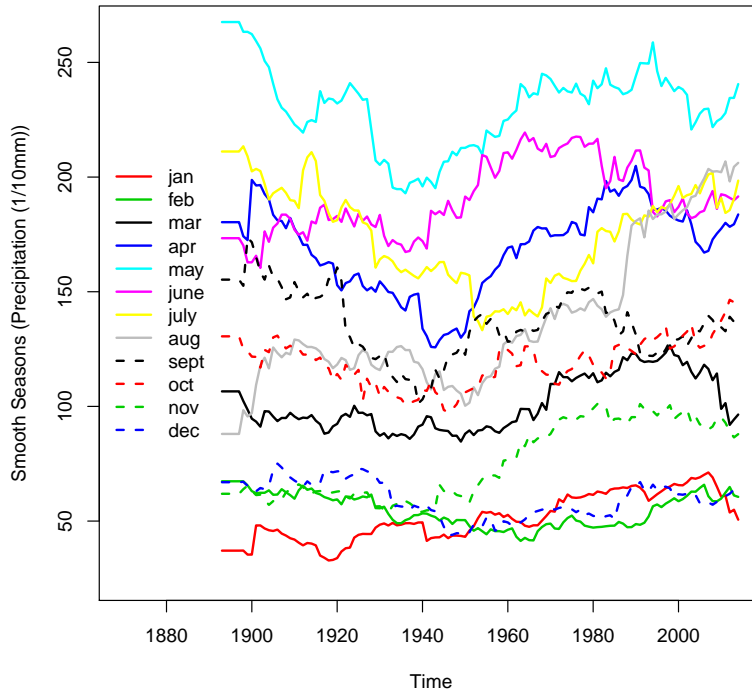


Figure 2.38: Seasonal time series (by month)

#### 2.5.4 PROBABILITIES OF EXCEEDING RAINFALL THRESHOLDS OVER TIME FROM ESTIMATED DISTRIBUTIONS

The top right plot in Figure 2.40 shows that the probability of at least 1 in of rain being recorded for a calendar day in a qualifying month is close to constant on average. Observing the variability in the plot shows that the overall change in the probability is not practically informative for understanding recent rainfall trends. Focusing on the lines generated from the 25 and 50 year smoothing windows it appears the probability of meeting and/or exceeding the 1 in rain threshold had increased since the 1950s to about the 1990s where the signal appears comparable to the average probability estimated over the first couple decades of the data. The tail end of the data shows a large increase in the probabilities for meeting

and/or exceeding all three rainfall thresholds. The probability time series for the both the probabilities of at least 2 in and 3 in of rainfall exhibit almost identical behavior. Both time

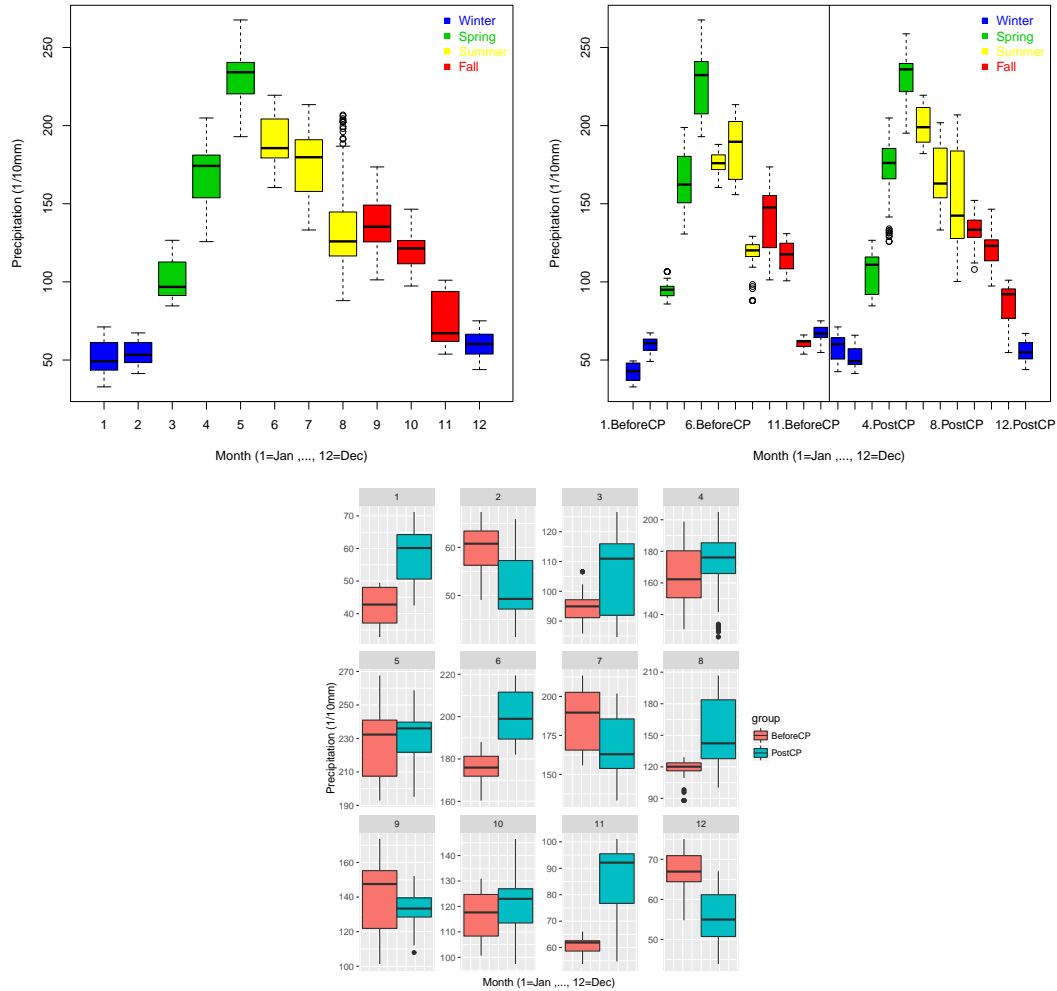


Figure 2.39: Left: Box plot of each month for smoothed data (1893 to 2014), Right: Split into groups (before and post-change-point), Bottom: Each month by group

series show some of the lowest probabilities from the 1990s to the earlier 2000s, until the probabilities sharply increase at the end of the dataset. The estimated probabilities for both thresholds are currently at one of the highest points for the entire range of the data, but not that dissimilar from the previous peaks.



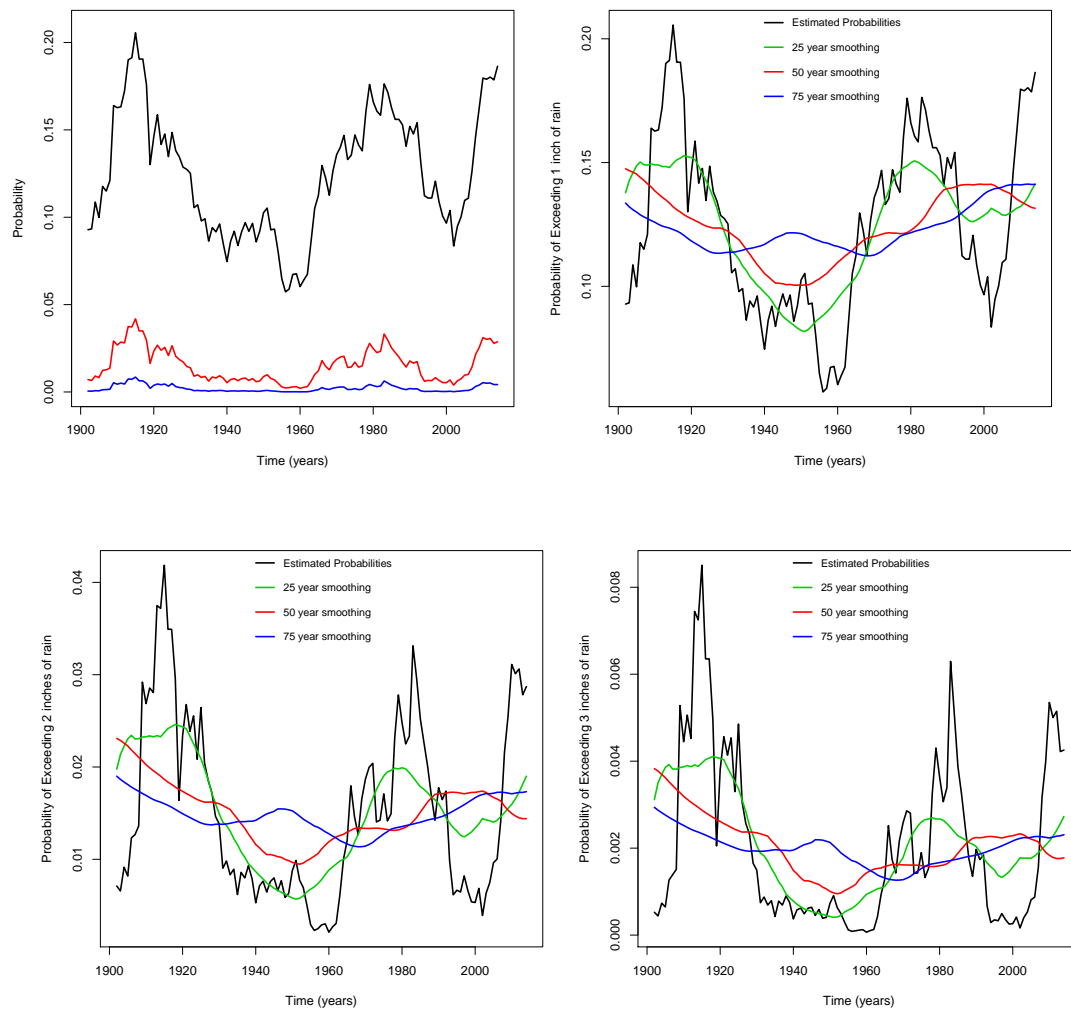


Figure 2.40: Top Left: All probabilities (meeting and/or exceeding 1 in, 2 in, or 3 in of rainfall), Top Right: Probability of meeting and/or exceeding 1 in of rainfall with smoothing lines, Bottom Left: Same with 2 in, Bottom Right: Same with 3 in

## CHAPTER 3

### GEOSPATIAL EXPLORATORY DATA ANALYSIS

The area investigated for this report showed varying behavior for the climate signals, as they relate to rainfall, of the investigated cities. The intent of this section is to examine maximum rainfall in a way that could be more insightful in context. The plots were generated

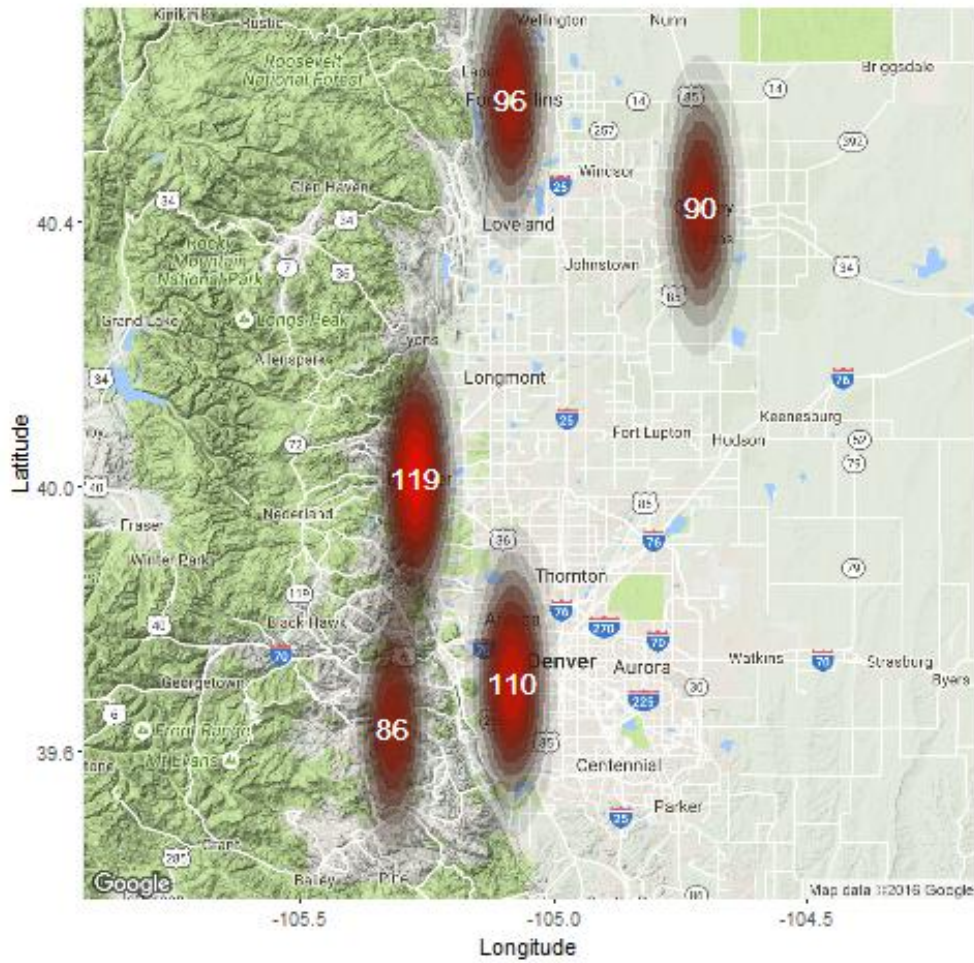


Figure 3.1: Density and frequency for 1 in of rainfall observed in the data set from 1963 to 2014

using ggmap (Kahle and Wickham, 2013). Figure 3.1 shows that the weather station in Boulder has recorded 119 months in which the rainfall for one calendar day was at least 1 in. The information does not carry the same weight as also knowing that Evergreen recorded 33 fewer such months since 1963 and/or that Boulder has the most such months on record, in the qualifying data set, among the five cities in the investigation. The data for this section was a subset of the observed monthly 24-h maximum rainfall values after 1962 since 1963 was the shortest time ranged observed among the cities (Lakewood). Comparing the data on the longest time range available dilutes the information gained by direct comparisons since dating back to 1898 the city of Boulder had over 200 months satisfying the criteria, yet the number of months for Lakewood does not change.

The information provided in Figures 3.1, 3.2, and 3.3 relates the number of qualifying months since 1963 that each of the cities had at least 1 one calendar day in which 1 in (25.4 mm) of rainfall was recorded. Additionally, a relative density gradient is provided. The gradient is the richest/brightest shade of red for a high density of points as well as relatively higher density than the surrounding cities. The gradient fades to gray for low density of points and relatively low occurrences. The gradient is also used in Appendix Figures E.1, E.2, E.3.

Table 3.1: Number of times at least 1 in of rain was recorded for qualifying months

	Jan	Feb	Mar	Apr	May	Jun	Jul	Aug	Sep	Oct	Nov	Dec
Boulder	1	1	10	19	20	15	14	11	11	13	2	2
Fort Collins	0	0	8	15	21	15	10	10	8	6	1	2
Lakewood	1	0	8	13	17	22	19	12	9	4	4	1
Evergreen	0	0	7	12	14	14	10	8	5	8	4	4
Greeley	0	0	5	12	20	15	11	9	8	6	3	1

Figure 3.1 shows that Boulder has the most months with 1 in of rainfall (with conditions described above and throughout the report). Preliminarily, from this viewpoint, it seems that it would be more likely to observe the September 2013 event in Boulder than the other cities - this conjecture is addressed throughout the section. The same geospatial approach

was applied in Figure E.1 to decompose the information in Figure 3.1. The decomposed information is summarized in Table 3.1. The information in Table 3.1 also shows that Boulder could be the most likely to experience the 9/13 Event with the most occurrences in September among the cities, however, the table shows that late Spring and early Summer have far more qualifying months across the cities. The table also shows that only 3 qualifying months among all the cities recorded at least 1 in of rain in January and February. Without those 3 months, January and February would not have made it into this portion of the summary.

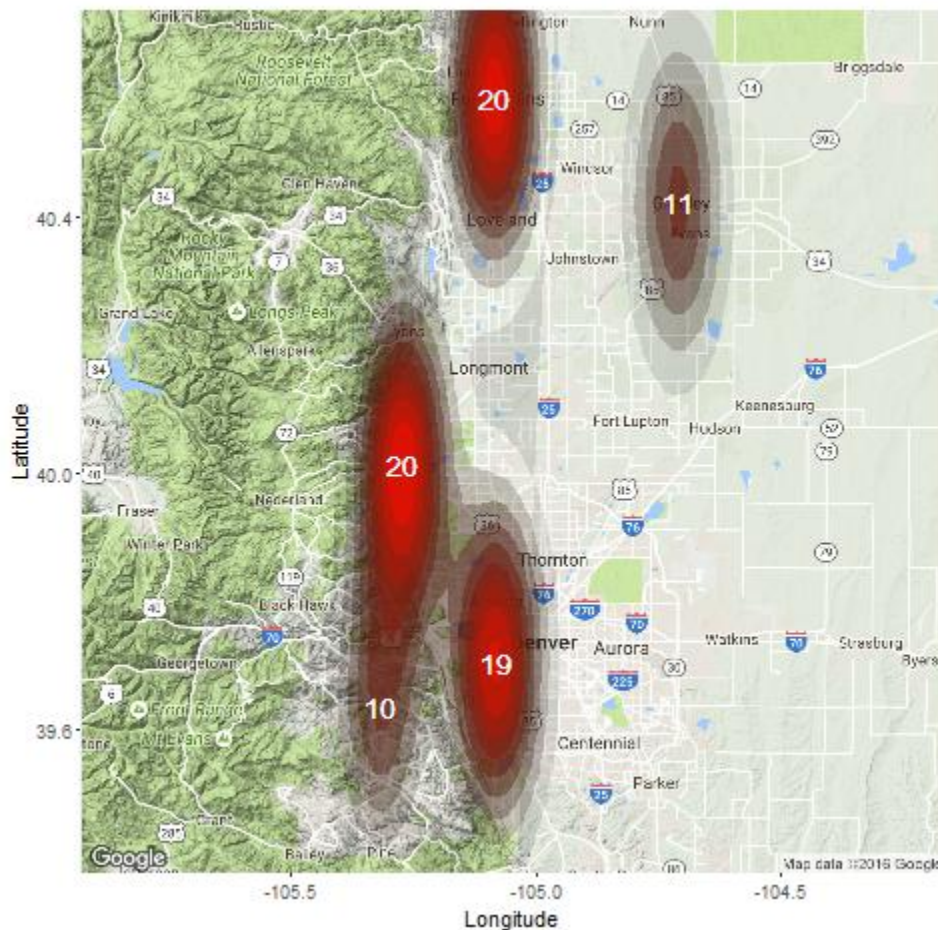


Figure 3.2: Density and frequency for 2 in of rainfall observed in the data set from 1963 to 2014

Increasing the rainfall threshold from 1 in to 2 in (50.8 mm), Figure 3.2 shows Boulder and Fort Collins now have the same number (20) of occurrences (Lakewood has just 1 less). Boulder, while having more frequent occurrences of breaking the 1 in rain threshold,

appears to have a comparable number of more extreme rainfalls. The other important piece of information in the plot is the relative shift in the proportion of occurrences. There appears to be two clusters of rainfall densities with Boulder, Fort Collins, and Lakewood recording almost double the occurrences of Evergreen and Greeley.

Table 3.2: Number of times at least 2 in of rain were recorded for qualifying months

	Mar	Apr	May	Jun	Jul	Aug	Sep	Oct
Boulder	2	4	5	5	2	1	1	0
Fort Collins	2	3	3	5	3	4	0	0
Lakewood	2	2	2	5	2	3	2	1
Evergreen	2	1	2	4	1	0	0	0
Greeley	0	1	3	3	2	2	0	0

Decomposing the information to produce Appendix Figure E.2 and Table 3.2 shows that at least 2 in of rainfall in a calendar day was recorded only in non-Winter months since 1963. The only rainfall to exceed 2 in during September for Boulder was the September 2013 event.

Lastly, Figure 3.3 shows the number of occurrences for the largest rainfall threshold of interest (3 in). Boulder and Fort Collins have the highest number of occurrences. Evergreen and Lakewood only have a single qualifying occurrence each. If the September 2013 event is omitted from the geospatial investigation then Fort Collins and Boulder have the same number of occurrences. Looking at Table E.3 it appears rainfall of this magnitude occurs only in Spring and Summer months because the only occurrence in September was for Boulder in 2013, which is an outlier based on this investigation.



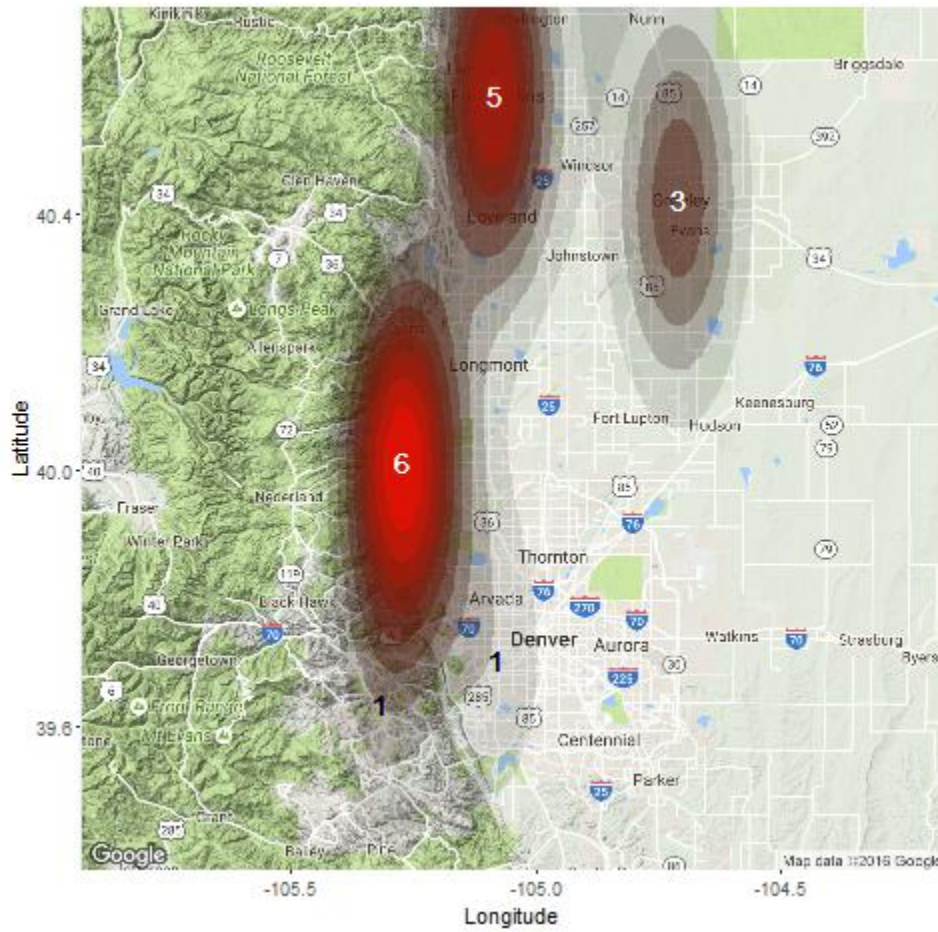


Figure 3.3: Density and frequency for 3 in of rainfall observed in the data set from 1963 to 2014

Table 3.3: Number of times at least 3 in of rain were recorded for qualifying months

	Mar	Apr	May	Jun	Jul	Aug	Sep
Boulder	0	2	2	1	0	0	1
Fort Collins	2	0	1	0	2	0	0
Lakewood	1	0	0	0	0	0	0
Evergreen	0	0	1	0	0	0	0
Greeley	0	0	0	1	1	1	0

## CHAPTER 4

### CONCLUSIONS

#### 4.1 CLIMATE SIGNAL EDA

The climate signal investigation yielded some interesting similarities from a data viewpoint. It is possible the insights gained in this report are less novel to climatologists and/or those familiar with the climate of the area. The primary conclusions of the climate signal EDA is Boulder, Lakewood, and Fort Collins exhibit similar trends that might be explained by geographic features. Each of the cities borders the national forest present on the map in Figure 1.1, has a significant change point around 1980 that results in difference in the average of the pre and post-change-point groups of at least 2 mm of precipitation, and each had a general increasing trend in the mean maximum monthly 24-h precipitation over their respective time ranges. Had only these three weather stations been analyzed, it would be possible some change in the precipitation collecting, recording, and/or cataloging could be responsible for the increases across the cities, however, considering the analyses performed on Evergreen and Greeley, this scenario is unlikely. The two cities that did not border the eastern edge of the national forest had vastly different behaviors in the areas analyzed. Evergreen, which is west of the border and resides in a gray portion of the national forest in the map, experienced a decrease in the mean trend line, observed variances, and probabilities of meeting and/or exceeding all of the precipitation thresholds. The overall trends for Evergreen are negative; however, in the most recent years Evergreen appears to have hit a stable low point for all values of interest. The data for Greeley, which is a city east of the border, showed great variability over the time range, however, the values of interest for Greeley do not appear to have any long term increase or decrease to their trend. The signal is essentially

as variable as it has been since 1893 and the averages of the values is essentially the same as they were then as well. If the earlier years of the data are ignored (before 1950s), the trend lines for Greeley's values of interest have similar behavior to the trends of the same values for Boulder, Lakewood, and Fort Collins.

The seasonal effect of each city shows that if there was an increasing trend present (Boulder, Fort Collins, and Lakewood), then that change was not evenly spread across the mean trend lines for the individual months. This implies that as the signal has increased, and continues to increase, some months are experiencing a higher mean of maximum precipitation while others are remaining the same or decreasing. This could have negative implications such as more extreme storms during the wetter months.

## 4.2 GEOSPATIAL EXPLORATORY DATA ANALYSIS

The geospatial investigation helped provide a way to standardize an element of the climate signals. Boulder has the most months, in the qualifying data set, that have at least 1 in of rain recorded - followed by Lakewood, then Fort Collins. Interestingly, the second precipitation threshold (2 in) shows that these three cities, with similar climate signals and that all border the national forest line, have almost the same number of months in which at least one day recorded 2 in of rainfall or more. The other two cities, Evergreen and Greeley, are about half that. The third rainfall threshold (3 in) shows that Boulder and Fort Collins have the most occurrences while Lakewood and Evergreen have only seen rainfall on that magnitude in one month each since 1963 (for the qualifying data).

## 4.3 SHORTCOMINGS

The immediate shortcoming is also a strength. The EDA performed in this report was primarily done by a statistician with little-to-no direction from a climatologist. The insights and implications, which are data driven, should be largely unbiased in context.



The method used for the change point analyses required both the normality and independence assumptions. The application of the method yielded the expected results, but should be additionally verified and/or compared to alternative method (perhaps a non-parametric method).

Since the focus of this report was EDA, which yielded interesting results, little was done to claim and support statistical significance at many points. An argument can be made about the validity of determining statistical significance from the smoothed data provided in Chapter 2 - as compared to the full data primarily referenced in the appendix. For instance, had a client provided the smoothed data set and wanted inferential analysis performed on the change points and the time series, most (if not all) the results could be statistically significant in the absence of the original data.

#### 4.4 FUTURE WORK

If deemed worthy, the discoveries in this study can be published after some statistically sound review and debate. Additionally, partnerships with climatologists would aid to remove information trivial to climatologists and emphasize significant results (if any exist from a climatological viewpoint).

The specific topics we would like added, improve upon, solidified, hear conclusions about in context by a subject matter expert, and/or have a conclusive measure of statistical significance attached to are:

- The location of the change points identified. The change points presented in this report were detected using statistical tests that were not technically valid. The resulting points in time seemed logical and intuitive, however, there could be room for improvement in the accuracy of the points themselves. Better identification of the points could lead to more informative conclusions. For instance, if the true change points are closer together (temporally speaking), there might be an informative climatological element that simultaneously explains the change points.

- The shifts in seasonal patterns over time, especially as they relate to the change points. Direct conclusions about the probability, location, and magnitude of flooding cannot be made in this report; however, an intent of the report is to investigate elements of rainfall that could be helpful in reducing and preventing the severity of future floods. One of the more telling aspects of this investigation was shifts in seasonal mean monthly 24-h maximum observed rainfall. The fact that long term increasing trends were detected for maximum rainfall is potentially problematic for flooding on its own. Coupled with the information that these increases in time appear to be concentrated in certain months, while other months show decreasing trends, implies that greater and more severe rainfalls are in store for Boulder, Fort Collins, Lakewood and Greeley. The components of flood prevention that relate to rainfall would need to improve accordingly to maintain the status quo and/or reduce the frequency and magnitude of floods (as they relate to rainfall).
- Bayesian updated distributions. An unachieved research goal was to compare the probabilities of exceeding the established rainfall thresholds from the estimated distribution to Bayesian updated distributions. One benefit of this approach is stability in the parameter estimates over time, since the updated distribution would be robust to the variability among observed distributions throughout the investigation. Another benefit could be estimating the probability that precipitation exceeds the established thresholds using the full range of the data, as well as looking at the changes in the probabilities with the Bayesian approach. This approach should yield smoother probability trend lines than those presented in this report. Similar to the overall investigation, the robust distribution over time and the robust probability trend lines could provide conservative information akin to the smoothing procedures that were applied. What information can be added remains to be seen. It should be noted that while smoothing proved informative in this report, the greater variability presented throughout carries more contextual weight since conservative results have greater negative implications (loss

of lives, greater property and community damage, etc.) than less conservative results (overspending on maintenance and/or infrastructure that would still prove useful for future extreme rainfalls).

- Investigating the definition of the data. As was mentioned, when the data was defined in the introduction, not all months qualified for this data set. The perceived intent was that this helps prevent against including maximums that were not the true maximums for that month, leaving only data that provides the best attempt at working with the true maximums over time. It might lead to more conservative results, but the data used for this investigation could be augmented with a semi-subjective look at the original data in which reasonable extremes are added to this dataset regardless of how many days were observed that month. Adding data points could potentially stabilize elements of the analysis, specifically the observed variances over time. In some cases this would lead to conservative results while the best case result is that the observed maximum is the true maximum for that month. Using the original data is recommended since the imputation attempted during this investigation produced results that were below the observed maximums for months that did not qualify.
- Quantifying the trends. Several approximations about the magnitude of the change in the trends were stated throughout this investigation. The approximations were based on visual inspection and have room for improvement. Rigorous approximations for the rate of change in the trends and overall changes in the trends should be calculated for all cities and values of interest. Once better approximations have been obtained, simultaneous comparisons, perhaps geospatially, could prove useful in understanding how the climate signal for the region is changing.

## REFERENCES

- [1] Chakravarti, I.M., R. G. Laha, and J. Roy. 1967. Pp. 392-394 in *Handbook of Methods of Applied Statistics*, Volume I, John Wiley and Sons.
- [2] Clark, Robert A., Jonathan J. Gourley, Zachary L. Flamig, Yang Hong, and Edward Clark. 2014. "CONUS-Wide Evaluation of National Weather Service Flash Flood Guidance Products." *Weather & Forecasting* **29**: 377-392. doi: 10.1175/WAF-D-12-00124.1.
- [3] Delignette-Muller, Marie Laure, and Christophe Dutang. 2015. "fitdistrplus: An R Package for Fitting Distributions". *Journal of Statistical Software* **64**(4).
- [4] Doodge, James C.I. 1968. "The Hyrdrologic Cycle as a Closed System." *International Association of Scientific Hydrology*. **13**(1): 58-68. doi:10.1080/02626666809493568
- [5] Drossos, Constantine A., and Andreas N. Philippou. 1980. "A Note on Minimum Distance Estimates." *Annals of the Institute of Statistical Mathematics*. Institute of Statistical Mathematics **32**(1): 121123. doi:10.1007/BF02480318.
- [6] JRC (Joint Research Centre). 2008. *Urbanization: 95% Of The World's Population Lives On 10% Of The Land*. European Commission. ScienceDaily. Retrieved October 14, 2016 ([www.sciencedaily.com/releases/2008/12/081217192745.htm](http://www.sciencedaily.com/releases/2008/12/081217192745.htm)).
- [7] Hays, J.D., John Imbrie, and N.J. Shackleton. 1976. "Variations in the Earth's Orbit: Pacemaker of the Ice Ages." *Science* textbf194(4270): 1121-1132.
- [8] HDSC (Hydrometeorological Design Studies Center). 2013. "Exceedance Probability Analysis for the Colorado Flood Event 9-16 September 2013." National Weather Service. National Oceanic and Atmospheric Administration. Retrieved October 14, 2016 ([http://www.nws.noaa.gov/oh/hdsc/aep\\_storm\\_analysis/8\\_Colorado\\_2013.pdf](http://www.nws.noaa.gov/oh/hdsc/aep_storm_analysis/8_Colorado_2013.pdf)).

- [9] Kahle, D. and H. Wickham. 2013. “ggmap: Spatial Visualization with ggplot2”. *The R Journal* **5(1)**: 144-161. Retrieved October 26, 2016 (<http://journal.r-project.org/archive/2013-1/kahle-wickham.pdf>).
- [10] Killick, Rebecca, and Idris A. Eckley. 2014. “chanepoint: An R Package for Changepoint Analysis.” *Journal of Statistical Software* **58(3)**.
- [11] Marvel, Kate, and Cline Bonfils. 2013. “Identifying external influences on global precipitation.” *PNAS* **110(48)**: 19301-19306; published ahead of print November 11, 2013. doi:10.1073/pnas.1314382110.
- [12] Mattingly, K., P. Miller, and L. Seymour. 2016. “Estimates of Extreme Precipitation Frequency Derived from Spatially Dense Rain Gauge Observations: A Case Study of Two Urban Areas in the Colorado Front Range Region.” Submitted for publication.
- [13] NCEI (NOAA National Centers for Environmental Information). 2016. *U.S. Billion-Dollar Weather and Climate Disasters*. Retrieved October 19, 2016 (<https://www.ncdc.noaa.gov/billions/>).
- [14] Stewart, Kevin. 2010. *Extreme Rains Not Required*. Flood Hazard News. Denver, CO: Urban Drainage and Flood Control District. Retrieved September 26, 2016 ([http://www.udfcd.org/FWP/floodhistory/Understanding\\_Extremes.pdf](http://www.udfcd.org/FWP/floodhistory/Understanding_Extremes.pdf)).
- [15] Stewart, Kevin. 2007. *Understanding Extremes - Part IV*. Flood Hazard News. Denver, CO: Urban Drainage and Flood Control District. Retrieved September 26, 2016 ([http://www.udfcd.org/FWP/floodhistory/Understanding\\_Extremes.pdf](http://www.udfcd.org/FWP/floodhistory/Understanding_Extremes.pdf)).
- [16] Watkins, Joseph C. 2011. “Introduction to the Science of Statistics: From Theory to Implementation - Topic 15: Maximum Likelihood Estimation.” Preliminary Edition. Tucson, AZ: University of Arizona Department of Mathematics.

## APPENDIX

### A.1 DISTRIBUTION TESTING WITH FITDISTRPLUS IN R

This portion of the appendix contains the results from fitting the distributions for the decade long intervals from each weather station/city. The maximum likelihood estimation method is described in the introduction to Chapter 2 Climate Signal EDA, while the maximum goodness-of-fit (a.k.a. minimum distance estimation) with Anderson-Darling distance with right tailed weights (ADR) is described in Section 2.1.4.

#### A.1.1 DISTRIBUTION TESTING: BOULDER

Table A.1: Goodness-of-Fit test results using K-S GoF Test		
DISTRIBUTION	NULL REJECTED	NULL NOT REJECTED
Exponential (MLE)	46	62
Gamma (MLE)	37	71
Weibull (MLE)	15	93
Gamma (MGE)	0	108

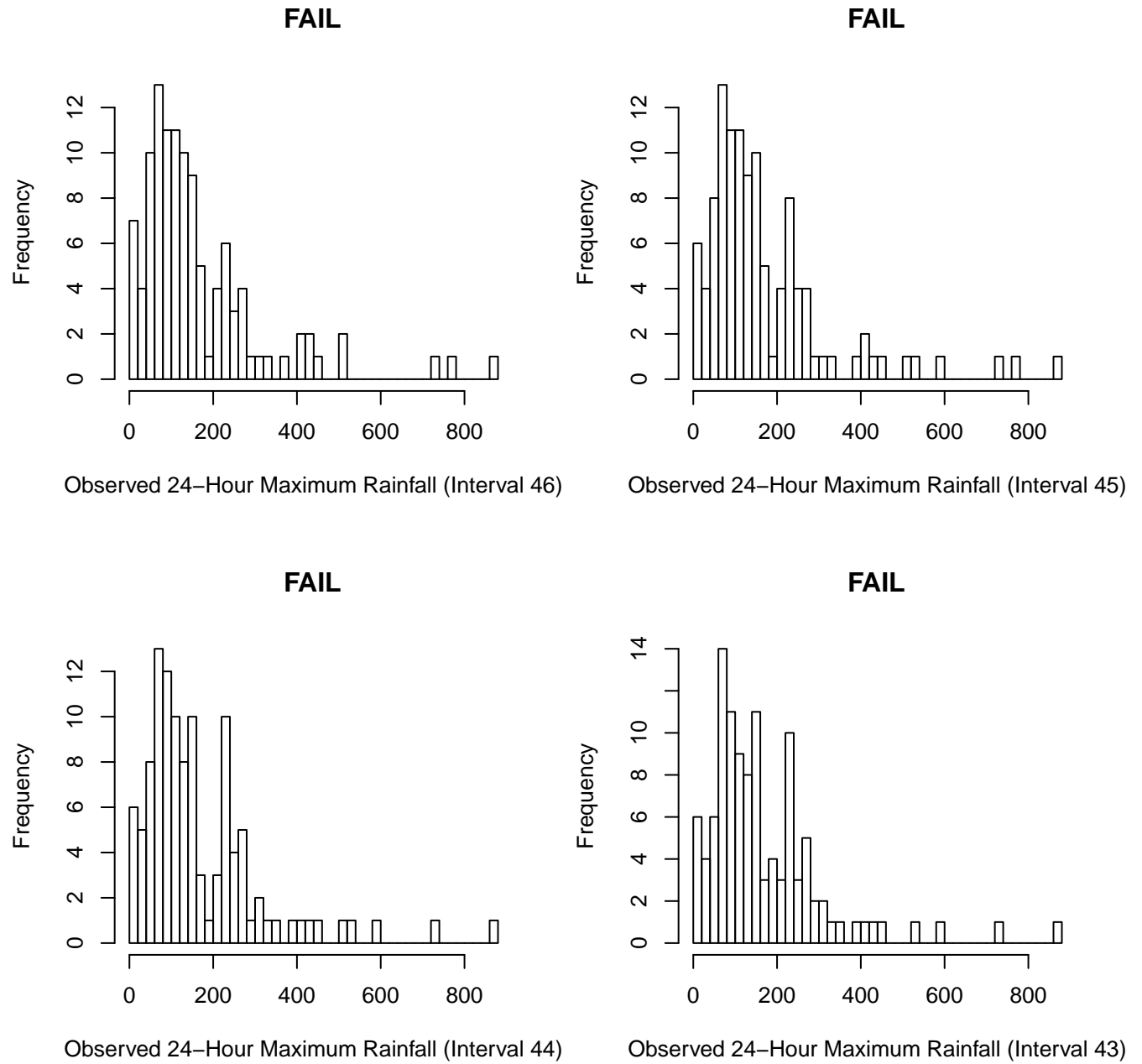


Figure A.1: Distributions of Observed 24-Hour Maximum Rainfall for Intervals that failed K-S GoF tests with parameter estimates from MLE (Boulder)

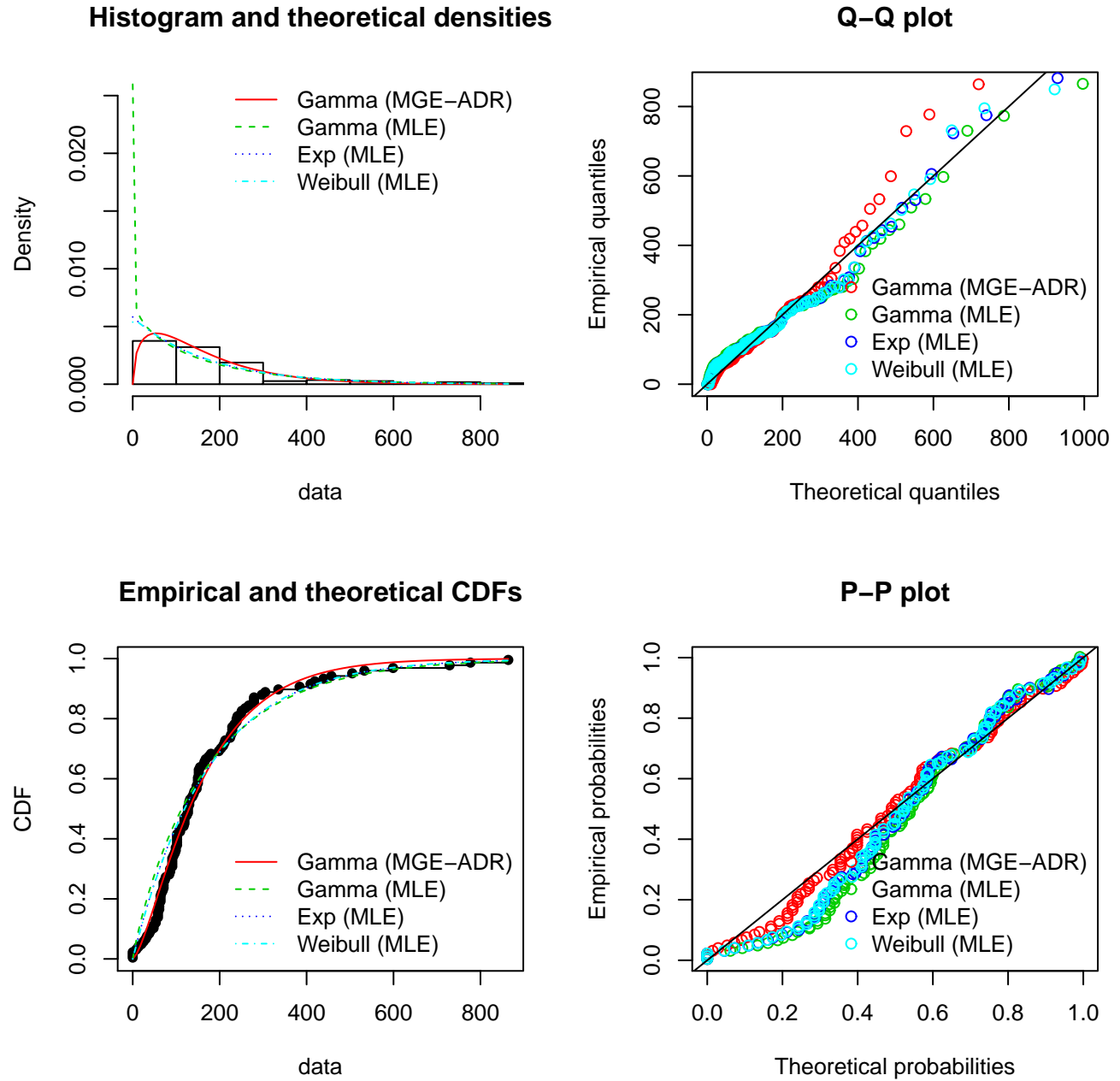


Figure A.2: Boulder time interval 45, suboptimal fit



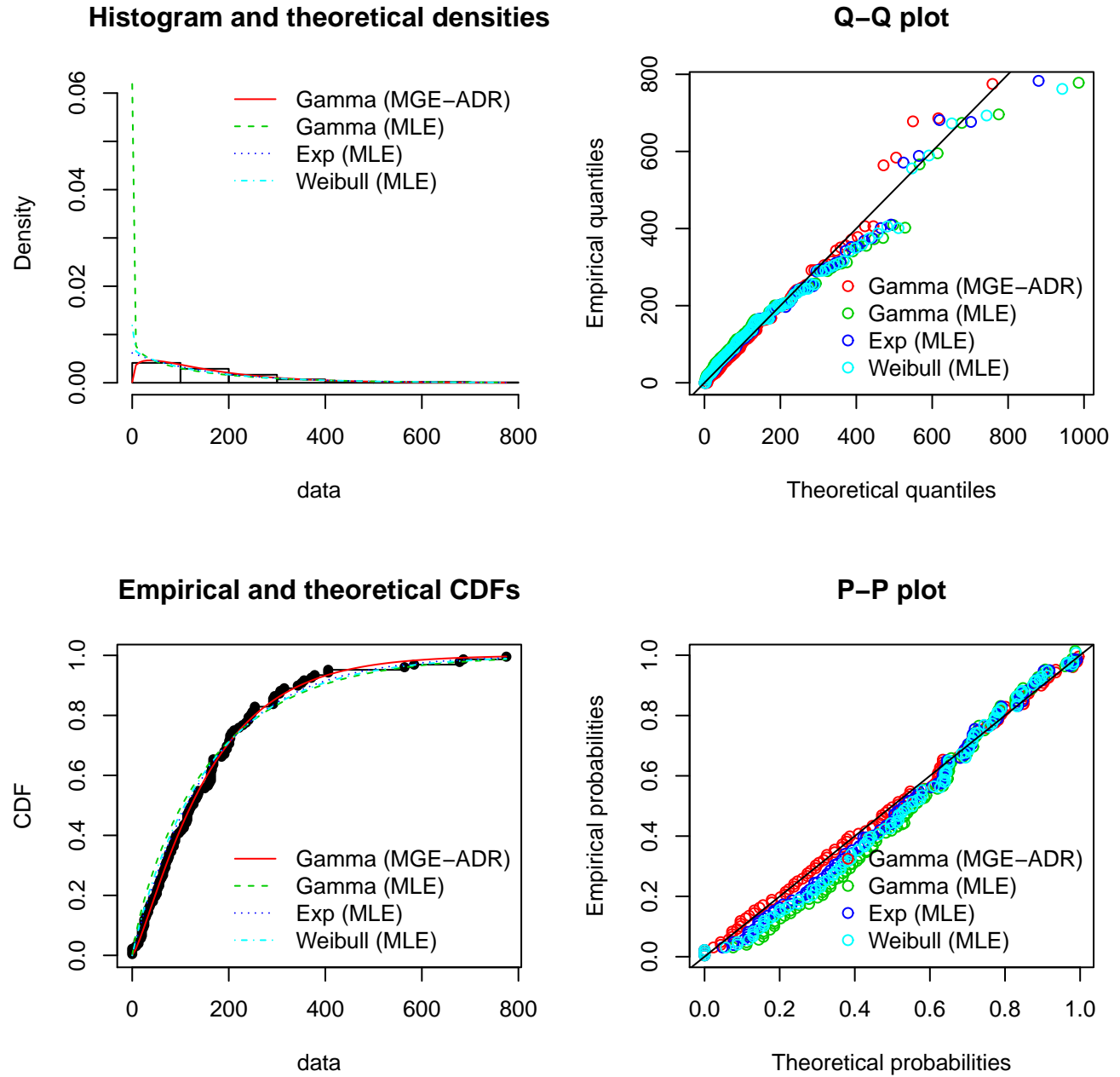


Figure A.3: Boulder time interval 3, optimal fit

## A.1.2 DISTRIBUTION TESTING: FORT COLLINS

Table A.2: Goodness-of-Fit test results using K-S GoF Test

DISTRIBUTION	NULL REJECTED	NULL NOT REJECTED
Exponential (MLE)	0	110
Gamma (MLE)	18	92
Weibull (MLE)	12	98
Gamma (MGE)	0	110

## A.1.3 DISTRIBUTION TESTING: EVERGREEN

Table A.3: Goodness-of-Fit test results using K-S GoF Test

DISTRIBUTION	NULL REJECTED	NULL NOT REJECTED
Exponential (MLE)	0	44
Gamma (MLE)	10	34
Weibull (MLE)	0	44
Gamma (MGE)	0	44

## A.1.4 DISTRIBUTION TESTING: LAKEWOOD

Table A.4: Goodness-of-Fit test results using K-S GoF Test

DISTRIBUTION	NULL REJECTED	NULL NOT REJECTED
Exponential (MLE)	14	29
Gamma (MLE)	13	30
Weibull (MLE)	4	39
Gamma (MGE)	0	43

## A.1.5 DISTRIBUTION TESTING: GREELEY

Table A.5: Goodness-of-Fit test results using K-S GoF Test

DISTRIBUTION	NULL REJECTED	NULL NOT REJECTED
Exponential (MLE)	1	112
Gamma (MLE)	50	63
Weibull (MLE)	26	87
Gamma (MGE)	0	113

## B.1 CHANGE POINT ANALYSIS IN R

### B.1.1 CHANGE POINT: BOULDER

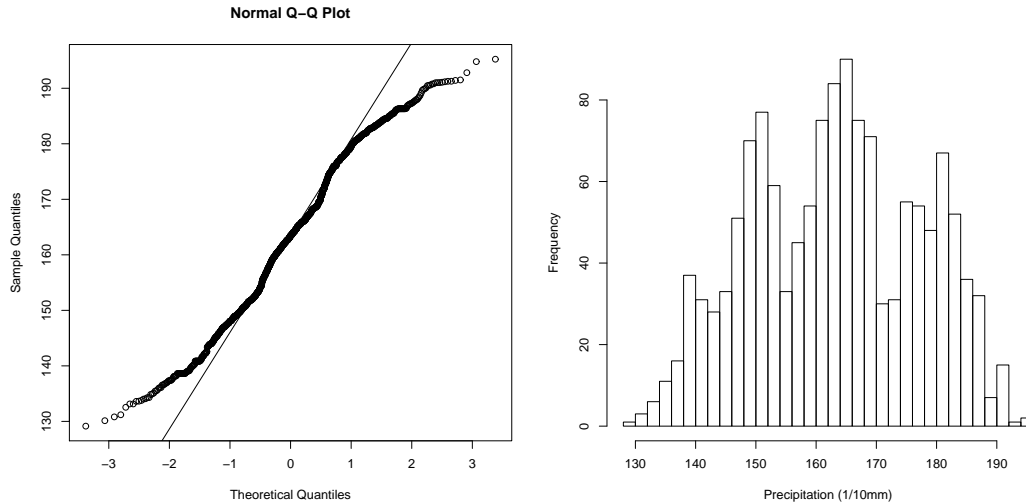


Figure B.1: QQ plot (left); Distribution of smoothed precipitation values (right)

Change point detection requires both independence and normality assumptions to be valid. As discussed in the context of the Trend Analysis for Behavior of Mean in the Boulder section, the independence assumption is violated. As seen in Figure B.1, the normality assumption is also violated. The Shapiro-Wilk test yields a test statistic of 0.98 and a p-value less than .0001, which means the null hypothesis that the distribution can be assumed to be normal is rejected. Although both assumptions were violated, the change point detected by performing change point analysis on the mean was employed in Figure 2.4. The successful detection of the change point is presumed to be due to the symmetry and relative bell-shape of the histogram on the right in Figure B.1, as well as the stark contrast in the means of the groups before and after the change point (i.e. it did not require a powerful or precise test to identify). The results of the change point analysis are displayed below as R output, where Changepoint Location 1007 corresponds to November 1981.

```
Class 'cpt' : Changepoint Object
~~      : S4 class containing 12 slots with names
```

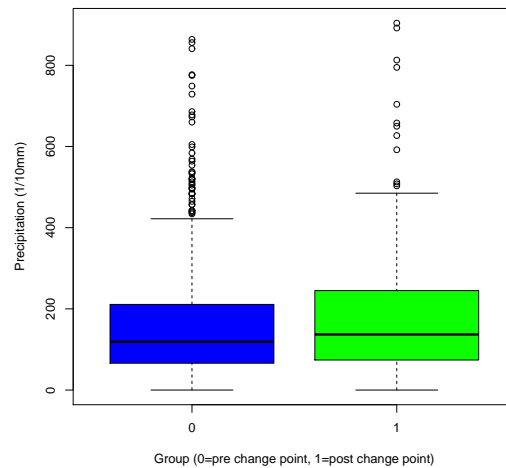


Figure B.2: Box plot for pre and post-change-point groups for full dataset (event omitted)

```

date version data.set cpttype method test.stat pen.type pen.value minseglen cpts ncpts.m
Created on   : Tue Sep 13 17:22:34 2016
summary(.)   :
-----
Created Using changepoint version 2.2.1
Changepoint type      : Change in mean
Method of analysis    : AMOC
Test Statistic       : Normal
Type of penalty       : MBIC with value, 21.68952
Minimum Segment Length : 1
Maximum no. of cpts   : 1
Changepoint Locations : 1007

```

### B.1.2 CHANGE POINT: FORT COLLINS

As discussed in the context of the Boulder section, the independence assumption is violated. As seen in Figure B.3, the normality assumption is also violated. The Shapiro-Wilk test yields a test statistic of 0.99 and a p-value less than .0001, which means the null hypothesis that the distribution can be assumed to be normal is rejected. Although both assumptions were violated, the change point detected by performing change point analysis on the mean

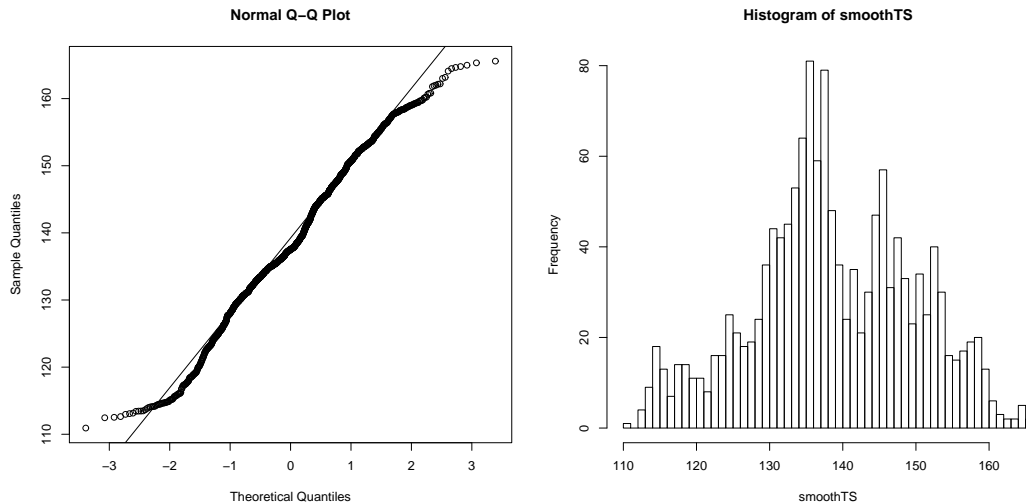


Figure B.3: QQ plot (left); Distribution of smoothed precipitation values (right)

was employed in Figure 2.14. The successful detection of the change point is presumed to be due to the symmetry and relative bell-shape of the histogram on the right in Figure B.3, as well as the stark contrast in the means of the groups before and after the change point (i.e. it did not require a powerful or precise test to identify). The results of the change point analysis are displayed below as R output, where Changepoint Location 976 corresponds to April 1977. Like Boulder, this change point will be used since it is detectable without a formal analysis, so the power/validity of the test is of less consequence.

```
Class 'cpt' : Changepoint Object
~~      : S4 class containing 12 slots with names
date version data.set cpttype method test.stat pen.type pen.value minseglen cpts ncpts.m
Created on   : Tue Sep 13 17:22:34 2016
summary(.)  :
-----

Created Using changepoint version 2.2.1
Changepoint type      : Change in mean
Method of analysis    : AMOC
Test Statistic       : Normal
Type of penalty       : MBIC with value, 21.79209
Minimum Segment Length : 1
```

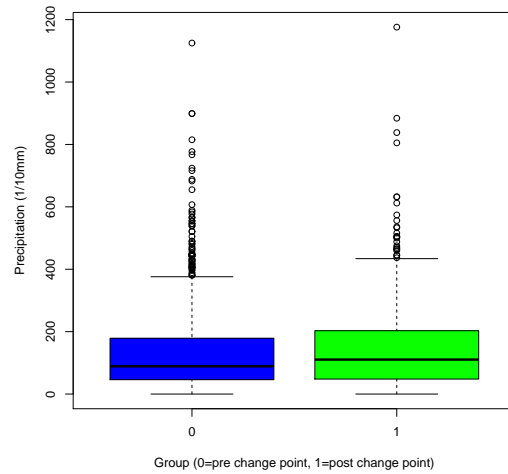


Figure B.4: Box plot for pre and post-change-point groups for full dataset

Maximum no. of cpts : 1  
 Changepoint Locations : 976

### B.1.3 CHANGE POINT: EVERGREEN

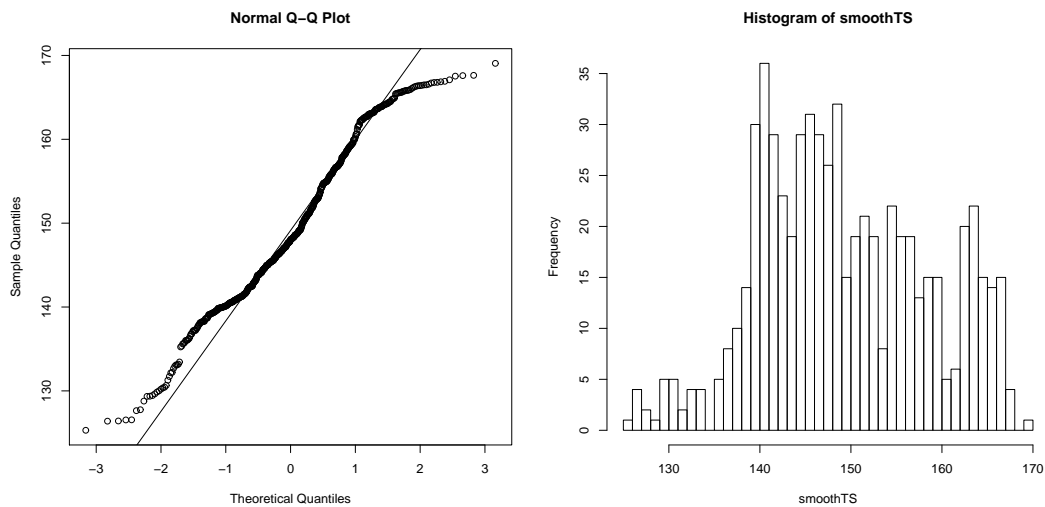


Figure B.5: QQ plot (left); Distribution of smoothed precipitation values (right)

The Shapiro-Wilk test yields a test statistic of 0.977 and a p-value less than .0001, which means the null hypothesis that the distribution can be assumed to be normal is rejected. Although both assumptions were violated, the change point detected by performing change point analysis on the mean was employed in Figure B.5. The results of the change point analysis are displayed below as R output, where Changepoint Location 358 corresponds to October 1991. This change point is less obvious than the change points determined during the Boulder and Fort Collins investigations, but will be utilized for the EDA purposes of this paper.

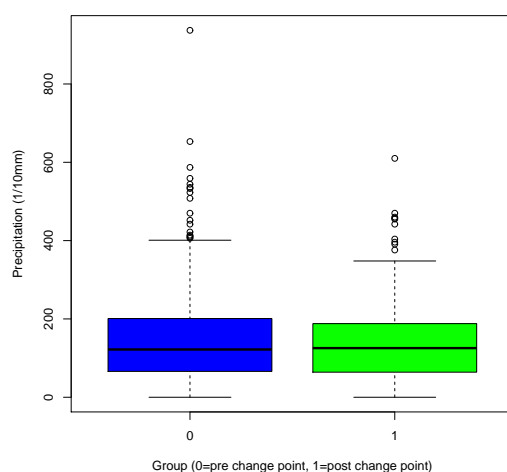


Figure B.6: Box plot for pre and post-change-point groups for full dataset

```
Class 'cpt' : Changepoint Object
~~      : S4 class containing 12 slots with names
date version data.set cpttype method test.stat pen.type pen.value minseglen cpts ncpts.m

Created on   : Tue Sep 13 17:22:34 2016

summary(.)  :
-----
Created Using changepoint version 2.2.1
Changepoint type      : Change in mean
Method of analysis    : AMOC
Test Statistic       : Normal
Type of penalty       : MBIC with value, 19.3656
```

```

Minimum Segment Length : 1
Maximum no. of cpts    : 1
Changepoint Locations  : 358

```

#### B.1.4 CHANGE POINT: LAKEWOOD

The Shapiro-Wilk test yields a test statistic of 0.952 and a p-value less than .0001, which means the null hypothesis that the distribution can be assumed to be normal is rejected. Although both assumptions were violated, the change point detected by performing change point analysis on the mean was employed in Figure B.7. The results of the change point analysis are displayed below as R output, where Changepoint Location 239 corresponds to November 1982. This change point was another sharp contrast between the two groups and an obvious shift in the climate signal. Similar to Boulder, this point could have been manually selected looking at the data and/or plot of the time series.

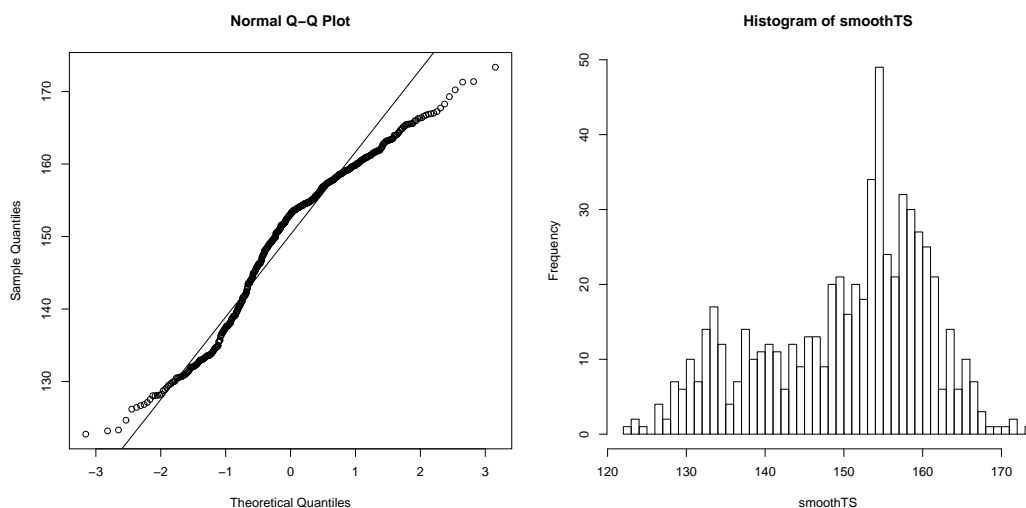


Figure B.7: QQ plot (left); Distribution of smoothed precipitation values (right)

```

Class 'cpt' : Changepoint Object
~~
: S4 class containing 12 slots with names
date version data.set cpttype method test.stat pen.type pen.value minseglen cpts ncpts.m

```

Created on : Tue Sep 13 17:22:34 2016



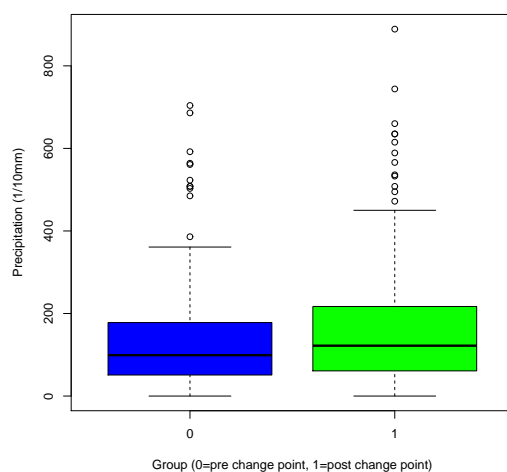


Figure B.8: Box plot for pre and post-change-point groups for full dataset

```
summary(.) :
-----
Created Using changepoint version 2.2.1
Changepoint type      : Change in mean
Method of analysis    : AMOC
Test Statistic       : Normal
Type of penalty       : MBIC with value, 19.30845
Minimum Segment Length : 1
Maximum no. of cpts   : 1
Changepoint Locations : 239
```

### B.1.5 CHANGE POINT: GREELEY

The Shapiro-Wilk test yields a test statistic of 0.975 and a p-value less than .0001, which means the null hypothesis that the distribution can be assumed to be normal is rejected. Although both assumptions were violated, the change point detected by performing change point analysis on the mean was employed in Figure B.9. The results of the change point analysis are displayed below as R output, where Changepoint Location 876 corresponds to December 1965. This change point is less obvious than the change points determined during

the Boulder and Fort Collins investigations, but will be utilized for the EDA purposes of this paper.

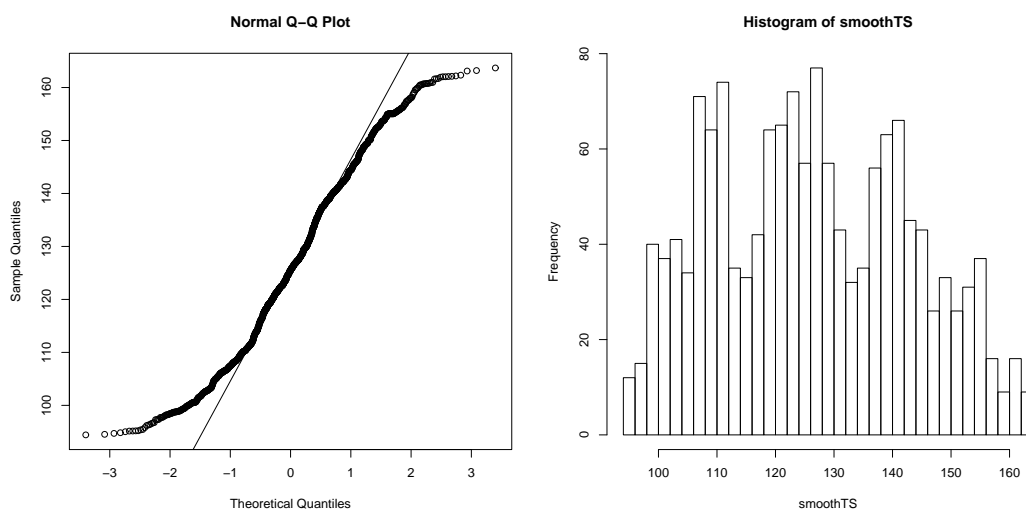


Figure B.9: QQ plot (left); Distribution of smoothed precipitation values (right)

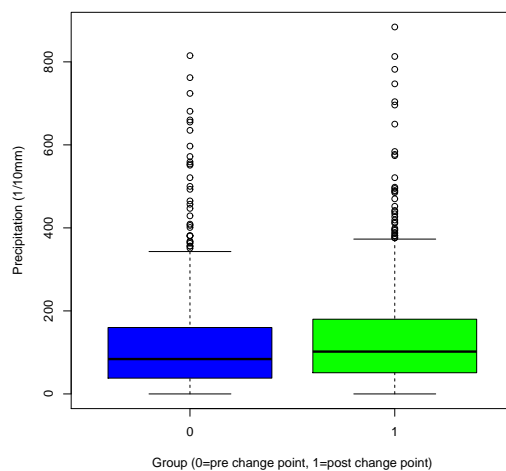


Figure B.10: Box plot for pre and post-change-point groups for full dataset

```
Class 'cpt' : Changepoint Object
~~ : S4 class containing 12 slots with names
date version data.set cpttype method test.stat pen.type pen.value minseglen cpts ncpts.m
```

Created on : Tue Sep 13 17:22:34 2016

```
summary(.) :
```

```
-----
```

```
Created Using changepoint version 2.2.1
```

```
Changepoint type      : Change in mean
```

```
Method of analysis    : AMOC
```

```
Test Statistic       : Normal
```

```
Type of penalty       : MBIC with value, 21.89127
```

```
Minimum Segment Length : 1
```

```
Maximum no. of cpts   : 1
```

```
Changepoint Locations : 876
```

## C.1 SEASONAL EFFECTS FOR CLIMATE SIGNAL EDA

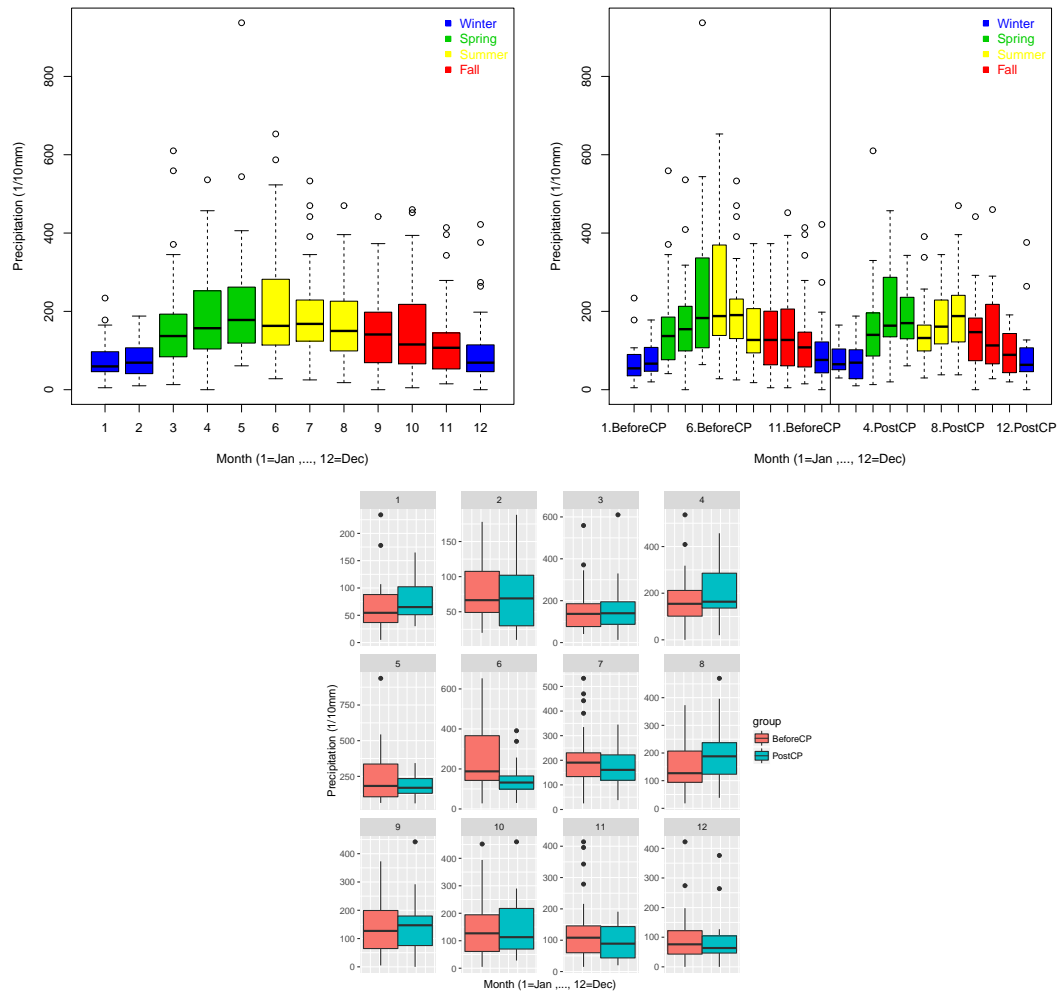


Figure C.1: Left: Box plot of each month for full dataset (1962 to 2014), Right: Split into groups (before and post-change-point), Bottom: Each month by group (Evergreen)

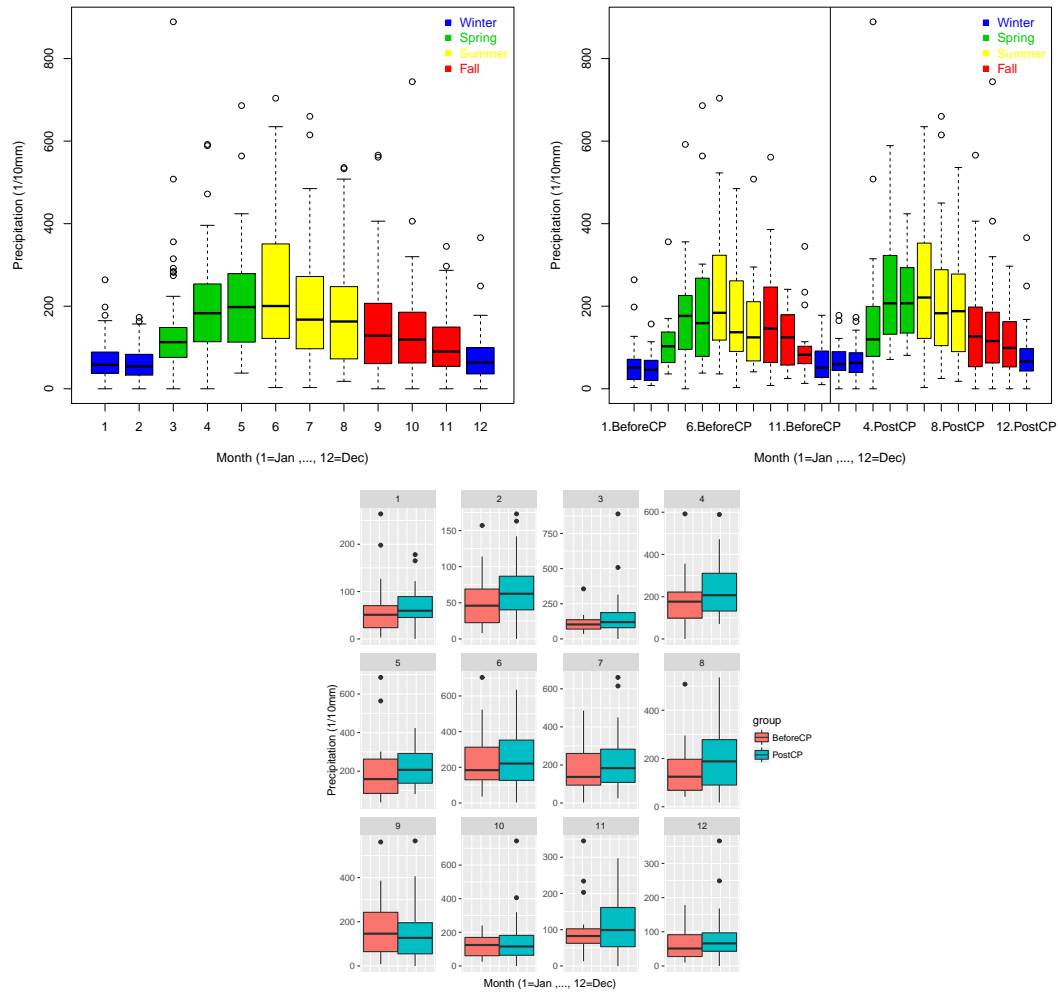


Figure C.2: Left: Box plot of each month for full dataset (1963 to 2014), Right: Split into groups (before and post-change-point), Bottom: Each month by group (Lakewood)

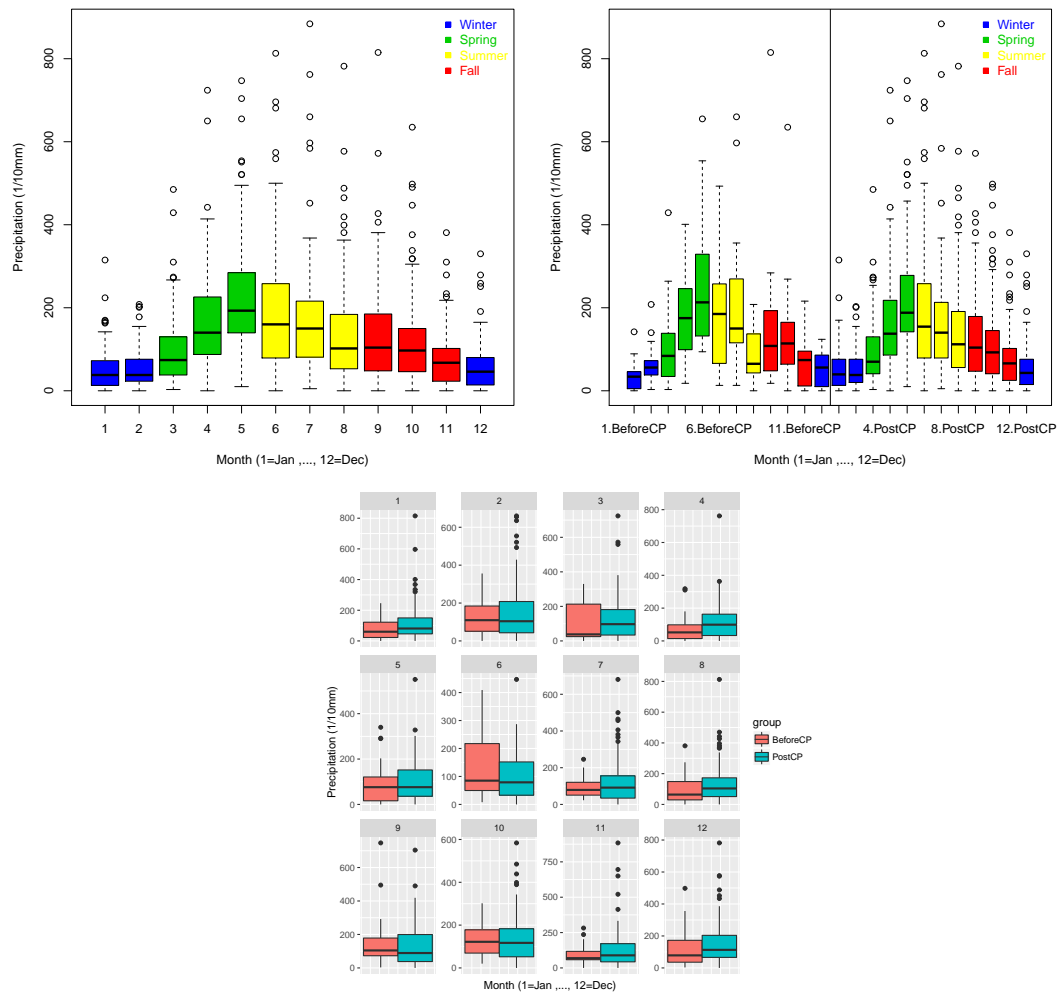


Figure C.3: Left: Box plot of each month for full dataset (1893 to 2014), Right: Split into groups (before and post-change-point), Bottom: Each month by group (Greeley)

## D.1 STANDARD DEVIATION PLOTS FOR CLIMATE SIGNAL EDA

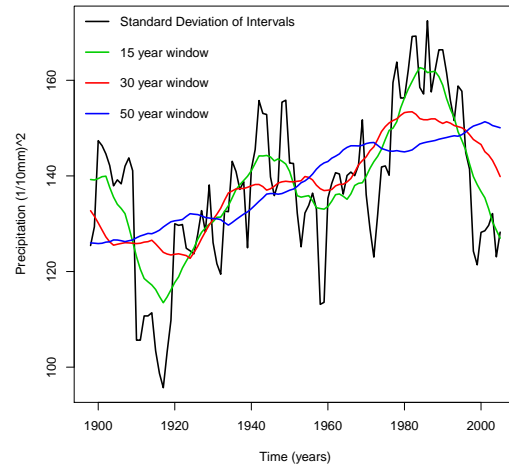


Figure D.1: Observed Standard deviations over time (Boulder)

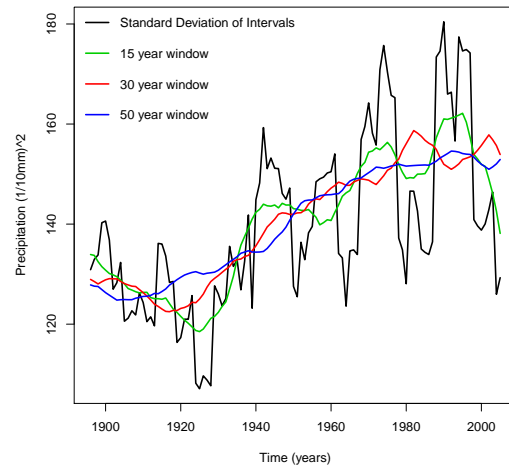


Figure D.2: Observed Standard deviations over time (Fort Collins)

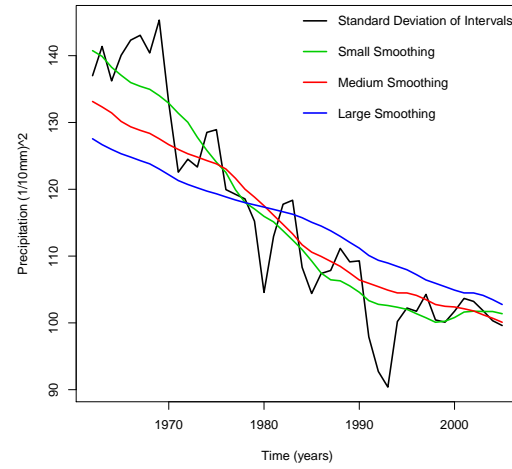


Figure D.3: Observed Standard deviations over time (Evergreen)

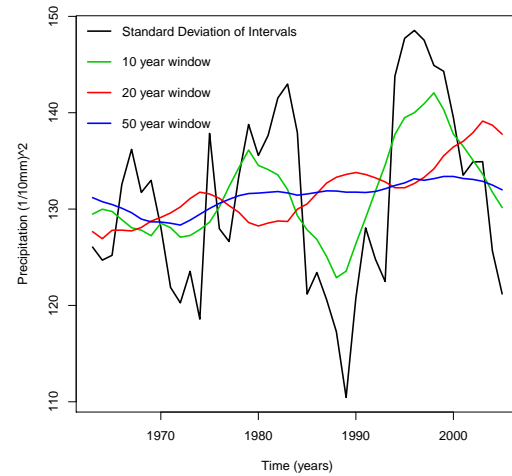


Figure D.4: Observed Standard deviations over time (Lakewood)



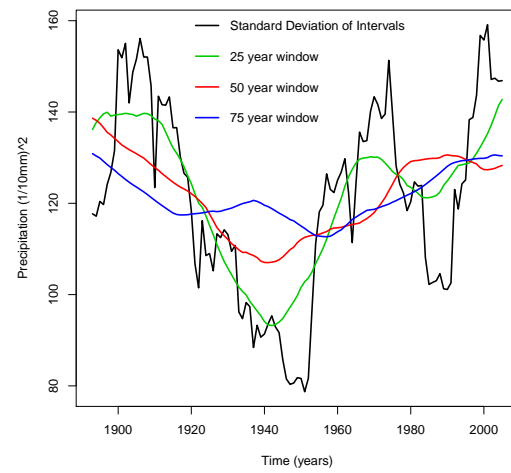


Figure D.5: Observed Standard deviations over time (Greeley)

## E.1 GEOSPATIAL SUPPORT PLOTS

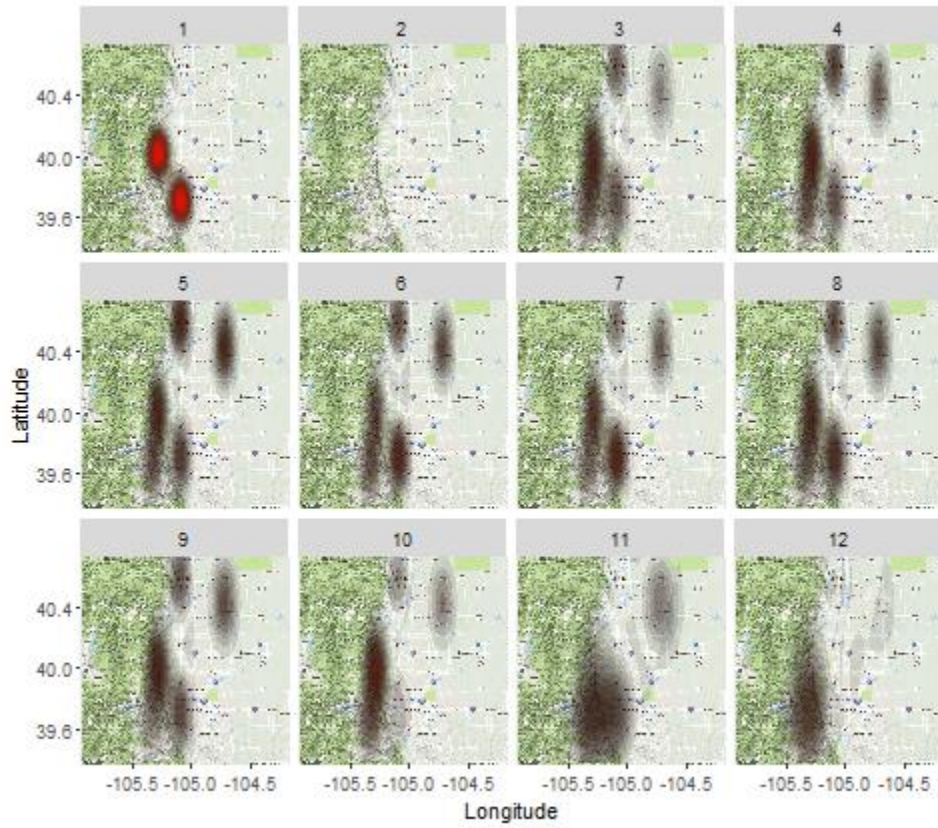


Figure E.1: Number of times the weather stations recorded 1 in of rain or more for qualifying each month in the data set

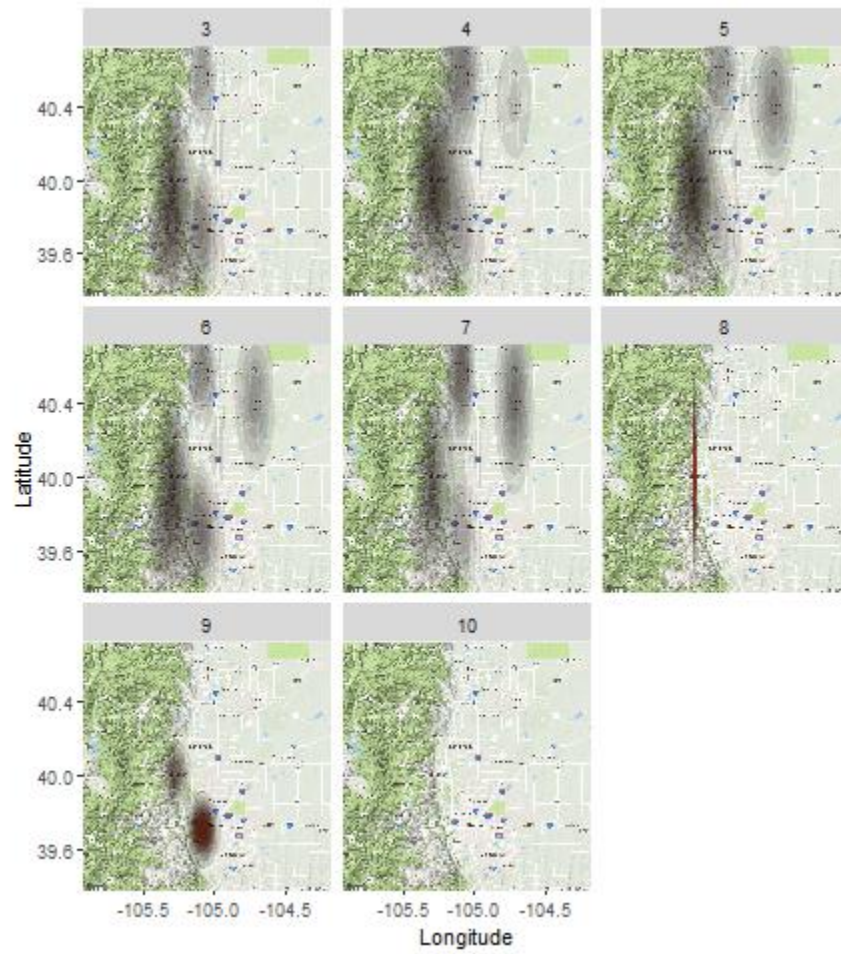


Figure E.2: Number of times the weather stations recorded 2 in of rain or more for each qualifying month in the data set

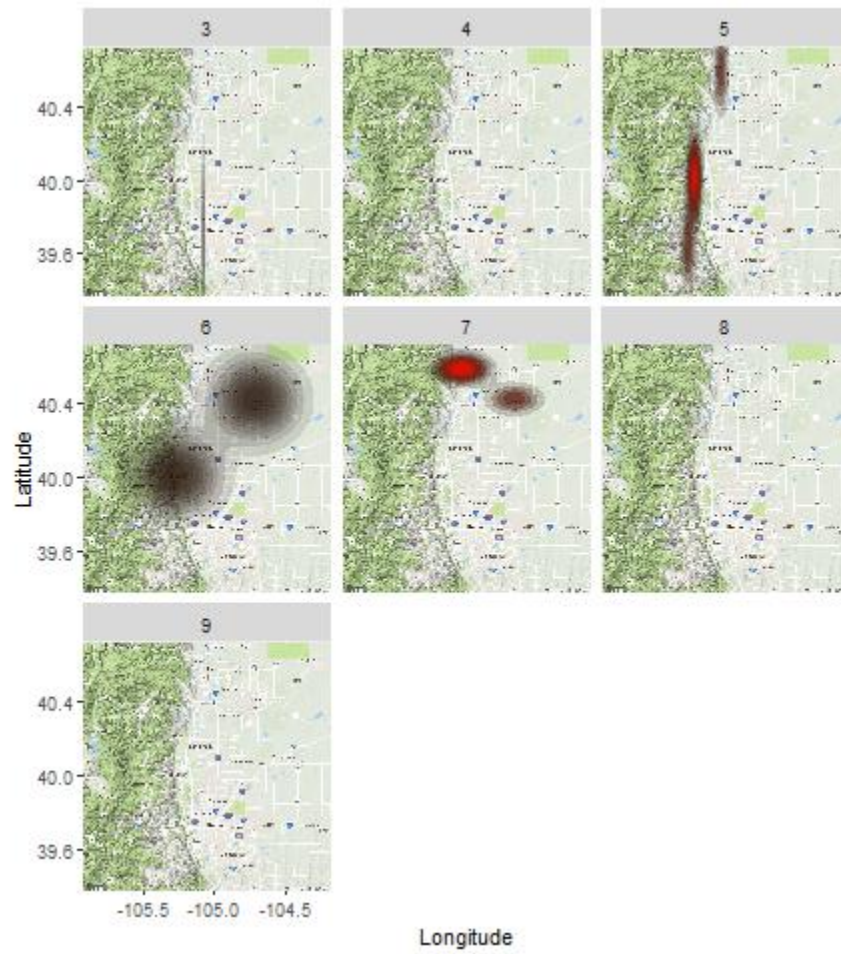


Figure E.3: Number of times the weather stations recorded 3 in of rain or more for each qualifying month in the data set